

Neural Inference Functions for Margins for Time Series Copula Models

Daniel Fynn^a, David Gunawan^a and Andrew Zammit-Mangion^{b,a}

^aSchool of Mathematics and Physics, University of Wollongong,
Wollongong, New South Wales, Australia

^bSchool of Mathematics and Statistics, University of New South Wales,
Sydney, New South Wales, Australia

March 24, 2026

Abstract

Copula models are widely employed in multivariate time series analysis because they permit flexible modelling of marginal distributions independently of the dependence structure, which is fully characterised by the copula function. However, Bayesian inference with these models becomes computationally demanding as the number of variables in the time series increases. Motivated by the classical inference functions for margins (IFM) approach, we propose a new neural-network based inference framework for estimating parameters in copula models, termed the neural inference functions for margins (N-IFM). N-IFM enables rapid parameter estimation for new data, fast sequential prediction, and efficient model comparison via time-series validation. We assess the performance of N-IFM using both simulated and real datasets and compare

it to Hamiltonian Monte Carlo, demonstrating substantial computational gains with comparable inferential accuracy.

Keywords: amortised inference; Gaussian approximation; neural networks; time series validation

1 Introduction

Multivariate time series models are an important inferential tool in several applications, as they provide a powerful framework for analysing volatility and dependence across multiple series. In financial applications, analysing high-dimensional time series is crucial for understanding how asset returns move together, managing portfolio risk, and assessing systemic risk arising from complex dependence across assets (Patton, 2009; Kastner, 2019; Deng et al., 2025). A commonly-used class of multivariate time series models are copula-based models, which offer a flexible framework that separates the modelling of marginal distributions from the dependence structure, which is captured by the copula function.

Exact Bayesian inference for high-dimensional copula models using Markov chain Monte Carlo (MCMC) methods is computationally expensive (Smith et al., 2012; Smith, 2015; Gunawan et al., 2020). Recently, variational Bayes (VB) inference has been used to estimate high-dimensional time-series copula models, reducing computational cost and improving scalability (Loaiza-Maya and Smith, 2019; Nguyen et al., 2020; Deng et al., 2025). However, financial and economics practitioners are interested in updating parameter and volatility estimates in real time, in order to regularly produce one-step or multi-step ahead predictive distributions. Sequential updating using MCMC or VB methods is computationally intensive, as each new observation requires rerunning full MCMC and VB algorithms.

Neural amortised inference, a type of simulation-based inference method, has recently emerged as a powerful approach for Bayesian inference; see Zammit-Mangion et al. (2025) for a recent review. Rather than performing computationally intensive inference from scratch for each new dataset, these methods train neural networks to learn reusable mappings from

data to posterior distributions of model parameters (Radev et al., 2020; Zammit-Mangion et al., 2025). Once trained, these neural networks amortise their training cost by providing fast, near-instantaneous inference for new observations, making them particularly well suited to scenarios that require repeated inference, such as sequential parameter updating or time-series validation for model selection. Often, flexible deep learning architectures (Goodfellow et al., 2016) are employed to model the mapping between observations and the posterior distribution of the model parameters.

In this paper, we propose an efficient neural amortised inference to fit high-dimensional time series copula models. Motivated by the classical inference functions for margins (IFM) approach (Joe, 1997), which first estimates the parameters of the marginal distributions and subsequently estimates the copula parameters conditional on the marginal parameter estimates, we propose neural inference functions for margins (N-IFM), which leverages neural networks to perform both stages of inference in an amortised manner. Two copula models — Gaussian copula (Song, 2000) and t copula (Demarta and McNeil, 2005) models — are considered. We empirically evaluate the performance of N-IFM on simulated and real datasets, benchmarking it against Hamiltonian Monte Carlo (HMC, Neal, 2011) and showing substantial computational gains with comparable inferential accuracy.

The rest of this paper is organised as follows. Section 2 presents background material on copula models, while Section 3 presents N-IFM. Section 4 outlines the criteria used to assess predictive performance. Section 5 describes simulation studies conducted to evaluate the accuracy of N-IFM, and Section 6 applies N-IFM to a real-world dataset. Section 7 discusses our results and findings. The paper also has an online supplement with additional technical details and examples.

2 Background

Section 2.1 provides a brief overview of copula models. Section 2.2 introduces implicit copula models, and Section 2.3 describes the Gaussian and t copula specifications. Section 2.4 details the factor-based parameterisation of the correlation structure for the Gaussian and t copulas. Finally, Section 2.5 presents the Generalised Autoregressive Conditional Heteroskedasticity (GARCH) model that we use to model the marginal time series.

2.1 Copula models

Copulas offer a general framework for modelling multivariate distributions in which the marginal distributions and the dependence structure across variables are modelled separately. By Sklar's theorem (Sklar, 1959), the joint cumulative distribution function of a multivariate continuous random variable $\mathbf{Y} \equiv (Y_1, \dots, Y_D)^\top$ is given by

$$F_{\mathbf{Y}}(\mathbf{y}) = C(F_{Y_1}(y_1), \dots, F_{Y_D}(y_D)), \quad (1)$$

where $\mathbf{y} \equiv (y_1, \dots, y_D)^\top$ denotes a realisation of the random vector \mathbf{Y} , $F_{Y_d}(y_d)$ is the marginal cumulative distribution function (CDF) of the d -th component Y_d , and $C : [0, 1]^D \rightarrow [0, 1]$ is the copula function, which captures the dependence structure among the components of \mathbf{Y} .

To obtain the joint probability density function (PDF) $p_{\mathbf{Y}}(\mathbf{y})$, we differentiate (1) with respect to all components of \mathbf{Y} :

$$p_{\mathbf{Y}}(\mathbf{y}) = \frac{\partial^D}{\partial y_1 \dots \partial y_D} F_{\mathbf{Y}}(\mathbf{y}) = c(F_{Y_1}(y_1), \dots, F_{Y_D}(y_D)) \prod_{d=1}^D p_{Y_d}(y_d), \quad (2)$$

where $p_{Y_d}(y_d) = \frac{\partial}{\partial y_d} F_{Y_d}(y_d)$ is the marginal density of Y_d and $c(\mathbf{u}) = \frac{\partial^D}{\partial u_1 \dots \partial u_D} C(\mathbf{u})$ is the copula density, where $\mathbf{u} \equiv (u_1, \dots, u_D)^\top \in [0, 1]^D$ with $u_d = F_{Y_d}(y_d)$.

2.2 Implicit copula models

McNeil et al. (2015) use the term implicit copula to refer to the copula that is implicitly defined by the multivariate distribution of a continuous random vector $\mathbf{Z} \equiv (Z_1, \dots, Z_D)^\top$. This copula is obtained by inverting Sklar's theorem, through what is called the inversion method (Nelsen, 2006). If \mathbf{Z} has a joint distribution function $F_{\mathbf{Z}}$ with marginal distributions F_{Z_1}, \dots, F_{Z_D} , then the implicit copula function is given by

$$C(\mathbf{u}) = F_{\mathbf{Z}}(F_{Z_1}^{-1}(u_1), \dots, F_{Z_D}^{-1}(u_D)). \quad (3)$$

Then, by the change of variables formula, we obtain the copula density

$$c(\mathbf{u}) = \frac{\partial^D}{\partial u_1 \cdots \partial u_D} C(\mathbf{u}) = \frac{p_{\mathbf{Z}}(\mathbf{z})}{\prod_{d=1}^D p_{Z_d}(z_d)}, \quad (4)$$

where $\mathbf{z} \equiv (z_1, \dots, z_D)^\top$ with $z_d = F_{Z_d}^{-1}(u_d)$ for $d = 1, \dots, D$; further details are given in Section S1 of the online supplement. Here, $p_{\mathbf{Z}}(\mathbf{z})$ denotes the joint density of \mathbf{Z} ,

$$p_{\mathbf{Z}}(\mathbf{z}) = \frac{\partial^D}{\partial z_1 \cdots \partial z_D} F_{\mathbf{Z}}(\mathbf{z}),$$

and $p_{Z_d}(z_d)$ denotes the marginal density of Z_d ,

$$p_{Z_d}(z_d) = \frac{\partial}{\partial z_d} F_{Z_d}(z_d), \quad d = 1, \dots, D.$$

In this paper we consider two commonly used implicit copula models, the Gaussian copula (Song, 2000) and the t copula (Demarta and McNeil, 2005). Since their margins are constrained to be uniform, copula models are invariant to location and scale. Therefore, when defining the joint distribution $F_{\mathbf{Z}}$, the location parameters are largely irrelevant, and the scale matrices can be restricted to correlation matrices (Nelsen, 2006).

2.3 Gaussian and t copulas

This section briefly describes the widely-used Gaussian copula of Song (2000) and t copula of Demarta and McNeil (2005). Both these copulas are constructed using the implicit method of Section 2.2.

Let $\Phi(\cdot)$ and $\phi(\cdot)$ be the CDF and PDF, respectively, of a univariate standard Gaussian random variable \mathbf{Z} , and let $\Phi_D(\cdot; \boldsymbol{\mu}, \boldsymbol{\Omega})$ and $\phi_D(\cdot; \boldsymbol{\mu}, \boldsymbol{\Omega})$ be the CDF and PDF of a D -dimensional multivariate normal distribution with mean vector $\boldsymbol{\mu}$ and correlation matrix $\boldsymbol{\Omega}$, respectively. The Gaussian copula is derived from a multivariate normal distribution $\mathbf{Z} \sim \mathcal{N}_D(\mathbf{0}, \boldsymbol{\Omega})$, where $\boldsymbol{\Omega}$ is a $D \times D$ correlation matrix. From (3), the Gaussian copula function is defined as

$$C_G(\mathbf{u}; \boldsymbol{\Omega}) = \Phi_D(\Phi^{-1}(u_1), \dots, \Phi^{-1}(u_D); \mathbf{0}, \boldsymbol{\Omega}), \quad (5)$$

where $\Phi^{-1}(\cdot)$ is the inverse of the standard normal CDF, applied component-wise to the vector $\mathbf{u} \equiv (u_1, \dots, u_D)^\top$. The Gaussian copula density is given by:

$$c_G(\mathbf{u}; \boldsymbol{\Omega}) = \frac{\phi_D(\mathbf{z}; \mathbf{0}, \boldsymbol{\Omega})}{\prod_{d=1}^D \phi(z_d)},$$

where $\mathbf{z} \equiv (\Phi^{-1}(u_1), \dots, \Phi^{-1}(u_D))^\top$. Despite its popularity, the Gaussian copula does not allow for tail dependence: the tendency of variables to exhibit dependence during extreme co-movements.

The t copula is constructed by modelling the vector \mathbf{Z} as a multivariate t -distributed with degrees of freedom $\nu > 2$. A key advantage of the t copula over the Gaussian copula lies in its ability to model tail dependence. The t copula also allows for heavy tails, providing a more realistic description of dependence for financial data.

Let $T_D(\cdot; \mathbf{0}, \boldsymbol{\Omega}, \nu)$ and $t_D(\cdot; \mathbf{0}, \boldsymbol{\Omega}, \nu)$ denote the CDF and PDF, respectively, of the D -dimensional multivariate t -distribution with $\nu > 2$ degrees of freedom, a zero mean vector,

and a positive definite scale matrix $\mathbf{\Omega}$. For $0 \leq u_1, \dots, u_D \leq 1$, the D -dimensional t copula (C_T) and its joint copula density (c_T) are given by

$$C_T(\mathbf{u}; \mathbf{\Omega}, \nu) = T_D(z_1, \dots, z_D; \mathbf{0}, \mathbf{\Omega}, \nu), \quad (6)$$

$$c_t(\mathbf{u}; \mathbf{\Omega}, \nu) = \frac{t_D(z_1, \dots, z_D; \mathbf{0}, \mathbf{\Omega}, \nu)}{\prod_{d=1}^D t_\nu(z_d)}, \quad (7)$$

where $t_\nu(\cdot)$ is the PDF of a univariate t -distribution with $\nu > 2$ degrees of freedom and $z_d = T_\nu^{-1}(u_d)$ for $d = 1, \dots, D$, where $T_\nu^{-1}(\cdot)$ is the quantile function of standard univariate t -distribution with ν degrees of freedom.

2.4 Factor correlation matrix

When the dimensionality D is large, estimating an unrestricted correlation matrix $\mathbf{\Omega}$ for Gaussian and t copulas becomes challenging due to the large number of parameters and the constraints required for positive definiteness. To address this issue, we follow the approach of Murray et al. (2013) and employ a factor structure for the correlation matrix for \mathbf{Z} . Specifically, we factorise the correlation matrix as

$$\bar{\mathbf{\Omega}} = \mathbf{R}_1 \mathbf{R} \mathbf{R}_1 = \mathbf{R}_1 (\mathbf{G} \mathbf{G}^\top + \mathbf{I}_D) \mathbf{R}_1, \quad (8)$$

where \mathbf{I}_D denotes the $D \times D$ identity matrix, $\mathbf{R}_1 = \text{diag}(\mathbf{R})^{-1/2}$ scales \mathbf{R} to have unit diagonal entries thereby converting it into a valid correlation matrix, and \mathbf{G} is a $D \times k$ factor loading matrix with $k < D$. For identifiability, \mathbf{G} is constrained so that $G_{ij} = 0$ for $j > i$ and $G_{ii} > 0$ for $i = 1, \dots, k$. To facilitate satisfying the positivity constraints when making inference, we reparameterise the loading matrix \mathbf{G} as $\tilde{\mathbf{G}}$ where

$$\tilde{G}_{ij} = \begin{cases} \log(G_{ij}), & \text{if } i = j, \\ G_{ij}, & \text{if } i \neq j. \end{cases}$$

2.5 Marginal time series model

The GARCH model is one of the most commonly used for modelling volatility clustering (Bollerslev, 1986). In most applications, the GARCH(1,1) model is sufficient for capturing the volatility dynamics of financial data, and it is hence the model we use for each (marginal) time series. Let $y_{d,t}$ denote an observation of the d -th time series at time t , where $d = 1, \dots, D$ and $t = 1, \dots, T$. The GARCH(1,1) model with Gaussian errors is given by

$$y_{d,t} = \sigma_{d,t} \epsilon_{d,t} \quad \text{for } t = 1, \dots, T, \quad (9)$$

$$\sigma_{d,t}^2 = \gamma_d + \alpha_{1,d} y_{d,t-1}^2 + \alpha_{2,d} \sigma_{d,t-1}^2 \quad \text{for } t = 2, \dots, T, \quad (10)$$

$$\sigma_{d,1}^2 = \frac{\gamma_d}{1 - \alpha_{1,d} - \alpha_{2,d}}, \quad (11)$$

where $\gamma_d > 0$, $\alpha_{1,d} \geq 0$, $\alpha_{2,d} \geq 0$, $\alpha_{1,d} + \alpha_{2,d} < 1$, and $\epsilon_{d,t} \sim \mathcal{N}(0, 1)$ for $d = 1, \dots, D$. Instead of making inference on the constrained $\alpha_{1,d}$, $\alpha_{2,d}$ and γ_d , we instead make inference on the transformed parameters $\varphi_{1,d}$, $\varphi_{2,d}$ and $\varphi_{3,d}$, where the transformations are detailed in Section S2 of the online supplement. In addition to Gaussian errors, in Section 6 we also consider error terms that follow a Student's- t distribution with $\tilde{\nu}_d$ degrees of freedom, for $d = 1, \dots, D$.

3 Neural Posterior Inference

Section 3.1 discusses the classical inference functions for margins (IFM). Section 3.2 discusses the proposed neural inference functions for margins (N-IFM).

3.1 Classical inference functions for margins

This section discusses the classical IFM approach proposed by Joe and Xu (1996). The IFM method applies to models in which the univariate marginal distributions can be modelled separately from the dependence structure, as is the case when the dependence is modelled

using a copula discussed in Section 2.1. Here, we consider the case where the margins are generated through a time series. Let $\boldsymbol{\theta}_d$ denote the vector of (possibly transformed) marginal parameters for the d -th series, $d = 1, \dots, D$, and let $\boldsymbol{\theta}_{\text{cop}}$ denote the vector of (possibly transformed) copula parameters. The full parameter vector is then given by

$$\boldsymbol{\theta} \equiv (\boldsymbol{\theta}_1^\top, \dots, \boldsymbol{\theta}_D^\top, \boldsymbol{\theta}_{\text{cop}}^\top)^\top.$$

Consider observations $\mathbf{y}_t \equiv (y_{1,t}, \dots, y_{D,t})^\top$, for $t = 1, \dots, T$ from the copula model with parameters $\boldsymbol{\theta}$, and let $\mathbf{y} \equiv (\mathbf{y}_1^\top, \dots, \mathbf{y}_T^\top)^\top$. Based on the joint density of \mathbf{Y} given in (2) and the observed data \mathbf{y}_t , $t = 1, \dots, T$, the corresponding full log-likelihood is given by

$$\ell(\boldsymbol{\theta}; \mathbf{y}) = \sum_{t=1}^T \ell_{C,t}(\boldsymbol{\theta}_{\text{cop}}; F_{Y_{1,t}}(y_{1,t}; \boldsymbol{\theta}_1), \dots, F_{Y_{D,t}}(y_{D,t}; \boldsymbol{\theta}_D)) + \sum_{d=1}^D \sum_{t=1}^T \ell_{d,t}(\boldsymbol{\theta}_d; y_{d,t}), \quad (12)$$

where $\ell_{C,t}(\boldsymbol{\theta}_{\text{cop}}; F_{Y_{1,t}}(y_{1,t}; \boldsymbol{\theta}_1), \dots, F_{Y_{D,t}}(y_{D,t}; \boldsymbol{\theta}_D)) = \log c(F_{Y_{1,t}}(y_{1,t}; \boldsymbol{\theta}_1), \dots, F_{Y_{D,t}}(y_{D,t}; \boldsymbol{\theta}_D); \boldsymbol{\theta}_{\text{cop}})$ and $\ell_{d,t}(\boldsymbol{\theta}_d; y_{d,t}) = \log p_{Y_{d,t}}(y_{d,t}; \boldsymbol{\theta}_d)$, for $d = 1, \dots, D$. The full maximum likelihood (ML) estimator $\hat{\boldsymbol{\theta}}_{\text{ML}}$ is then defined by

$$\hat{\boldsymbol{\theta}}_{\text{ML}} = \arg \max_{\boldsymbol{\theta} \in \Theta} \ell(\boldsymbol{\theta}; \mathbf{y}),$$

where Θ is some suitable parameter space. This optimisation is typically performed using numerical optimisation methods and can be computationally prohibitive, particularly in high-dimensional settings, which motivates the need for IFM. Consider the D log-likelihood functions for the univariate marginal distributions:

$$\ell_d(\boldsymbol{\theta}_d; y_{d,t}) = \sum_{t=1}^T \ell_{d,t}(\boldsymbol{\theta}_d; y_{d,t}) = \sum_{t=1}^T \log p_{Y_{d,t}}(y_{d,t}; \boldsymbol{\theta}_d), \quad d = 1, \dots, D,$$

and the log-likelihood function for the copula:

$$\ell_C(\boldsymbol{\theta}_{\text{cop}}; F_{Y_{1,1}}(y_{1,1}; \boldsymbol{\theta}_1), \dots, F_{Y_{D,T}}(y_{D,T}; \boldsymbol{\theta}_D)) = \sum_{t=1}^T \log c(F_{Y_{1,t}}(y_{1,t}; \boldsymbol{\theta}_1), \dots, F_{Y_{D,t}}(y_{D,t}; \boldsymbol{\theta}_D); \boldsymbol{\theta}_{\text{cop}}).$$

IFM proceeds as follows:

- (a) Maximise the univariate log-likelihoods ℓ_d , for $d = 1, \dots, D$, separately, to obtain the ML estimates $\hat{\boldsymbol{\theta}}_1, \dots, \hat{\boldsymbol{\theta}}_D$.
- (b) Maximise the log-likelihood function ℓ_C with respect to the copula parameter vector $\boldsymbol{\theta}_{\text{cop}}$ to obtain the ML estimate $\hat{\boldsymbol{\theta}}_{\text{cop}}$ given the marginal parameter estimates $\hat{\boldsymbol{\theta}}_1, \dots, \hat{\boldsymbol{\theta}}_D$ and the copula “data” $\mathbf{u} \equiv (\mathbf{u}_1^\top, \dots, \mathbf{u}_T^\top)^\top$, where $\mathbf{u}_t \equiv (u_{1,t}, \dots, u_{D,t})^\top$, and where $u_{d,t} = F_{Y_{d,t}}(y_{d,t}; \hat{\boldsymbol{\theta}}_d)$.

The two-step estimation procedure is computationally simpler than jointly estimating all parameters $\boldsymbol{\theta}$ by directly maximising the full log-likelihood in (12). By decoupling the estimation of marginal and dependence parameters, IFM reduces computational complexity while still providing consistent estimators under standard regularity conditions (Joe and Xu, 1996). In a Bayesian version of the IFM one equips $\boldsymbol{\theta}_1, \dots, \boldsymbol{\theta}_D$ with a prior distribution, and then uses a Bayesian functional of the posterior distribution (e.g., the posterior mean) of $\boldsymbol{\theta}_1, \dots, \boldsymbol{\theta}_D$ as plug-in for finding the posterior distribution of $\boldsymbol{\theta}_{\text{cop}}$.

3.2 Neural inference functions for margins

For ease of exposition, from here on we omit variable subscripts and write conditional and marginal densities simply as $p(\cdot | \cdot)$; for example, $p(\mathbf{y})$ denotes the density of \mathbf{Y} .

In this section we propose a two-stage approach, which we call N-IFM, to obtain an approximation to the posterior distribution of marginal and copula parameters motivated by the classical IFM discussed in Section 3.1. The approach leverages the representation capacity of neural networks to efficiently compute high quality approximations of posterior distributions from data (Zammit-Mangion et al., 2025).

We begin by expressing the full Bayesian posterior distribution of all model parameters using an IFM representation, which factorises the parameters into marginal-model and copula components:

$$p(\boldsymbol{\theta}_1, \dots, \boldsymbol{\theta}_D, \boldsymbol{\theta}_{\text{cop}} \mid \mathbf{y}) \approx p(\boldsymbol{\theta}_{\text{cop}} \mid \mathbf{y}, \hat{\boldsymbol{\theta}}_1, \dots, \hat{\boldsymbol{\theta}}_D) \prod_{d=1}^D p(\boldsymbol{\theta}_d \mid \mathbf{y}_{(d)}), \quad (13)$$

where $\mathbf{y}_{(d)} \equiv (y_{d,1}, \dots, y_{d,T})^\top$ is the d -th time series data, and $\hat{\boldsymbol{\theta}}_1, \dots, \hat{\boldsymbol{\theta}}_D$ are plug-in estimates for the marginal parameters. This factorisation separates inference for the marginal parameters from inference for the dependence structure.

To enable scalable computation, we approximate the posterior distribution in (13) using a posterior approximation that mirrors the same factorisation:

$$q(\boldsymbol{\theta}_1, \dots, \boldsymbol{\theta}_D, \boldsymbol{\theta}_{\text{cop}}; \boldsymbol{\lambda}) = q_{\text{cop}}(\boldsymbol{\theta}_{\text{cop}}; \boldsymbol{\lambda}_{\text{cop}}) \prod_{d=1}^D q_d(\boldsymbol{\theta}_d; \boldsymbol{\lambda}_d), \quad (14)$$

where $\boldsymbol{\lambda} = (\boldsymbol{\lambda}_1^\top, \dots, \boldsymbol{\lambda}_D^\top, \boldsymbol{\lambda}_{\text{cop}}^\top)^\top$ denotes the vector of parameters of the approximate posterior distributions, $\boldsymbol{\lambda}_d$ are the parameters associated with the approximate posterior distribution $q_d(\boldsymbol{\theta}_d; \boldsymbol{\lambda}_d)$ of the parameters $\boldsymbol{\theta}_d$ in the d -th marginal model for $d = 1, \dots, D$, and $\boldsymbol{\lambda}_{\text{cop}}$ are the parameters governing the approximation $q_{\text{cop}}(\boldsymbol{\theta}_{\text{cop}}; \boldsymbol{\lambda}_{\text{cop}})$ of the copula parameters $\boldsymbol{\theta}_{\text{cop}}$.

N-IFM is carried out in two stages. In the first stage, we train a set of neural networks to approximate the posterior distributions of the marginal model parameters $\boldsymbol{\theta}_d$ for $d = 1, \dots, D$. In the second stage, we train a separate neural network to approximate the posterior distribution of the copula parameters $\boldsymbol{\theta}_{\text{cop}}$, using the copula “data” \mathbf{u} as the inputs, using estimates of the marginal model parameters estimated from the first stage. Sections 3.2.1 and 3.2.2 discuss the neural approximation for the posterior distributions of marginal and copula parameters, respectively. Section 3.2.3 gives the N-IFM algorithm.

3.2.1 Neural approximation for marginal models

This section discusses the neural approximation for the posterior distribution of the marginal model parameters. Consider the prior density $p(\boldsymbol{\theta}_d)$, and the likelihood for the d -th marginal model $p(\mathbf{y}_{(d)} \mid \boldsymbol{\theta}_d)$ where $\mathbf{Y}_{(d)} \equiv (Y_{d,1}, \dots, Y_{d,T})^\top$. Write the posterior density of the d -th marginal model as $p(\boldsymbol{\theta}_d \mid \mathbf{y}_{(d)})$, for $d = 1, \dots, D$. For a given $\mathbf{y}_{(d)}$, $\boldsymbol{\lambda}_d$ can be optimised by minimising the (forward) Kullback-Leibler divergence between $p(\boldsymbol{\theta}_d \mid \mathbf{y}_{(d)})$ and $q_d(\boldsymbol{\theta}_d; \boldsymbol{\lambda}_d)$, for $d = 1, \dots, D$, as follows:

$$\boldsymbol{\lambda}_d^* = \arg \min_{\boldsymbol{\lambda}_d} \text{KL} \{p(\boldsymbol{\theta}_d \mid \mathbf{y}_{(d)}) \parallel q_d(\boldsymbol{\theta}_d; \boldsymbol{\lambda}_d)\}, \quad (15)$$

for $d = 1, \dots, D$. The optimisation problem in (15) is typically computationally expensive to solve for a single dataset $\mathbf{y}_{(d)}$. When this inference procedure must be repeated for many different datasets (e.g., in validation and real-time forecasting), the computational burden becomes prohibitive. As a result, such approaches are often impractical in applications that demand fast, repeated inference.

In neural amortised inference, we construct neural network models that map the observed data to the parameters defining the approximate posterior distribution of the model parameters. We replace $q_d(\boldsymbol{\theta}_d; \boldsymbol{\lambda}_d)$ with $q_d(\boldsymbol{\theta}_d; \boldsymbol{\lambda}_d(\mathbf{y}_{(d)}; \boldsymbol{\gamma}_d))$, where $\boldsymbol{\gamma}_d$ are the neural network parameters. The problem of estimating the posterior distribution $p(\boldsymbol{\theta}_d \mid \mathbf{y}_{(d)})$ can be written as an optimisation problem of finding the optimal neural-network parameters, $\boldsymbol{\gamma}_d^*$, using the expected forward Kullback-Leibler divergence, as follows (Zammit-Mangion et al., 2025):

$$\boldsymbol{\gamma}_d^* = \arg \min_{\boldsymbol{\gamma}_d} \mathbb{E}_{\mathcal{Y}_{(d)}} [\text{KL} (p(\boldsymbol{\theta}_d \mid \mathbf{y}_{(d)}) \parallel q_d(\boldsymbol{\theta}_d; \boldsymbol{\lambda}_d(\mathbf{y}_{(d)}; \boldsymbol{\gamma}_d)))] \quad (16)$$

$$= \arg \min_{\boldsymbol{\gamma}_d} \int_{\Theta} \int_{\mathcal{Y}_{(d)}} [-\log q_d(\boldsymbol{\theta}_d; \boldsymbol{\lambda}_d(\mathbf{y}_{(d)}; \boldsymbol{\gamma}_d))] p_{Y_d}(\mathbf{y}_{(d)} \mid \boldsymbol{\theta}_d) p(\boldsymbol{\theta}_d) d\mathbf{y}_{(d)} d\boldsymbol{\theta}_d, \quad (17)$$

where $\mathcal{Y}_{(d)}$ is the sample space of $\mathbf{y}_{(d)}$. We approximate (17) with a Monte Carlo approximation using N sets of simulated parameters and corresponding datasets from our prior

distribution and marginal models: $\left\{ \left\{ \boldsymbol{\theta}_d^{(n)}, \mathbf{y}_{(d)}^{(n)} \right\} : n = 1, \dots, N \right\}$. The optimisation problem is therefore approximated as

$$\boldsymbol{\gamma}_d^* \approx \arg \min_{\boldsymbol{\gamma}_d} \frac{1}{N} \sum_{n=1}^N -\log q_d \left(\boldsymbol{\theta}_d^{(n)}; \boldsymbol{\lambda}_d(\mathbf{y}_{(d)}^{(n)}; \boldsymbol{\gamma}_d) \right), \quad (18)$$

where $\boldsymbol{\theta}_d^{(n)} \sim p(\boldsymbol{\theta}_d)$ and $\mathbf{y}_{(d)}^{(n)} \sim p(\mathbf{y}_{(d)} \mid \boldsymbol{\theta}_d^{(n)})$ for $d = 1, \dots, D$.

As posterior approximation for the (possibly transformed) marginal parameters, we use a Gaussian distribution of the form

$$q_d \left(\boldsymbol{\theta}_d; \boldsymbol{\lambda}_d(\mathbf{y}_{(d)}; \boldsymbol{\gamma}_d) \right) = \mathcal{N} \left(\boldsymbol{\mu}_d \left(\mathbf{y}_{(d)}; \boldsymbol{\gamma}_d \right), \boldsymbol{\Sigma}_d \left(\mathbf{y}_{(d)}; \boldsymbol{\gamma}_d \right) \right), \quad (19)$$

where $\boldsymbol{\mu}_d \left(\mathbf{y}_{(d)}; \boldsymbol{\gamma}_d \right)$ is an $m_d \times 1$ mean vector and $\boldsymbol{\Sigma}_d \left(\mathbf{y}_{(d)}; \boldsymbol{\gamma}_d \right)$ is an $m_d \times m_d$ covariance matrix of the approximate posterior, where m_d is the number of parameters in the d -th marginal model. We reparameterise the covariance matrix

$$\boldsymbol{\Sigma}_d \left(\mathbf{y}_{(d)}; \boldsymbol{\gamma}_d \right) = \mathbf{L}_d \left(\mathbf{y}_{(d)}; \boldsymbol{\gamma}_d \right) \mathbf{L}_d \left(\mathbf{y}_{(d)}; \boldsymbol{\gamma}_d \right)^\top, \quad (20)$$

where $\mathbf{L}_d \left(\mathbf{y}_{(d)}; \boldsymbol{\gamma}_d \right)$ is an $m_d \times m_d$ lower triangular Cholesky factor with positive diagonal elements. Once the neural network has been trained, given a new dataset, the trained neural network outputs the mean and covariance matrix of the approximate posterior distribution for the parameters of the d -th marginal model. In this case, $\boldsymbol{\lambda}_d(\cdot; \boldsymbol{\gamma}_d) = \left(\boldsymbol{\mu}_d(\cdot; \boldsymbol{\gamma}_d)^\top, \text{vech}(\mathbf{L}_d(\cdot; \boldsymbol{\gamma}_d))^\top \right)^\top$.

In our applications, all marginal models are a GARCH(1,1) model (described in Section 2.5), so it is sufficient to train a single neural network $\boldsymbol{\lambda}_{\text{mar}}(\cdot; \boldsymbol{\gamma}_{\text{mar}}) = \left(\boldsymbol{\mu}_{\text{mar}}(\cdot; \boldsymbol{\gamma}_{\text{mar}})^\top, \text{vech}(\mathbf{L}_{\text{mar}}(\cdot; \boldsymbol{\gamma}_{\text{mar}}))^\top \right)^\top$, for all marginal time series, where $\boldsymbol{\gamma}_{\text{mar}}$ are the neural network parameters. We let $\boldsymbol{\theta}_d \equiv (\varphi_{1,d}, \varphi_{2,d}, \varphi_{3,d})^\top$ denote the vector of transformed GARCH(1,1) parameters (see Section S2 of the online supplement) and $\mathbf{y}_{(d)}$ denote the training observations generated from the corresponding GARCH(1,1) model,

Algorithm 1 Marginal Posterior Approximation

Require: Prior density $p(\boldsymbol{\theta}_{\text{mar}}) \equiv p(\boldsymbol{\theta}_1) = \dots = p(\boldsymbol{\theta}_D)$, likelihood $p(\mathbf{y}_{\text{mar}} | \boldsymbol{\theta}_{\text{mar}}) \equiv p(\mathbf{y}_{(1)} | \boldsymbol{\theta}_1) = \dots = p(\mathbf{y}_{(D)} | \boldsymbol{\theta}_D)$.

1: Draw N Monte Carlo samples $\{(\boldsymbol{\theta}_{\text{mar}}^{(n)}, \mathbf{y}_{\text{mar}}^{(n)})\}_{n=1}^N$ with

$$\boldsymbol{\theta}_{\text{mar}}^{(n)} \sim p(\boldsymbol{\theta}_{\text{mar}}), \quad \mathbf{y}_{\text{mar}}^{(n)} \sim p(\mathbf{y}_{\text{mar}} | \boldsymbol{\theta}_{\text{mar}}^{(n)}).$$

2: Optimise $\boldsymbol{\gamma}_{\text{mar}}$ through

$$\boldsymbol{\gamma}_{\text{mar}}^* = \arg \min_{\boldsymbol{\gamma}_{\text{mar}}} \frac{1}{N} \sum_{n=1}^N -\log q_{\text{mar}}(\boldsymbol{\theta}_{\text{mar}}^{(n)}; \boldsymbol{\lambda}_{\text{mar}}(\mathbf{y}_{\text{mar}}^{(n)}; \boldsymbol{\gamma}_{\text{mar}})),$$

where

$$q_{\text{mar}}(\boldsymbol{\theta}_{\text{mar}}; \boldsymbol{\lambda}_{\text{mar}}(\mathbf{y}_{\text{mar}}^{(n)}; \boldsymbol{\gamma}_{\text{mar}})) = \mathcal{N}(\boldsymbol{\mu}_{\text{mar}}(\mathbf{y}_{\text{mar}}^{(n)}; \boldsymbol{\gamma}_{\text{mar}}), \boldsymbol{\Sigma}_{\text{mar}}(\mathbf{y}_{\text{mar}}^{(n)}; \boldsymbol{\gamma}_{\text{mar}})),$$

with covariance matrix

$$\boldsymbol{\Sigma}_{\text{mar}}(\mathbf{y}_{\text{mar}}^{(n)}; \boldsymbol{\gamma}_{\text{mar}}) = \mathbf{L}_{\text{mar}}(\mathbf{y}_{\text{mar}}^{(n)}; \boldsymbol{\gamma}_{\text{mar}}) \mathbf{L}_{\text{mar}}(\mathbf{y}_{\text{mar}}^{(n)}; \boldsymbol{\gamma}_{\text{mar}})^\top.$$

3: **Output:** Trained neural network with parameters $\boldsymbol{\gamma}_{\text{mar}}^*$ to map the observations from each marginal series $\mathbf{y}_{(d)}$ to the mean $\boldsymbol{\mu}_{\text{mar}}(\mathbf{y}_{(d)}; \boldsymbol{\gamma}_{\text{mar}}^*)$ and covariance matrix $\boldsymbol{\Sigma}_{\text{mar}}(\mathbf{y}_{(d)}; \boldsymbol{\gamma}_{\text{mar}}^*)$ to obtain the approximate posterior distribution $q_d(\boldsymbol{\theta}_d; \boldsymbol{\lambda}_d(\mathbf{y}_{(d)}; \boldsymbol{\gamma}_{\text{mar}}^*))$, for $d = 1, \dots, D$.

for $d = 1, \dots, D$.

Algorithm 1 gives the steps needed to find optimal neural network parameters $\boldsymbol{\gamma}_{\text{mar}}^*$, which map the observations from each marginal time series $\mathbf{y}_{(d)}$ to the mean $\boldsymbol{\mu}_{\text{mar}}(\mathbf{y}_{(d)}; \boldsymbol{\gamma}_{\text{mar}}^*)$ and Cholesky factor $\mathbf{L}_{\text{mar}}(\mathbf{y}_{(d)}; \boldsymbol{\gamma}_{\text{mar}}^*)$ to obtain the approximate posterior distribution $q_d(\boldsymbol{\theta}_d; \boldsymbol{\lambda}_{\text{mar}}(\mathbf{y}_{(d)}; \boldsymbol{\gamma}_{\text{mar}}^*))$, for $d = 1, \dots, D$. The details of the algorithm to generate observations from the GARCH(1,1) model, and the convolutional neural network model used to map between observations $\mathbf{y}_{(d)}$ and $\boldsymbol{\lambda}_d \equiv \boldsymbol{\lambda}_{\text{mar}}(\mathbf{y}_{(d)}; \boldsymbol{\gamma}_{\text{mar}}^*)$ are given in Sections S2 and S3 of the online supplement, respectively.

Figure 1 summarises the inference framework for the marginal models. The observed marginal data $\mathbf{y}_{(d)}$ are first passed through a neural network, which outputs $\boldsymbol{\lambda}_d(\mathbf{y}_{(d)}; \boldsymbol{\gamma}_{\text{mar}}^*)$, the parameters of the approximate posterior distribution for the marginal model parameters.

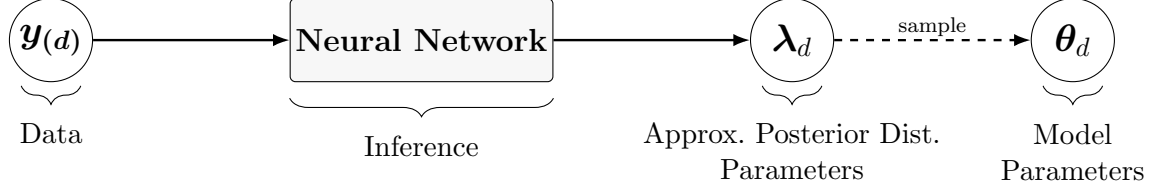


Figure 1: Inference framework for the marginal models in N-IFM.

Conditional on $\lambda_d(\mathbf{y}(d); \gamma_{\text{mar}}^*)$, samples of the marginal parameters θ_d are then drawn from this approximate posterior distribution.

3.2.2 Neural approximation for copula models

This section discusses the neural approximation for the posterior distribution of the copula parameters. Let θ_{cop} be the vector of copula parameters of dimension m_{cop} , and consider the prior density $p(\theta_{\text{cop}})$ and the joint copula density $c(\mathbf{u}; \theta_{\text{cop}})$. For the Gaussian copula, $\theta_{\text{cop}} \equiv (\text{vech}(\tilde{\mathbf{G}}))$, while for the t copula, $\theta_{\text{cop}} \equiv (\text{vech}(\tilde{\mathbf{G}})^\top, \nu)^\top$. The posterior density is $p(\theta_{\text{cop}} \mid \mathbf{u})$. We aim to construct a flexible neural network architecture to map the copula “data” \mathbf{u} to the parameters of the approximate posterior distribution of the copula parameters $q_{\text{cop}}(\theta_{\text{cop}}; \lambda_{\text{cop}}(\mathbf{u}; \gamma_{\text{cop}}))$, where γ_{cop} are the neural network parameters. Similar to the marginal model in Section 3.2.1, the problem of estimating the posterior distribution can be written as an optimisation problem of finding the optimal neural-network parameters, γ_{cop}^* , using the expected forward Kullback-Leibler divergence, as follows:

$$\gamma_{\text{cop}}^* = \arg \min_{\gamma_{\text{cop}}} \mathbb{E}_U [\text{KL} (p(\theta_{\text{cop}} \mid \mathbf{u}) \parallel q_{\text{cop}}(\theta_{\text{cop}}; \lambda_{\text{cop}}(\mathbf{u}; \gamma_{\text{cop}})))] \quad (21)$$

$$= \arg \min_{\gamma_{\text{cop}}} \int_{\Theta} \int_{[0,1]^D} [-\log q_{\text{cop}}(\theta_{\text{cop}}; \lambda_{\text{cop}}(\mathbf{u}; \gamma_{\text{cop}}))] c(\mathbf{u} \mid \theta_{\text{cop}}) p(\theta_{\text{cop}}) d\mathbf{u} d\theta_{\text{cop}}. \quad (22)$$

We approximate (22) with a Monte Carlo approximation using N sets of simulated parameters and corresponding “data” simulated with standard uniform margins,

$\left\{ \left\{ \boldsymbol{\theta}_{\text{cop}}^{(n)}, \mathbf{u}^{(n)} \right\} : n = 1, \dots, N \right\}$. The optimisation problem then becomes

$$\boldsymbol{\gamma}_{\text{cop}}^* = \arg \min_{\boldsymbol{\gamma}_{\text{cop}}} \frac{1}{N} \sum_{n=1}^N -\log q_{\text{cop}} \left(\boldsymbol{\theta}_{\text{cop}}^{(n)}; \boldsymbol{\lambda}_{\text{cop}}(\mathbf{u}^{(n)}; \boldsymbol{\gamma}_{\text{cop}}) \right), \quad (23)$$

where $\boldsymbol{\theta}_{\text{cop}}^{(n)} \sim p(\boldsymbol{\theta}_{\text{cop}})$ and $\mathbf{u}^{(n)} \sim c(\mathbf{u} \mid \boldsymbol{\theta}_{\text{cop}}^{(n)})$. The algorithm to generate copula “data” for the Gaussian and t copulas is given in Algorithm 5 in Section S2 of the online supplement.

We now discuss the posterior approximation for the copula parameters. We adopt a mean-field Gaussian approximation of the form

$$q_{\text{cop}}(\boldsymbol{\theta}_{\text{cop}}; \boldsymbol{\lambda}_{\text{cop}}(\mathbf{u}; \boldsymbol{\gamma}_{\text{cop}})) = \prod_{\ell=1}^{m_{\text{cop}}} \mathcal{N} \left(\boldsymbol{\theta}_{\text{cop},\ell} \mid \mu_{\text{cop},\ell}(\mathbf{u}; \boldsymbol{\gamma}_{\text{cop}}), \sigma_{\text{cop},\ell}^2(\mathbf{u}; \boldsymbol{\gamma}_{\text{cop}}) \right), \quad (24)$$

where $\boldsymbol{\lambda}_{\text{cop}}(\cdot; \boldsymbol{\gamma}_{\text{cop}}) \equiv \left(\mu_{\text{cop},1}(\cdot; \boldsymbol{\gamma}_{\text{cop}}), \dots, \mu_{\text{cop},m_{\text{cop}}}(\cdot; \boldsymbol{\gamma}_{\text{cop}}), \sigma_{\text{cop},1}^2(\cdot; \boldsymbol{\gamma}_{\text{cop}}), \dots, \sigma_{\text{cop},m_{\text{cop}}}^2(\cdot; \boldsymbol{\gamma}_{\text{cop}}) \right)$, $\mathbf{u} \equiv (\mathbf{u}_1^\top, \dots, \mathbf{u}_T^\top)^\top$ are the copula “data”, m_{cop} is the number of copula parameters, and $\boldsymbol{\gamma}_{\text{cop}}$ parameterises the neural network that outputs the marginal means and variances of the univariate Gaussian approximation for each copula parameter. The mean-field assumption enforces posterior independence among the copula parameters. Algorithm 2 gives the steps needed to find optimal neural network parameters $\boldsymbol{\gamma}_{\text{cop}}^*$, which map the copula “data”, \mathbf{u} , to the mean $\mu_{\text{cop},\ell}(\mathbf{u}; \boldsymbol{\gamma}_{\text{cop}}^*)$ and variances $\sigma_{\text{cop},\ell}^2(\mathbf{u}; \boldsymbol{\gamma}_{\text{cop}}^*)$ for $\ell = 1, \dots, m_{\text{cop}}$, to obtain the approximate posterior distribution $q_{\text{cop}}(\boldsymbol{\theta}_{\text{cop}}; \boldsymbol{\lambda}_{\text{cop}}(\mathbf{u}; \boldsymbol{\gamma}_{\text{cop}}^*))$.

Since $\mathbf{u}_1, \dots, \mathbf{u}_T$ are mutually independent, we employ the Deep Sets neural network architecture of Zaheer et al. (2017) to learn a flexible mapping from sets of copula “data” to copula parameters; see Section S4 of the online supplement and also Sainsbury-Dale et al. (2024) for further details.

Figure 2 illustrates the neural inference framework for the copula model. The copula “data” \mathbf{u} are first fed into a neural network. This network outputs $\boldsymbol{\lambda}_{\text{cop}}(\mathbf{u}; \boldsymbol{\gamma}_{\text{cop}}^*)$, the parameters of the approximate posterior distribution for the copula parameters. Conditional on $\boldsymbol{\lambda}_{\text{cop}}(\mathbf{u}; \boldsymbol{\gamma}_{\text{cop}}^*)$, we then draw samples of the copula parameters $\boldsymbol{\theta}_{\text{cop}}$ from this approximate

Algorithm 2 Copula Posterior Approximation

Require: Prior density $p(\boldsymbol{\theta}_{\text{cop}})$, likelihood $c(\mathbf{u} \mid \boldsymbol{\theta}_{\text{cop}})$.

- 1: Draw N Monte Carlo samples

$$\{(\boldsymbol{\theta}_{\text{cop}}^{(n)}, \mathbf{u}^{(n)})\}_{n=1}^N$$

with

$$\boldsymbol{\theta}_{\text{cop}}^{(n)} \sim p(\boldsymbol{\theta}_{\text{cop}}), \quad \mathbf{u}^{(n)} \sim c(\mathbf{u} \mid \boldsymbol{\theta}_{\text{cop}}^{(n)}) \quad (\text{see lines 1–12 of Algorithm 5 of the online supplement}).$$

- 2: Optimise neural network parameters $\boldsymbol{\gamma}_{\text{cop}}$ through

$$\boldsymbol{\gamma}_{\text{cop}}^* = \arg \min_{\boldsymbol{\gamma}_{\text{cop}}} \frac{1}{N} \sum_{n=1}^N -\log q_{\text{cop}}(\boldsymbol{\theta}_{\text{cop}}^{(n)}; \boldsymbol{\lambda}_{\text{cop}}(\mathbf{u}^{(n)}; \boldsymbol{\gamma}_{\text{cop}})).$$

- 3: **Output:** Trained neural network, with parameters $\boldsymbol{\gamma}_{\text{cop}}^*$, to map copula “data” \mathbf{u} to approximate posterior means $\mu_{\text{cop},\ell}(\mathbf{u}; \boldsymbol{\gamma}_{\text{cop}}^*)$ and variances $\sigma_{\text{cop},\ell}^2(\mathbf{u}; \boldsymbol{\gamma}_{\text{cop}}^*)$ for $\ell = 1, \dots, m_{\text{cop}}$.
-

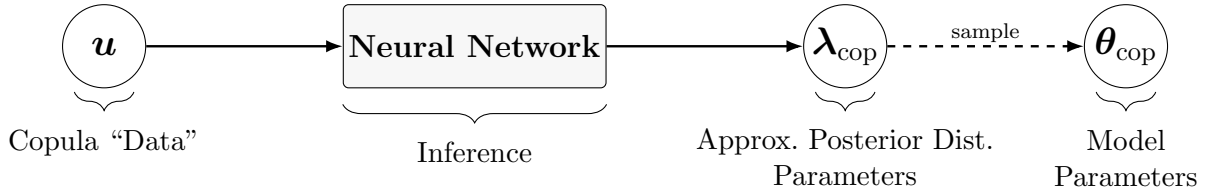


Figure 2: Inference framework for the copula model in N-IFM.

posterior distribution.

3.2.3 Neural inference functions for margins (N-IFM) algorithm

Given the trained neural network parameters $\boldsymbol{\gamma}_{\text{mar}}^*$ for the marginal models and the observed data $\mathbf{y}_{(d)}$ as input, the “marginal” neural-network outputs the parameters of the approximate posterior distribution of the marginal model parameters, denoted by $\boldsymbol{\lambda}_{\text{mar}}(\mathbf{y}_{(d)}; \boldsymbol{\gamma}_{\text{mar}}^*)$, for $d = 1, \dots, D$. From each approximate posterior $q_d(\boldsymbol{\theta}_d; \boldsymbol{\lambda}_{\text{mar}}(\mathbf{y}_{(d)}; \boldsymbol{\gamma}_{\text{mar}}^*))$, we then draw $J = 1000$ samples and compute the posterior mean estimates $\hat{\boldsymbol{\theta}}_d$ for each marginal model. Using these posterior mean estimates, we then construct the copula “data” \mathbf{u} , which serve as the input to the neural network for the copula model. Finally, given the trained copula-network parameters $\boldsymbol{\gamma}_{\text{cop}}^*$ and the copula “data” as input, the network outputs the parameters of the

Algorithm 3 Neural Inference Functions for Margins

Require: Trained marginal neural network parameters $\boldsymbol{\gamma}_{\text{mar}}^*$, trained copula neural network parameters $\boldsymbol{\gamma}_{\text{cop}}^*$, data $\{\mathbf{y}_{(d)}\}_{d=1}^D$.

- 1: **for** $d = 1$ to D **do**
- 2: Compute marginal posterior parameters: $\boldsymbol{\lambda}_{\text{mar}}(\mathbf{y}_{(d)}; \boldsymbol{\gamma}_{\text{mar}}^*)$.
- 3: Compute posterior means of marginal parameters:

$$\widehat{\boldsymbol{\theta}}_d = \mathbb{E}_{q_d(\boldsymbol{\theta}_d; \boldsymbol{\lambda}_{\text{mar}}(\mathbf{y}_{(d)}; \boldsymbol{\gamma}_{\text{mar}}^*))}[\boldsymbol{\theta}_d], \quad \text{for } d = 1, \dots, D.$$

- 4: Compute copula “data” \mathbf{u} through:

$$u_{d,t} = F_{Y_{d,t}}(\mathbf{y}_{d,t}; \widehat{\boldsymbol{\theta}}_d), \quad \text{for } d = 1, \dots, D \text{ and } t = 1, \dots, T.$$

- 5: **end for**

- 6: Compute copula posterior parameters: $\boldsymbol{\lambda}_{\text{cop}}(\mathbf{u}; \boldsymbol{\gamma}_{\text{cop}}^*)$.
 - 7: Output: $\{\boldsymbol{\lambda}_{\text{mar}}(\mathbf{y}_{(d)}; \boldsymbol{\gamma}_{\text{mar}}^*)\}_{d=1}^D$ and $\boldsymbol{\lambda}_{\text{cop}}(\mathbf{u}; \boldsymbol{\gamma}_{\text{cop}}^*)$.
-

approximate posterior distributions of the copula parameters, $\boldsymbol{\lambda}_{\text{cop}}(\mathbf{u}; \boldsymbol{\gamma}_{\text{cop}}^*)$ to obtain the approximate posterior $q_{\text{cop}}(\boldsymbol{\theta}_{\text{cop}}; \boldsymbol{\lambda}_{\text{cop}}(\mathbf{u}; \boldsymbol{\gamma}_{\text{cop}}^*))$.

We write the full approximate posterior distribution based on N-IFM as:

$$q(\boldsymbol{\theta}; \boldsymbol{\lambda}(\mathbf{y}; \boldsymbol{\gamma}^*)) = q_{\text{cop}}(\boldsymbol{\theta}_{\text{cop}}; \boldsymbol{\lambda}_{\text{cop}}(\mathbf{u}; \boldsymbol{\gamma}_{\text{cop}}^*)) \prod_{d=1}^D q_d(\boldsymbol{\theta}_d; \boldsymbol{\lambda}_{\text{mar}}(\mathbf{y}_{(d)}; \boldsymbol{\gamma}_{\text{mar}}^*)), \quad (25)$$

where $\boldsymbol{\gamma}^* \equiv (\boldsymbol{\gamma}_{\text{mar}}^{*\top}, \boldsymbol{\gamma}_{\text{cop}}^{*\top})^\top$ is the trained neural network parameters and the copula “data” $\mathbf{u} \equiv (\mathbf{u}_1^\top, \dots, \mathbf{u}_T^\top)^\top$ where $\mathbf{u}_t \equiv (u_{1,t}, \dots, u_{D,t})^\top$, and $u_{d,t} = F_{Y_{d,t}}(y_{d,t}; \widehat{\boldsymbol{\theta}}_d)$. Algorithm 3 describes the proposed neural inference functions for margins.

4 Measure of predictive performance

This section outlines the performance criteria used to evaluate and compare the predictive accuracy of the competing models. Section 4.1 discusses the approximate predictive density. Section 4.2 discusses the time-series validation.

4.1 Approximate predictive density

Let \mathbf{Y}_{T+h} denote the unobserved value of the variable \mathbf{Y} at time $T+h$, where $h > 0$. The h -step-ahead predictive density of $\mathbf{Y}_{T+h} = \mathbf{y}_{T+h}$ is

$$p(\mathbf{y}_{T+h} | \mathbf{y}) = \int_{\mathcal{Y}_{T+h}} p(\mathbf{y}_{T+h} | \boldsymbol{\theta}) p(\boldsymbol{\theta} | \mathbf{y}) d\boldsymbol{\theta}, \quad (26)$$

where \mathcal{Y}_{T+h} is the sample space of \mathbf{y}_{T+h} and $p(\boldsymbol{\theta} | \mathbf{y})$ denotes the posterior distribution given the data up to time T . A consistent Monte Carlo estimate of (26) is

$$\widehat{p}(\mathbf{y}_{T+h} | \mathbf{y}) = \frac{1}{J} \sum_{j=1}^J p(\mathbf{y}_{T+h} | \boldsymbol{\theta}^{(j)}), \quad \boldsymbol{\theta}^{(j)} \sim p(\boldsymbol{\theta} | \mathbf{y}). \quad (27)$$

When evaluated at the observed value $\mathbf{y}_{T+h} = \mathbf{y}_{T+h}^{\text{obs}}$, (27) yields the h -step-ahead predictive density $\widehat{p}(\mathbf{y}_{T+h}^{\text{obs}} | \mathbf{y})$. One may also simulate $\mathbf{y}_{T+h}^{(j)} \sim p(\cdot | \boldsymbol{\theta}^{(j)})$, for $j = 1, \dots, J$ and form a kernel density estimate of $p(\mathbf{y}_{T+h} | \mathbf{y})$.

For high-dimensional time-series copula models, obtaining the exact posterior $p(\boldsymbol{\theta} | \mathbf{y})$ can be computationally expensive. By applying (25), we obtain the corresponding approximate h -step-ahead predictive density

$$g(\mathbf{y}_{T+h} | \mathbf{y}) = \int_{\mathcal{Y}_{T+h}} p(\mathbf{y}_{T+h} | \boldsymbol{\theta}) q(\boldsymbol{\theta}; \boldsymbol{\lambda}(\mathbf{y}; \boldsymbol{\gamma}^*)) d\boldsymbol{\theta}. \quad (28)$$

We approximate (28) by

$$\widehat{g}(\mathbf{y}_{T+h} | \mathbf{y}) = \frac{1}{J} \sum_{j=1}^J p(\mathbf{y}_{T+h} | \boldsymbol{\theta}^{(j)}), \quad \boldsymbol{\theta}^{(j)} \sim q(\boldsymbol{\theta}; \boldsymbol{\lambda}(\mathbf{y}; \boldsymbol{\gamma}^*)). \quad (29)$$

Evaluating (29) at the observed value $\mathbf{y}_{T+h} = \mathbf{y}_{T+h}^{\text{obs}}$ yields the approximate predictive density $\widehat{g}(\mathbf{y}_{T+h}^{\text{obs}} | \mathbf{y})$. Simulations of $\mathbf{y}_{T+h}^{(j)} \sim p(\cdot | \boldsymbol{\theta}^{(j)})$, for $j = 1, \dots, J$, can also be used to construct a kernel density estimate of $g(\mathbf{y}_{T+h} | \mathbf{y})$.

4.2 Time series validation

We assess out-of-sample performance using time-series validation with a fixed-width rolling window of length T . Assume that we have a time series of length $T+K$. For $i = 0, \dots, K-h$, we fit the model on data starting from \mathbf{y}_{1+i} to \mathbf{y}_{T+i} , and produce an h -step-ahead forecast for \mathbf{y}_{T+h+i} . For each $i = 0, \dots, K-h$, given J posterior draws from the approximate posterior $\{\boldsymbol{\theta}^{(i,j)}\}_{j=1}^J$, we compute the corresponding h -step-ahead predictive density $p(\mathbf{y}_{T+h+i}^{\text{obs}} \mid \boldsymbol{\theta}^{(i,j)})$. The h -step-ahead log-predictive density score (LPDS) is the sum of the log of the h -step posterior predictive density score over the $K-h+1$ rolls:

$$\text{LPDS} = \sum_{i=0}^{K-h} \log \left\{ \frac{1}{J} \sum_{j=1}^J p(\mathbf{y}_{T+h+i}^{\text{obs}} \mid \boldsymbol{\theta}^{(i,j)}) \right\}.$$

In all experiments we set $J = 1000$. Larger LPDS values are indicative of better predictive performance (Gelman et al., 2014).

5 Simulation Study

This section details a simulation study designed to assess the proposed N-IFM method for data simulated from a Gaussian copula model. A second simulation study, based on a t -copula, is provided in Section S8 of the online supplement. We compare N-IFM to Hamiltonian Monte Carlo (HMC), specifically the No-U-Turn Sampler (NUTS) of Hoffman et al. (2014), as implemented in `Stan` (Carpenter et al., 2017). The posterior distributions obtained from HMC are treated used as ground truth. In addition, we consider HMC-IFM, which mirrors the two-step structure of N-IFM. HMC-IFM first fits each marginal time series separately to obtain posterior draws and the corresponding posterior mean estimates of the marginal parameters; conditional on these marginal estimates, it then estimates the copula parameters. We assess agreement across methods by comparing posterior densities of both marginal and copula parameters. We also conduct the time-series validation procedure

described in Section 4.2 using the N-IFM, HMC and HMC-IFM methods, to highlight the computational advantages of N-IFM in repeated, time-consuming predictive exercises.

For all examples, we run the HMC algorithm for 4000 iterations, discarding the first 2000 iterations as burn-in, unless stated otherwise. These settings were chosen to target a minimum effective sample size (ESS) of approximately 1000 for all parameters. Training and validation of N-IFM was carried out on a high-end server, with an NVIDIA Tesla A100 80GB graphics processing unit.

Section 5.1 describes the prior distributions specified for the marginal and copula parameters. Section 5.2 outlines the procedure used to generate the training data, while Section 5.3 discusses the training of the neural network models. Section 5.4 presents a simulation study based on a Gaussian copula with GARCH(1,1) marginals with Gaussian errors.

5.1 Simulating parameters from priors

Training the N-IFM models requires generating large collections of synthetic datasets from the GARCH(1,1) and copula models. This is accomplished by first sampling model parameters from their prior distributions and then simulating data conditional on these parameters.

Certain model parameters are subject to validity constraints enforced through the choice of prior distributions. For the GARCH(1,1) parameters, the prior is specified subject to the constraint $\alpha_{1,d} + \alpha_{2,d} < 1$ for $d = 1, \dots, D$, to ensure stationarity. For simplicity, here we use the same prior distribution for all GARCH marginals. Similarly, in the t copula model and in the GARCH(1,1) model with Student's- t errors, the degrees-of-freedom parameters are assigned gamma priors subject to the constraints $\nu > 2$ and $\tilde{\nu}_d > 2$ to ensure finite variance. Table 4 in Section S2 of the online supplement summarises the prior distributions assigned to all model parameters, and provides a detailed discussion of the associated prior choices. Since neural-network outputs are unconstrained, we apply suitable transformations to map the parameters to the real line; these transformed parameters are then used to define $\boldsymbol{\theta}_{\text{mar}}$ and $\boldsymbol{\theta}_{\text{cop}}$. The specific transformations used are described in Section S2 of the online

supplement. The resulting collection of parameter draws forms the basis for generating synthetic datasets used to train the neural networks in both stages of the neural inference functions for margins, which we discuss next.

5.2 Generation of simulated data

For the marginal time series, we consider two alternative specifications: a GARCH(1,1) model with Gaussian errors and a GARCH(1,1) model with Student’s- t errors. To generate the training datasets from GARCH(1,1) with Gaussian errors, we first generate $N = 30,000$ independent parameter draws per epoch from the prior distributions described in Section 5.1. Specifically, for $n = 1, \dots, N$, we sample $\boldsymbol{\theta}_{\text{mar}}^{(n)} \equiv (\varphi_{1,\text{mar}}^{(n)}, \varphi_{2,\text{mar}}^{(n)}, \varphi_{3,\text{mar}}^{(n)})^\top$, construct the GARCH parameters $\alpha_{1,\text{mar}}^{(n)}$, $\alpha_{2,\text{mar}}^{(n)}$, and $\gamma_{\text{mar}}^{(n)}$, and use these to simulate a synthetic time series $\mathbf{y}^{(n)}$, which is used to train the neural-networks for the marginal models. A similar process is used for GARCH(1,1) with Student’s- t errors, but an additional degrees-of-freedom parameter $\tilde{\nu}_{d,\text{mar}}$ is required to simulate $\mathbf{y}^{(n)}$. The number of epochs we use is determined during training, as detailed in Section 5.3.

For the Gaussian copula model, we simulate $N = 30,000$ draws per epoch for each non-zero element in factor loading matrix $\tilde{\mathbf{G}}^{(n)}$ for $n = 1, \dots, N$. Each factor loading matrix $\tilde{\mathbf{G}}^{(n)}$ is transformed into $\mathbf{G}^{(n)}$ and then into a correlation matrix $\bar{\boldsymbol{\Omega}}^{(n)}$ according to (8). For each $\bar{\boldsymbol{\Omega}}^{(n)}$, we generate 1000 independent realisation $\mathbf{z}^{(n)}$ from multivariate normal distribution with a zero mean and a covariance matrix $\bar{\boldsymbol{\Omega}}^{(n)}$. The variable $\mathbf{z}^{(n)}$ is then transformed to copula “data” $\mathbf{u}^{(n)}$ using an appropriate copula transformation; see Section S2 of the online supplement for further details. The $\mathbf{u}^{(n)}$ are used to train the neural networks for the copula models. Note that for the copula network we do not need data from the marginal models, only uniform variables constructed via \mathbf{Z} with the correct dependence.

5.3 Training the neural networks

In this paper, we consider two alternative specifications for the marginal distributions: a GARCH(1, 1) model with Gaussian errors and a GARCH(1, 1) model with Student’s- t errors. Accordingly, we train a separate neural network for each marginal specification. For the cross-sectional dependence structure, we consider both Gaussian and t copulas, each parameterised through a factor model with one to four factors. We train separate neural networks for each combination of copula family and factor dimension.

For the neural network used to estimate the GARCH(1,1) model with Gaussian errors, the inputs consist of the simulated datasets $\mathbf{y}^{(n)}$ for $n = 1, \dots, N$ generated in Section 5.2. The target outputs are the transformed GARCH(1,1) parameters: $\boldsymbol{\theta}_{\text{mar}}^{(n)} \equiv (\varphi_{1,\text{mar}}^{(n)}, \varphi_{2,\text{mar}}^{(n)}, \varphi_{3,\text{mar}}^{(n)})^\top$, which are obtained by transforming $\alpha_{1,\text{mar}}^{(n)}$, $\alpha_{2,\text{mar}}^{(n)}$, and $\gamma_{\text{mar}}^{(n)}$ as described in Section S2 of the online supplement. For the GARCH(1,1) model with Student’s- t error, the outputs of the neural network include the transformed degrees-of-freedom parameter as described in Section S2 of the online supplement.

The simulated datasets are split into training and validation sets, with 90% of the data used for training and the remaining 10% reserved for validation. An example of the training and validation loss curves is shown in Figure 9 in Section S5 of the online supplement. During training, the data are processed in mini-batches of size 32. Optimisation is performed using the Adam stochastic gradient descent algorithm (Kingma and Ba, 2015), with gradients of the objective function computed via backpropagation and a learning rate of 9×10^{-5} . The optimisation proceeds until either the validation loss does not decrease for 100 consecutive epochs or a maximum of 4000 epochs is reached. The total training time for all N-IFM models is shown in Table 10 in Section S5 of the online supplement. Training time ranges from approximately 3 hours for the GARCH(1, 1) model with Gaussian errors to about 3.7 days for the four-factor t copula model. As the number of factors increases, the number of parameters grows, leading to longer training times: training the t copula models was found to be more time consuming than training the corresponding Gaussian copula models.

Similarly, training the GARCH(1, 1) model with Student’s- t errors takes longer than training the corresponding GARCH(1, 1) model with Gaussian errors.

An analogous training procedure is employed for the neural network models to estimate the Gaussian and t copulas. In this case, the training inputs consist of the copula “data” $\mathbf{u}^{(n)}$ and their associated parameters $\tilde{\mathbf{G}}^{(n)}$ for $n = 1, \dots, N$ and degrees-of-freedom parameter ν for the t copula. The transformations required for the copula parameters are discussed in detail in Section S2 of the online supplement.

5.4 Simulation study: Gaussian copula

We conduct a simulation study to compare the accuracy of the N-IFM method to that of the HMC and HMC-IFM methods. The simulated data are generated from a one-factor Gaussian copula model with GARCH(1,1) marginals with Gaussian errors, comprising $D = 20$ series of length $T = 1000$, following Algorithm 5 in Section S2 of the online supplement.

We obtain the estimated parameters of the approximate posterior distributions of marginal parameters $\boldsymbol{\lambda}_d$ for $d = 1, \dots, D$ and copula parameters $\boldsymbol{\lambda}_{\text{cop}}$ using Algorithm 3 in Section 3.2.3. Then, we generate posterior samples of the marginal parameters $\boldsymbol{\theta}_d^{(j)}$ for $d = 1, \dots, D$ and the copula parameters $\boldsymbol{\theta}_{\text{cop}}^{(j)}$, for $j = 1, \dots, 1000$.

Figure 3 shows posterior distributions of selected GARCH(1,1) parameters and Gaussian copula parameters estimated using the N-IFM, HMC and HMC-IFM methods for a one-factor Gaussian copula model with GARCH(1,1) marginals with Gaussian errors, comprising $D = 20$ series of length $T = 1000$. The figure shows the posterior distributions of model parameters obtained using the N-IFM method closely matching the HMC and HMC-IFM posteriors, with only minor discrepancies.

Figures 10 to 13 in Section S6 of the online supplement present the posterior distributions of all model parameters obtained using N-IFM, HMC, and HMC-IFM. Across all parameters, the posterior distributions produced by N-IFM and HMC-IFM closely align with those obtained from HMC. This strong agreement indicates that the two-stage N-IFM and HMC-

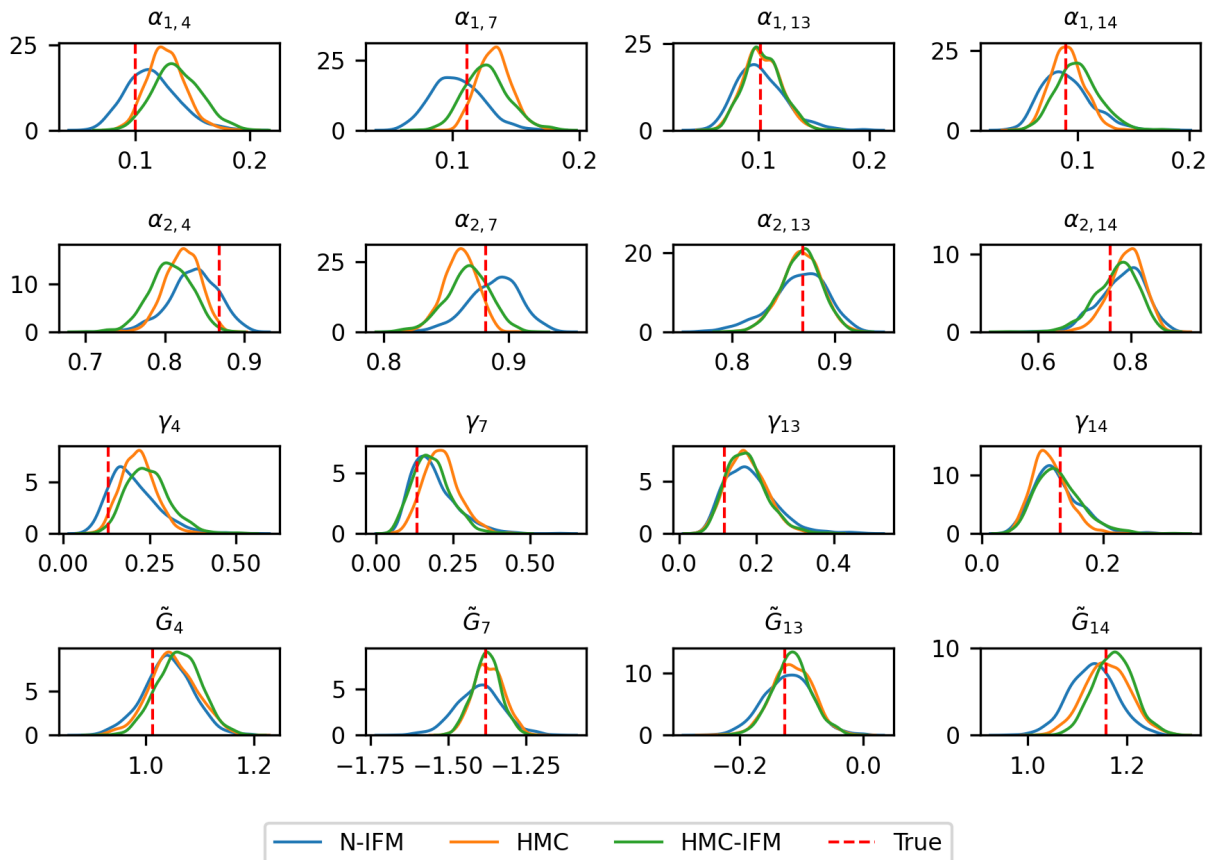


Figure 3: Posterior distributions of selected GARCH(1,1) parameters and Gaussian copula parameters estimated using the N-IFM, HMC and HMC-IFM methods for simulated data generated from a one-factor Gaussian copula model with GARCH(1,1) marginals with Gaussian errors, comprising $D = 20$ series of length $T = 1000$. Results from N-IFM, HMC and HMC-IFM are compared with the true parameter values, indicated by the vertical dotted lines.

IFM approaches provide accurate approximations to the full joint posterior distribution of the model parameters. Table 11 reports the effective sample sizes (ESS) and the potential scale reduction factors (\hat{R}) for all model parameters estimated using HMC. The large ESS values and \hat{R} close to 1 indicate good mixing across chains and provide evidence of satisfactory Markov chain convergence.

Figure 4 shows some of the univariate and bivariate one-step-ahead posterior predictive densities obtained from N-IFM, HMC and HMC-IFM for a one-factor Gaussian copula model with GARCH(1,1) marginals with Gaussian errors. The predictive densities obtained from

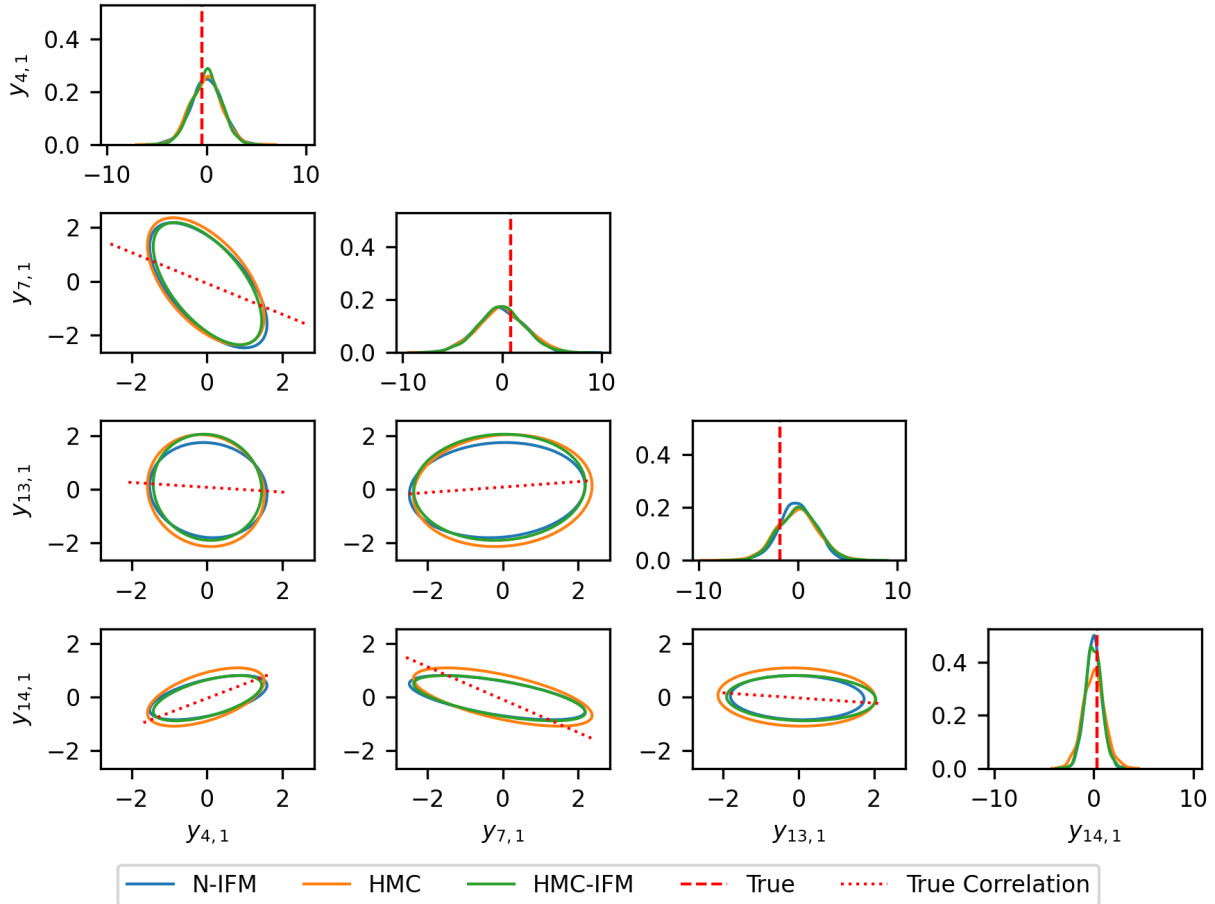


Figure 4: Selected one-step-ahead posterior predictive densities obtained from N-IFM, HMC and HMC-IFM for a one-factor Gaussian copula model with GARCH(1,1) marginals with Gaussian errors, comprising $D = 20$ series of length $T = 1000$. Diagonal panels show the marginal predictive distributions, while off-diagonal panels display the corresponding bivariate predictive distributions. In the diagonal panels, the vertical lines indicate the true parameter values, while in the off-diagonal panels, the dotted lines represent the true correlation between each pair of series.

N-IFM, HMC and HMC-IFM are very similar. The lower triangular panels display the corresponding bivariate predictive distributions, which exhibit strong agreement across the three methods. In particular, the ellipses obtained from N-IFM, HMC and HMC-IFM closely follow the true correlation structure. Table 12 in Section S7 of the online supplement shows the computing time of N-IFM, HMC and HMC-IFM for all simulation studies and real data applications. In terms of computational efficiency, N-IFM is approximately 3,500 times faster than HMC and 1,800 times faster than HMC-IFM post-training.

We now investigate the performance of the N-IFM and HMC-IFM methods using the one-step-ahead LPDS and computing time as evaluation criteria. We generate 1100 observations from a three-factor Gaussian copula model with GARCH(1,1) marginals with Gaussian errors, following Algorithm 5 in Section S2 of the online supplement. The one-step-ahead LPDS is computed using a rolling-window scheme with window length $T = 1000$. The approximate posterior distributions are first obtained using the first 1000 observations, and the log of the one-step-ahead predictive density is computed at time $t = 1001$. The window is then advanced by one time step, the approximate posterior distributions are obtained using observations $t = 2, \dots, 1001$, and the log of the one-step-ahead predictive density is evaluated at time $t = 1002$. This procedure is repeated until the final log of one-step-ahead predictive density is computed at time $t = 1100$. Then, the one step ahead LPDS is computed using (4.2) for models with one to four factor Gaussian copula models with GARCH(1,1) marginals with Gaussian errors.

Table 1 shows the one-step-ahead LPDS and computation time for one to four factor Gaussian copula models with GARCH(1,1) marginals with Gaussian errors for the 100 one-step-ahead predictions. The table shows that both N-IFM and HMC-IFM correctly identify the true data-generating process, namely the three-factor model. Moreover, the two methods produce identical rankings across all competing models. In terms of computational efficiency, N-IFM is much faster than HMC-IFM when performing model selection. From the simulation study, we conclude that N-IFM is substantially faster than both HMC and HMC-IFM, while producing posterior and predictive distributions that closely agree with those obtained from HMC-IFM that themselves are generally similar to those from HMC.

Further simulation studies reported in Section S8 of the online supplement also show that N-IFM performs well for the t copula, yielding posterior distributions that are closer to those obtained under HMC-IFM that in this case are slightly different to those from full HMC. Section S9 presents an additional simulation study demonstrating that N-IFM consistently recovers the true data-generating process. Taken together, these results indicate that N-IFM

Table 1: Comparison of N-IFM and HMC-IFM for one to four factor models in terms of the one-step-ahead LPDS and computational time (in seconds). The simulated data are generated from a three-factor Gaussian copula model with GARCH(1,1) marginals with Gaussian errors. Values shown in bold indicate the best-performing model according to the LPDS. The asterisk indicates the four-factor HMC-IFM model, which requires longer Markov chains (20,000 iterations) due to poor mixing and a low effective sample size.

Methods	Criteria	1-factor	2-factor	3-factor	4-factor
N-IFM	LPDS	-3046.04	-2667	-2414	-2470
	Time (s)	109	110	111	114
HMC-IFM	LPDS	-2989	-2655	-2370	-2371
	Time (s)	85,100	127,000	156,000	2,670,000*

constitutes a computationally efficient and reliable approach to model selection.

6 Real data application

We apply the proposed N-IFM method to a panel of $D = 20$ daily industry portfolio returns from 2 January 2015 to 16 May 2019. The dataset consists of 1100 de-meaned, average value-weighted daily returns obtained from the Center for Research in Security Prices (CRSP) database¹. Further details on the data are provided in Section S10 of the online supplement, including the list of industries, reported in Table 15.

Figure 20 in Section S10 of the online supplement shows the daily stock returns for the 20 industry portfolios. The agricultural industry is labelled as \mathbf{y}_1 . The \mathbf{y}_1 series has a minimum (-6.42) and maximum (7.66) return and shows the presence of some extreme movements and occasional large shocks. Several other series exhibit extreme movements and pronounced shocks, most notably \mathbf{y}_7 and \mathbf{y}_8 . The series \mathbf{y}_1 and \mathbf{y}_8 shows substantial excess kurtosis (8.23 and 33.16 respectively, compared with 0 under a Gaussian distribution), indicating heavy tails and a higher frequency of extreme observations. In addition, series \mathbf{y}_1 illustrates clear volatility clustering, highlighting the heteroskedastic nature of the data. These features support the use of GARCH-type volatility models with Student's- t errors

¹Tuck School of Business at Dartmouth, <https://mba.tuck.dartmouth.edu/pages/faculty/ken.french/index.html>

Table 2: Comparison of the LPDS values obtained using the N-IFM method for zero to four factor of the four models for the industry dataset: (1) The Gaussian copula with GARCH marginals with Gaussian errors; (2) The Gaussian copula with GARCH marginals with Student’s- t errors; (3) The t copula with GARCH marginals with Gaussian errors; (4) The t copula with GARCH marginals with Student’s- t errors. The zero-factor model is equivalent to assuming independent GARCH(1,1) processes for each series. Values shown in bold indicate the best-performing model according to the one-step-ahead LPDS.

Model	Zero-factor	One-factor	Two-factor	Three-factor	Four-factor
(1)	-3411	-2819	-2822	-2841	-2804
(2)	-3338	-2703	-2697	-2711	-2674
(3)	-3411	-2762	-2759	-2754	-2723
(4)	-3338	-2787	-2773	-2769	-2744

rather than Gaussian errors.

Figure 21 in Section S10 of the online supplement shows the histograms of all series, with some appearing Gaussian and others resembling a Student’s- t distribution. The histogram for the agricultural sector confirms that a Student’s- t distribution is appropriate.

We consider zero to four factors of the following models: (1) The Gaussian copula with GARCH(1,1) marginals with Gaussian errors; (2) The Gaussian copula with GARCH(1,1) marginals with Student’s- t errors; (3) The t copula with GARCH(1,1) marginals with Gaussian errors; (4) The t copula with GARCH(1,1) marginals with Student’s- t errors. The zero-factor model is equivalent to assuming independent GARCH(1,1) processes for each series. The best model is selected using the time series validation with the highest LPDS value discussed in Section 5.4.

Table 2 reports the LPDS for each model based on 100 one-step-ahead predictions. The zero-factor model delivers substantially lower LPDS values than the copula models with one to four factors, indicating markedly poorer predictive performance and highlighting the importance of modelling cross-series dependence via one or more factors. The highest LPDS, shown in bold, corresponds to the four-factor Gaussian copula model with GARCH(1,1) marginals with Student’s- t errors. Therefore, further analysis in this section is based on the four-factor Gaussian copula model with GARCH(1,1) marginals with Student’s- t errors.

We assess the accuracy of the posterior distributions of the model parameters estimated using N-IFM by comparing them with those obtained from the HMC and HMC-IFM methods on the real dataset. Figures 22 to 29 in Section S11 of the online supplement present the posterior distributions of all model parameters estimated using N-IFM, HMC and HMC-IFM. Overall, the three methods produce substantial overlap in the posterior distributions. However, noticeable discrepancies appear for some marginal model parameters. In particular, the N-IFM approximation for some $\alpha_{1,d}$ parameters, and to a lesser extent for $\alpha_{2,d}$ and γ_d , differs from the corresponding HMC, while still having strong agreement with HMC-IFM; this corroborates findings from the simulation studies. In contrast, the posterior distributions of $\tilde{\mathbf{G}}$ obtained using N-IFM, except for a few cases, closely agree with those from HMC and HMC-IFM. Table 16 reports the ESS and the \hat{R} for all model parameters estimated using HMC. The large ESS values and \hat{R} close to 1 indicate good mixing across chains and provide evidence of satisfactory Markov chain convergence.

Figure 5 shows selected univariate and bivariate one-step-ahead posterior predictive densities obtained from N-IFM, HMC and HMC-IFM for the industry dataset. The predictive densities obtained from N-IFM, HMC and HMC-IFM are very similar. The lower triangular panels display the corresponding bivariate predictive distributions, which exhibit strong agreement across the two methods. In terms of computational efficiency, N-IFM is approximately 19,000 times faster than HMC-IFM and 37,000 times faster than HMC post-training, while delivering posterior estimates of comparable accuracy, as shown in Table 12 in Section S7 of the online supplement.

Figure 6 (left panel) shows the predicted correlations from N-IFM for the 20 industry portfolio series. The correlations fluctuate across industry pairs. The highest correlation is 0.8 between Fabricated Metal Products and each of the following industries: Construction, Furniture and Fixtures, and Stone, Clay and Glass Products. The lowest correlation occurs between Tobacco Products and both Mining and Primary Metal Industries. There are no negative correlations among these series.

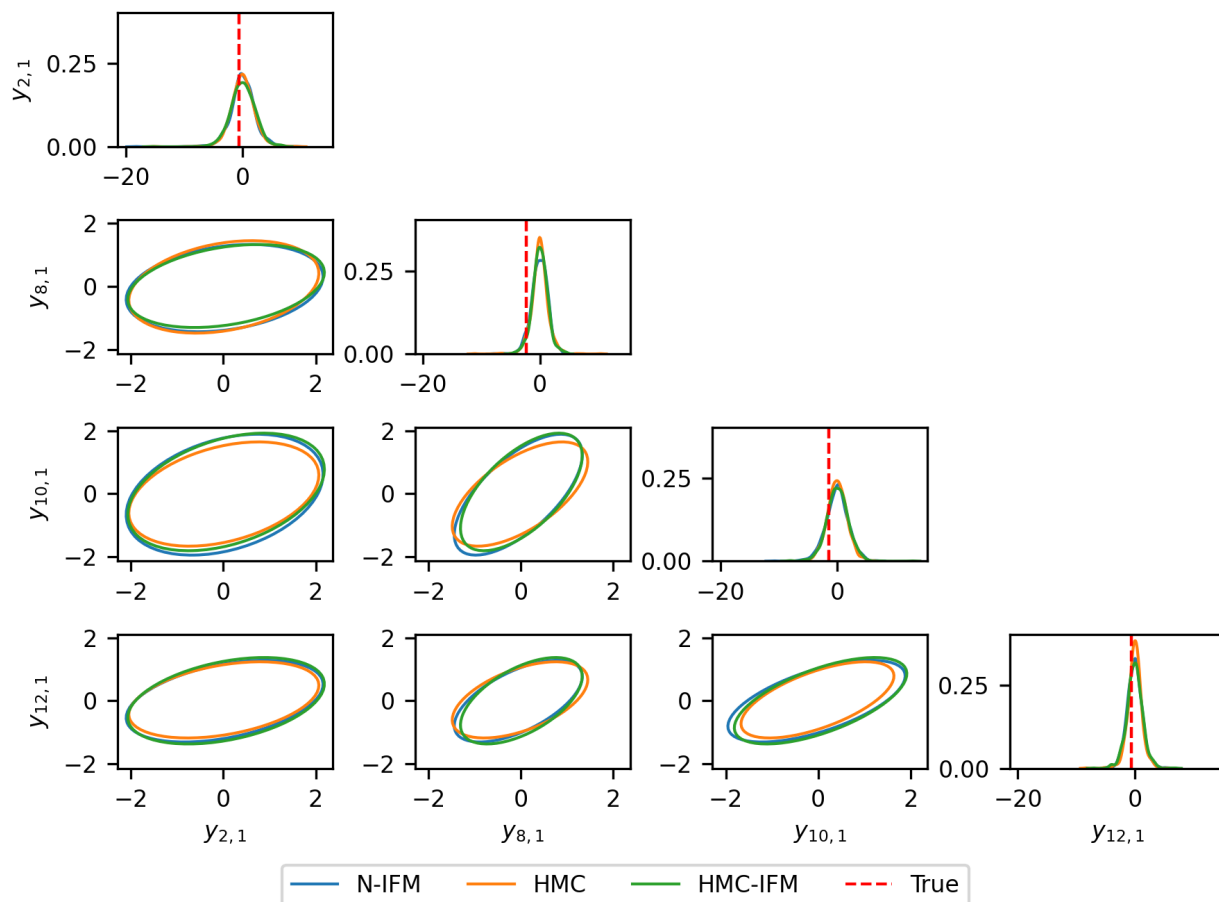


Figure 5: Selected one-step-ahead posterior predictive densities obtained from N-IFM, HMC and HMC-IFM for a four-factor Gaussian copula model with GARCH(1,1) marginals with Student’s- t errors, comprising $D = 20$ series of length $T = 1000$ for the industry dataset. Diagonal panels show the marginal predictive distributions, while off-diagonal panels display the corresponding bivariate predictive distributions. In the diagonal panels, the vertical lines indicate the true parameter values.

The right panel of Figure 6 shows the 90% prediction intervals across forecast horizons for the four-factor Gaussian copula model with GARCH(1,1) marginals with Student’s- t errors. The 90% prediction interval expands and contracts over time, reflecting volatility clustering, and only a small proportion of observations fall outside the interval. The 90% prediction interval of y_{12} is relatively wide, spanning approximately $[-4, 4]$. After around 20 time steps, the interval narrows to approximately $[-2, 2]$ and remains stable thereafter, closely tracking the observed values.

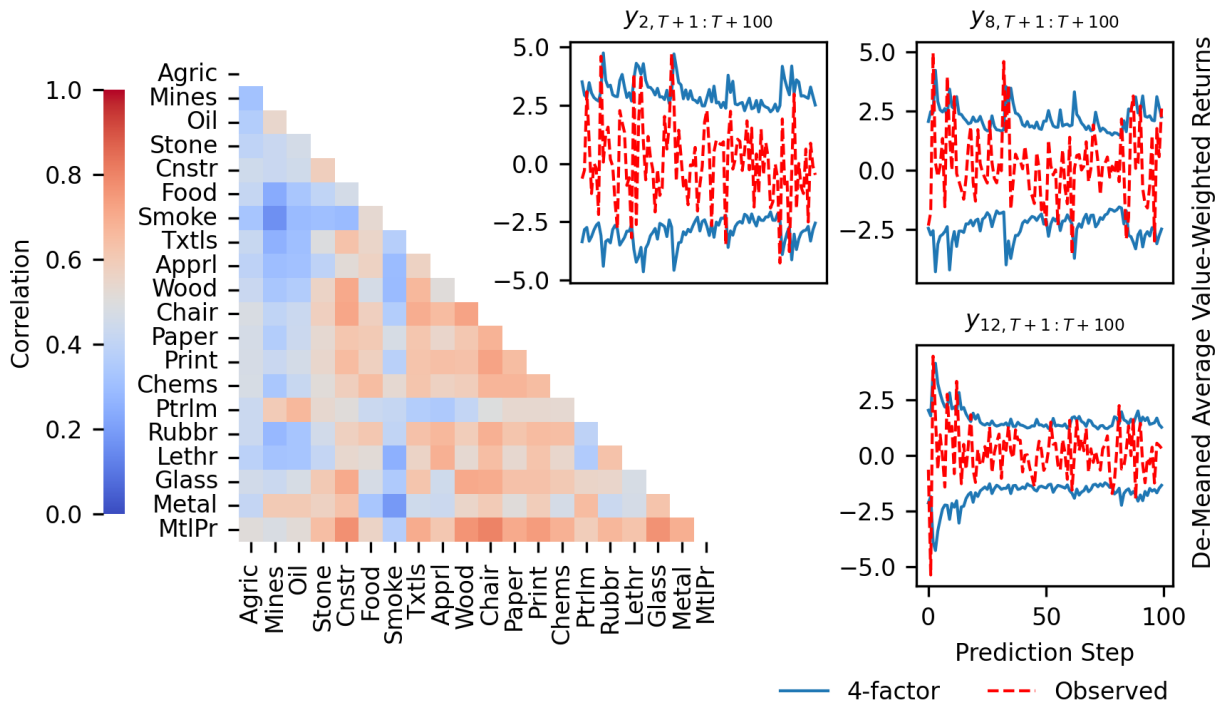


Figure 6: Left: estimated correlation coefficients between each pair of the 20 industry portfolio stock returns obtained using the N-IFM method. Right: the 90% prediction intervals over 100 forecast horizons for the four-factor Gaussian copula model with GARCH(1,1) marginals and Student’s- t errors, shown alongside the observed values for selected industry data series.

7 Conclusion

In this paper, we develop the N-IFM approach for fitting time series copula models. We consider Gaussian and t copula models with GARCH(1,1) marginals with Gaussian and Student’s- t errors. Two neural network models are developed. The first neural network maps the observations from each series to the parameters of the approximate posterior distribution of parameters of the GARCH(1,1) models. The second neural network maps the transformed copula “data” to the parameters of the approximate posterior distribution of parameters of the copula models. Across all simulated and real applications, these approximated posteriors closely align with those obtained using HMC-IFM and to a lesser extent HMC.

A key advantage of N-IFM is its substantial computational efficiency. The approximate posterior distributions are obtained in a fraction of the time required by HMC and HMC-

IFM, rendering tasks such as real-time prediction, model selection and time series validation effectively costless from a computational perspective, in contrast to the considerable burden imposed by HMC and HMC-IFM. In the simulation study, N-IFM and HMC-IFM agree in selecting the three-factor Gaussian copula with GARCH(1,1) marginals with Gaussian errors that generated the data.

When applied to the industry portfolio dataset, N-IFM identifies the four-factor Gaussian copula with GARCH(1,1) marginals with Student's- t errors as the preferred model. We then compare one-step-ahead predictions and the corresponding approximate posterior distributions of the model parameters obtained from N-IFM with those from HMC and HMC-IFM. Despite the dramatic reduction in computation time, N-IFM delivers highly comparable results in terms predictive distributions. The N-IFM posterior distributions align with those from HMC-IFM, although the HMC-based posterior distributions for the GARCH(1,1) parameters are generally narrower. Overall, the results suggest that the N-IFM method provides an accurate and computationally efficient alternative to HMC and HMC-IFM.

When conducting simulation experiments, we found that as the number of parameters increases, the quality of the posterior approximations tends to deteriorate. In addition, it is likely that the use of a mean-field variational approximation for the copula model overly limits posterior expressiveness by enforcing independence across parameters. While a Gaussian approximate distribution with a factor covariance matrix could capture posterior correlations, we found that neural network training became increasingly unstable as model complexity grew. Future work will attempt to address these issues by exploring more flexible neural network architectures, which in turn will allow the use of richer variational families—such as normalising flows, to better represent true posterior distributions. We will also extend N-IFM to more flexible copula specifications, including vine copulas, that are able to accommodate complex and high-dimensional dependence structures.

Acknowledgements

This research is supported by the ARC ITRH for Transforming Energy Infrastructure through Digital Engineering (TIDE), which is led by The University of Western Australia (UWA), delivered with The University of Wollongong and other research partners, and funded by the Australian Research Council, INPEX Operations Australia, Shell Australia, Wood-side Energy, Fugro Australia Marine, Wood Group Kenny Australia, RPSGroup, Bureau Veritas, and Lloyd’s Register Global Technology (grant No.IH200100009).

Data availability statement

The data that support the findings of this study are openly available in the Kenneth R. French Data Library at <https://mba.tuck.dartmouth.edu/pages/faculty/ken.french/index.html>, dataset: “38 Industry Portfolios”.

References

- Albawi, S., Mohammed, T. A., and Al-Zawi, S. (2017). Understanding of a convolutional neural network. In *2017 International Conference on Engineering and Technology (ICET)*, pages 1–6, Piscataway, NJ. IEEE.
- Bollerslev, T. (1986). Generalized autoregressive conditional heteroskedasticity. *Journal of Econometrics*, 31(3):307–327.
- Carpenter, B., Gelman, A., Hoffman, M. D., Lee, D., Goodrich, B., Betancourt, M., Brubaker, M., Guo, J., Li, P., and Riddell, A. (2017). Stan: A probabilistic programming language. *Journal of Statistical Software*, 76(1):1–32.
- Demarta, S. and McNeil, A. J. (2005). The t copula and related copulas. *International Statistical Review*, 73(1):111–129.

- Deng, L., Smith, M. S., and Maneesoonthorn, W. (2025). Large skew-t copula models and asymmetric dependence in intraday equity returns. *Journal of Business & Economic Statistics*, 43(2):269–285.
- Gelman, A., Hwang, J., and Vehtari, A. (2014). Understanding predictive information criteria for Bayesian models. *Statistics and Computing*, 24(6):997–1016.
- Goodfellow, I., Bengio, Y., and Courville, A. (2016). *Deep Learning*. MIT Press, Cambridge, MA.
- Gunawan, D., Khaled, M. A., and Kohn, R. (2020). Mixed marginal copula modeling. *Journal of Business & Economic Statistics*, 38(1):137–147.
- Hoffman, M. D., Gelman, A., et al. (2014). The No-U-Turn sampler: adaptively setting path lengths in Hamiltonian Monte Carlo. *Journal of Machine Learning Research*, 15(1):1593–1623.
- Joe, H. (1997). *Multivariate Models and Multivariate Dependence Concepts*. CRC press, Boca Raton, FL.
- Joe, H. and Xu, J. J. (1996). The estimation method of inference functions for margins for multivariate models. Technical report, Vancouver: University of British Columbia Library.
- Kastner, G. (2019). Sparse Bayesian time-varying covariance estimation in many dimensions. *Journal of Econometrics*, 210(1):98–115.
- Kingma, D. P. and Ba, J. (2015). Adam: A method for stochastic optimization. In Bengio, Y. and LeCun, Y., editors, *3rd International Conference on Learning Representations, ICLR 2015*, San Diego, CA.
- Li, X., Zheng, J., Li, M., Ma, W., and Hu, Y. (2021). Frequency-domain fusing convolutional neural network: a unified architecture improving effect of domain adaptation for fault diagnosis. *Sensors*, 21(2):450.

- Loaiza-Maya, R. and Smith, M. S. (2019). Variational Bayes estimation of discrete-margined copula models with application to time series. *Journal of Computational and Graphical Statistics*, 28(3):523–539.
- McNeil, A. J., Frey, R., and Embrechts, P. (2015). *Quantitative Risk Management: Concepts, Techniques and Tools*. Princeton University Press, Princeton, NJ.
- Murray, J. S., Dunson, D. B., Carin, L., and Lucas, J. (2013). Bayesian Gaussian copula factor models for mixed data. *Journal of the American Statistical Association*, 108:502:656–665.
- Neal, R. M. (2011). MCMC using Hamiltonian dynamics. In Brooks, S., Gelman, A., Jones, G., and Meng, X.-L., editors, *Handbook of Markov Chain Monte Carlo*, pages 113–162. Taylor & Francis, Andover, England.
- Nelsen, R. B. (2006). *An Introduction to Copulas*. Springer, New York, NY.
- Nguyen, H., Ausín, M. C., and Galeano, P. (2020). Variational inference for high dimensional structured factor copulas. *Computational Statistics & Data Analysis*, 151:107012.
- Paszke, A., Gross, S., Massa, F., Lerer, A., Bradbury, J., Chanan, G., Killeen, T., Lin, Z., Gimelshein, N., Antiga, L., Desmaison, A., Kopf, A., Yang, E., DeVito, Z., Raison, M., Tejani, A., Chilamkurthy, S., Steiner, B., Fang, L., Bai, J., and Chintala, S. (2019). Pytorch: An imperative style, high-performance deep learning library. In Wallach, H., Larochelle, H., Beygelzimer, A., d’Alché Buc, F., Fox, E., and Garnett, R., editors, *Advances in Neural Information Processing Systems*, volume 32, pages 8024–8035, Red Hook, NY. Curran Associates, Inc.
- Patton, A. J. (2009). Copula-based models for financial time series. In Mikosch, T., Kreiß, J.-P., Davis, R. A., and Andersen, T. G., editors, *Handbook of Financial Time Series*, pages 767–785. Springer, Berlin, Germany.

- Pitt, M. K., Hall, J., and Kohn, R. (2015). Bayesian inference for latent factor GARCH models. *arXiv:1507.01179*.
- Radev, S. T., Mertens, U. K., Voss, A., Ardizzone, L., and Köthe, U. (2020). BayesFlow: Learning complex stochastic models with invertible neural networks. *IEEE Transactions on Neural Networks and Learning Systems*, 33(4):1452–1466.
- Sainsbury-Dale, M., Zammit-Mangion, A., and Huser, R. (2024). Likelihood-free parameter estimation with neural bayes estimators. *The American Statistician*, 78(1):1–14.
- Sklar, A. (1959). Fonctions de répartition à n dimensions et leurs marges. *Publications de l'Institut de Statistique de l'Université de Paris*, 8:229–231.
- Smith, M. S. (2015). Copula modelling of dependence in multivariate time series. *International Journal of Forecasting*, 31(3):815–833.
- Smith, M. S., Gan, Q., and Kohn, R. J. (2012). Modelling dependence using skew t copulas: Bayesian inference and applications. *Journal of Applied Econometrics*, 27(3):500–522.
- Song, P. X.-K. (2000). Multivariate dispersion models generated from Gaussian copula. *Scandinavian Journal of Statistics*, 27(2):305–320.
- Wagstaff, E., Fuchs, F. B., Engelcke, M., Osborne, M. A., and Posner, I. (2022). Universal approximation of functions on sets. *Journal of Machine Learning Research*, 23(151):1–56.
- Zaheer, M., Kottur, S., Ravanbakhsh, S., Póczos, B., Salakhutdinov, R. R., and Smola, A. J. (2017). Deep sets. In Lee, D. D., Sugiyama, M., Luxburg, U. v., Guyon, I., and Garnett, R., editors, *Advances in Neural Information Processing Systems 30*, pages 3391–3401, Red Hook, NY. Curran Associates, Inc.
- Zammit-Mangion, A., Sainsbury-Dale, M., and Huser, R. (2025). Neural methods for amortized inference. *Annual Review of Statistics and its Application*, 12(1):311–335.

Supplementary Material

We use the following notation in the online supplement. (1), Algorithm 1, Section 1, etc, refer to the main paper, while (S1), Algorithm S1, Section S1, etc, refer to the supplement. All the acronyms used without definition in the supplement, are defined in the main paper.

Section S1 outlines the derivation of the implicit copula PDF. Section S2 outlines the model parameter transformations, prior calibration, and the algorithm for simulating data. Section S3 describes the convolutional neural network (CNN) architecture. Section S4 describes the Deep Sets (Zaheer et al., 2017) architecture. Section S5 provides additional implementation details on training the neural network within the N-IFM framework. Section S6 provides additional results for the Gaussian copula simulation study from Section 5.4 of the main paper. Section S7 provides a summary of the computing time of N-IFM, HMC and HMC-IFM. Section S8 presents a simulation study for the t copula with GARCH(1,1) marginals with Gaussian errors. Section S9 presents a simulation study on model selection. Section S10 provides further information on the industry portfolio dataset used in the real data application. Section S11 contains additional results from the real data application in Section 6 of the main paper.

S1 Implicit copula PDF derivation

Let $\mathbf{Z} \equiv (Z_1, \dots, Z_D)^\top$ be a continuous random vector with joint distribution function $F_{\mathbf{Z}}$ and marginal distribution functions F_{Z_1}, \dots, F_{Z_D} . The implicit copula function is defined as

$$C(\mathbf{u}) = F_{\mathbf{Z}}(F_{Z_1}^{-1}(u_1), \dots, F_{Z_D}^{-1}(u_D)), \quad \mathbf{u} \in [0, 1]^D. \quad (30)$$

The copula density is obtained by differentiation:

$$c(\mathbf{u}) = \frac{\partial^D}{\partial u_1 \cdots \partial u_D} C(\mathbf{u}) \quad (31)$$

$$= \frac{\partial^D}{\partial u_1 \cdots \partial u_D} F_{\mathbf{Z}}(\mathbf{z}), \quad (32)$$

where $\mathbf{z} \equiv (z_1, \dots, z_D)^\top$ denotes a realisation of \mathbf{Z} and $z_d = F_{Z_d}^{-1}(u_d)$ for $d = 1, \dots, D$.

Differentiating $z_d = F_{Z_d}^{-1}(u_d)$ with respect to u_d , gives

$$\frac{\partial z_d}{\partial u_d} = \frac{1}{p_{Z_d}(z_d)}, \quad d = 1, \dots, D.$$

Since the transformation $\mathbf{u} \mapsto \mathbf{z}$ is componentwise, the Jacobian determinant is

$$\left| \det \left(\frac{\partial \mathbf{z}}{\partial \mathbf{u}} \right) \right| = \prod_{d=1}^D \frac{1}{p_{Z_d}(z_d)}.$$

Applying the multivariate change-of-variables formula yields

$$c(\mathbf{u}) = p_{\mathbf{Z}}(\mathbf{z}) \left| \det \left(\frac{\partial \mathbf{z}}{\partial \mathbf{u}} \right) \right| = \frac{p_{\mathbf{Z}}(\mathbf{z})}{\prod_{d=1}^D p_{Z_d}(z_d)}. \quad (33)$$

Here,

$$p_{\mathbf{Z}}(\mathbf{z}) = \frac{\partial^D}{\partial z_1 \cdots \partial z_D} F_{\mathbf{Z}}(\mathbf{z}), \quad p_{Z_d}(z_d) = \frac{\partial}{\partial z_d} F_{Z_d}(z_d), \quad d = 1, \dots, D.$$

S2 Parameter transformations, prior calibration, and data generation

Section S2.1 outlines the transformations used to obtain the unrestricted GARCH(1,1) and degrees-of-freedom parameters. Section S2.2 outlines the algorithm used to obtain hyperparameters of the prior distributions of the model parameters. Section S2.3 outlines the data generation process for the copula model with GARCH(1,1) marginals.

S2.1 Parameter transformations

We apply the parameterisation used by Pitt et al. (2015) to obtain unrestricted GARCH(1,1) parameters. The transformation is carried out in two stages. In the first stage, we define

$$\begin{aligned}\psi_{1,d} &= \alpha_{1,d} + \alpha_{2,d}, \\ \psi_{2,d} &= \gamma_d / (1 - \psi_{1,d}), \\ \psi_{3,d} &= \alpha_{1,d} / \psi_{1,d},\end{aligned}\tag{34}$$

for $d = 1, \dots, D$. In the second stage, we map these parameters to an unconstrained space as follows:

$$\begin{aligned}\varphi_{1,d} &= \log(\psi_{1,d} / (1 - \psi_{1,d})), \\ \varphi_{2,d} &= \log(\psi_{2,d}), \\ \varphi_{3,d} &= \log(\psi_{3,d} / (1 - \psi_{3,d})),\end{aligned}\tag{35}$$

for $d = 1, \dots, D$. The parameters $\varphi_{1,d}$, $\varphi_{2,d}$, and $\varphi_{3,d}$ are unconstrained and ensure that the constrained GARCH(1,1) parameters satisfy the restrictions outlined in Section 2.5 of the main paper.

Second, we consider the degrees-of-freedom parameters. This parameterisation applies to both the t copula degrees-of-freedom parameter ν and the degrees-of-freedom parameters $\tilde{\nu}_d$ of the GARCH(1,1) marginals with Student's- t errors for $d = 1, \dots, D$. We use the following transformations:

$$\begin{aligned}df &= \log(\nu - 2), \\ \tilde{df}_d &= \log(\tilde{\nu}_d - 2).\end{aligned}\tag{36}$$

The transformed parameters df and \tilde{df}_d are unconstrained which ensures that $\nu > 2$ and $\tilde{\nu}_d > 2$.

Algorithm 4 Algorithm to obtain hyperparameters of the prior distributions of the model parameters

Require: Data y_{d,t^*} for $d = 1, \dots, D$ and $t^* = 1, \dots, T^*$.

1: **Estimate marginal (GARCH) parameters:**

2: **for** $d = 1$ to D **do**

3: Estimate GARCH(1,1) parameters using HMC (alternatively, ML can be used) and compute posterior means

$$\hat{\boldsymbol{\theta}}_d = (\hat{\varphi}_{1,d}, \hat{\varphi}_{2,d}, \hat{\varphi}_{3,d})^\top.$$

4: **end for**

5: **Compute pseudo-observations:**

$$u_{d,t^*} = F_{Y_{d,t^*}}(y_{d,t^*}; \hat{\boldsymbol{\theta}}_d), \quad t^* = 1, \dots, T^* \quad \text{and} \quad d = 1, \dots, D.$$

6: **Estimate copula parameters**

$$\tilde{\mathbf{G}}$$

using HMC (alternatively, ML can be used) and compute their posterior means to obtain $\boldsymbol{\mu}^*$.

7: **Estimate prior hyperparameters:**

(1) Use the posterior mean estimates $\{\hat{\alpha}_{1,d}, \hat{\alpha}_{2,d}, \hat{\gamma}_d\}_{d=1}^D$ as pseudo-observations.

(2) Fit beta distributions to $\{\hat{\alpha}_{1,d}\}_{d=1}^D$ and $\{\hat{\alpha}_{2,d}\}_{d=1}^D$ using either HMC or ML to obtain the hyperparameters (a_1, b_1) and (a_2, b_2) , respectively.

(3) Fit a gamma distribution to $\{\hat{\gamma}_d\}_{d=1}^D$ using either HMC or ML to obtain (a_3, b_3) .

8: **return** Hyperparameters of the prior distributions of the model parameters $(a_1, b_1, a_2, b_2, a_3, b_3, \boldsymbol{\mu}^{*\top})^\top$.

S2.2 Selecting hyperparameters for the prior distributions

In this paper, we consider copula models with one to four factors under four specifications: (1) a Gaussian copula with GARCH(1,1) marginals with Gaussian errors; (2) a Gaussian copula with GARCH(1,1) marginals with Student's- t errors; (3) a t copula with GARCH(1,1) marginals with Gaussian errors; and (4) a t copula with GARCH(1,1) marginals with Student's- t errors.

This section describes how we construct the prior hyperparameters for all model parameters. Algorithm 4 summarises the procedure used to calibrate the hyperparameters of the prior distributions using the historical industry stock return data of length $T^* = 1000$, spanning 11 January 2011 to 31 December 2014; see Section 6 of the main paper.

Algorithm 4 is now discussed. For each series $d = 1, \dots, D$, we assign beta priors,

$\text{beta}(a_1, b_1)$ and $\text{beta}(a_2, b_2)$ for $\alpha_{1,d}$ and $\alpha_{2,d}$ respectively, and a gamma prior, $\text{gamma}(a_3, b_3)$, to γ_d . To calibrate the hyperparameters $(a_1, b_1, a_2, b_2, a_3, b_3)$, we first use Hamiltonian Monte Carlo (HMC) to fit a GARCH(1,1) model to each separate series of the historical data, applying the weakly informative priors in Table 3 (alternatively, Maximum Likelihood (ML) can be used). This yields posterior mean estimates $\hat{\alpha}_{1,d}$, $\hat{\alpha}_{2,d}$, and $\hat{\gamma}_d$ for $d = 1, \dots, D$. We then treat $\{\hat{\alpha}_{1,d}\}_{d=1}^D$ as pseudo-observations from a $\text{beta}(a_1, b_1)$ distribution and estimate (a_1, b_1) using either HMC or ML. We apply the same approach to estimate (a_2, b_2) from $\{\hat{\alpha}_{2,d}\}_{d=1}^D$ and (a_3, b_3) from $\{\hat{\gamma}_d\}_{d=1}^D$. We use a truncated gamma prior, $\text{gamma}(a_\nu, b_\nu)$ for the degrees-of-freedom for the t copula, $\nu > 2$. We choose the hyperparameters (a_ν, b_ν) so that the prior mass is concentrated on empirically plausible values, with approximately 90% of the distribution lying between 3 and 20.

We initially adopt the same priors used for the GARCH(1,1) model with Gaussian errors for the GARCH(1,1) model with Student's- t errors. However, when simulating training data under these priors, the generated data are often unstable. We adjusted the values of the hyperparameters for the GARCH(1,1) model with Student's- t errors. The resulting calibrated priors are summarised in Table 4.

We now specify the prior distribution for the copula parameters, $\tilde{\mathbf{G}}$. We first fit the Gaussian copula to the copula “data”, constructed from the posterior means of the marginal model parameters, using HMC (although ML could also be used). Let $\boldsymbol{\mu}^*$ denote the resulting posterior mean estimate of the copula parameters. The dimension of $\tilde{\mathbf{G}}$ is given in Table 5. We then assign the prior

$$\tilde{\mathbf{G}} \sim \mathcal{N}(\boldsymbol{\mu}^*, \mathbf{I}),$$

where \mathbf{I} denotes the identity matrix of appropriate dimension. The full prior specification is reported in Table 4.

Table 3: Initial weakly informative priors used in HMC for historical industry stock return data from 11 January 2011 to 31 December 2014. The final column reports the 90% probability intervals. The Gaussian (\mathcal{N}) prior is parameterised by its mean and standard deviation.

Model	Parameter	Prior	90% probability intervals
GARCH(1,1)	$\varphi_{1,d}, \varphi_{2,d}, \varphi_{3,d}$	$\mathcal{N}(0, 1)$	(-1.64, 1.64)
Gaussian copula	$\tilde{\mathbf{G}}_{ij}$	$\mathcal{N}(0, 1)$	(-1.64, 1.64)
t copula	$\tilde{\mathbf{G}}_{ij}$	$\mathcal{N}(0, 1)$	(-1.64, 1.64)
	df	$\mathcal{N}(0, 1)$	(-1.64, 1.64)

Table 4: Summary of the prior distributions for all model parameters. The beta prior is parameterised by shape parameters a and b ; the gamma prior is parameterised by shape and rate; and the Gaussian (\mathcal{N}) prior is parameterised by its mean and standard deviation.

Model	Parameters	Prior	90% probability intervals
GARCH(1,1) Gaussian errors	w/ $\alpha_{1,d}$	beta(11.34, 85.12)	(0.069, 0.175)
	$\alpha_{2,d}$	beta(19.58, 4.62)	(0.667, 0.922)
	γ_d	gamma(4.69, 1/0.03)	(0.053, 0.262)
GARCH(1,1) Student's- t errors	w/ $\alpha_{1,d}$	beta(28.75, 324.57)	(0.059, 0.107)
	$\alpha_{2,d}$	beta(61.61, 22.40)	(0.651, 0.809)
	γ_d	gamma(3.53, 1/0.0276)	(0.030, 0.193)
	$\tilde{\nu}_d$	gamma(8.39, 1/1.45)	(6.173, 19.795)
Gaussian copula	$\tilde{\mathbf{G}}$	$\mathcal{N}(\boldsymbol{\mu}^*, \mathbf{I})$	$(\boldsymbol{\mu}^* - 1.64\mathbf{I}, \boldsymbol{\mu}^* + 1.64\mathbf{I})$
t copula	$\tilde{\mathbf{G}}$	$\mathcal{N}(\boldsymbol{\mu}^*, \mathbf{I})$	$(\boldsymbol{\mu}^* - 1.64\mathbf{I}, \boldsymbol{\mu}^* + 1.64\mathbf{I})$
	ν	gamma(4.74, 1/2.03)	(3.672, 17.852)

S2.3 Generating data from copula models with GARCH(1,1) margins

Algorithm 5 summarises our procedure for generating simulated data from one to four factor Gaussian and t copula models coupled with GARCH(1,1) marginals under both Gaussian and Student's- t innovations. We begin by sampling elements of the factor-loading matrix $\tilde{\mathbf{G}}$ from their prior distributions. For the t copula, we additionally draw the degrees-of-freedom parameter ν from its prior. Given $\tilde{\mathbf{G}}$, we construct the implied correlation matrix $\bar{\boldsymbol{\Omega}}$ following the factor-copula parameterisation in Section 2.4 of the main paper.

Conditional on $\bar{\boldsymbol{\Omega}}$, we generate copula “data” and transform them to uniform distribu-

Table 5: Number of non-zero elements in $\tilde{\mathbf{G}}$ for one to four factor 20-dimensional Gaussian and t copulas.

Number of Factors	Number of elements in $\tilde{\mathbf{G}}$
1	20
2	39
3	57
4	74

tions. For the Gaussian copula, we simulate $\mathbf{z}_t \sim \mathcal{N}_D(\mathbf{0}, \bar{\mathbf{\Omega}})$ for $t = 1, \dots, T$ and set

$$u_{d,t} = \Phi(z_{d,t}), \quad d = 1, \dots, D \text{ and } t = 1, \dots, T,$$

where $\Phi(\cdot)$ denotes the standard normal CDF. For the t copula, we simulate

$$\mathbf{z}_t \sim t_D(\mathbf{0}, \bar{\mathbf{\Omega}}, \nu), \quad t = 1, \dots, T,$$

via the scale-mixture representation

$$\mathbf{z}_t = \frac{1}{\sqrt{s_t/\nu}} \mathbf{x}_t, \quad \mathbf{x}_t \sim \mathcal{N}_D(\mathbf{0}, \bar{\mathbf{\Omega}}), \quad s_t \sim \chi_\nu^2,$$

with \mathbf{x}_t and s_t independent. The copula data are then obtained by

$$u_{d,t} = T_\nu(z_{d,t}), \quad d = 1, \dots, D \text{ and } t = 1, \dots, T,$$

where T_ν is the CDF of the univariate Student's t distribution with ν degrees of freedom.

For the marginal innovation process, we obtain the standardised shocks $\epsilon_{d,t}$ by transforming the copula “data” $u_{d,t}$. Specifically, under Gaussian errors, we set

$$\epsilon_{d,t} = \Phi^{-1}(u_{d,t}), \quad d = 1, \dots, D \text{ and } t = 1, \dots, T,$$

where $\Phi^{-1}(\cdot)$ denotes the standard normal quantile function. Under Student's- t errors, we

instead use

$$\epsilon_{d,t} = T_{\tilde{\nu}_d}^{-1}(u_{d,t}), \quad d = 1, \dots, D \quad \text{and} \quad t = 1, \dots, T,$$

where $T_{\tilde{\nu}_d}^{-1}(\cdot)$ is the quantile function of the Student's t distribution with $\tilde{\nu}_d$ degrees of freedom. The degrees-of-freedom parameter is generated independently for each margin, $\tilde{\nu}_d \sim p(\tilde{\nu}_d)$, for $d = 1, \dots, D$.

Finally, for each marginal series, we draw the GARCH(1,1) parameters $\alpha_{1,d}$, $\alpha_{2,d}$, and γ_d from their prior distributions. Given these draws and the innovations $\epsilon_{d,t}$, we recursively compute the conditional variances $\sigma_{d,t}^2$ and observations $y_{d,t}$ using (10) and (9) from the main paper, respectively, for all $d = 1, \dots, D$ and $t = 1, \dots, T$.

Algorithm 5 can also be used in reduced form, depending on the simulation objective. For copula-only simulation, Steps 1–12 are sufficient, as they generate the copula parameters from their prior distributions, form $\bar{\Omega}$, simulate $z_{d,t}$, and produce the uniform variables $u_{d,t}$, for $d = 1, \dots, D$ and $t = 1, \dots, T$. If interest instead lies solely in simulating the GARCH(1,1) marginals, then Steps 19–21 are sufficient, provided that the innovations $\epsilon_{d,t}$ are generated independently from either a standard Gaussian distribution or a Student's- t distribution.

Algorithm 5 Simulation of a copula with GARCH(1,1) marginals

Require: Dimension D , number of factors $k \in \{1, 2, 3, 4\}$, series length $T = 1000$, copula type (Gaussian or t), prior distributions for the model parameters from Table 4.

- 1: Sample $\tilde{\mathbf{G}} \sim p(\tilde{\mathbf{G}})$.
 - 2: **if** t copula **then**
 - 3: Sample copula degrees of freedom $\nu \sim p(\nu)$.
 - 4: **end if**
 - 5: Compute $\bar{\mathbf{\Omega}}$ following Section 2.4 of the main paper.
 - 6: **if** Gaussian copula **then**
 - 7: Generate $\mathbf{z}_t \sim \mathcal{N}_D(\mathbf{0}, \bar{\mathbf{\Omega}})$ for $t = 1, \dots, T$.
 - 8: Compute $u_{d,t} = \Phi(z_{d,t})$ for $d = 1, \dots, D$ and $t = 1, \dots, T$.
 - 9: **else** ▷ t copula
 - 10: Generate $\mathbf{z}_t \sim t_D(\mathbf{0}, \bar{\mathbf{\Omega}}, \nu)$ for $t = 1, \dots, T$.
 - 11: Compute $u_{d,t} = T_\nu(z_{d,t})$ for $d = 1, \dots, D$ and $t = 1, \dots, T$.
 - 12: **end if**
 - Explanation:* If the goal is only to simulate copula data, then Steps 1–12 are sufficient. These steps generate the copula parameters, construct $\bar{\mathbf{\Omega}}$, simulate $z_{d,t}$, and transform them to the uniform variables $u_{d,t}$.
 - 13: **if** Gaussian errors **then**
 - 14: Set $\epsilon_{d,t} = \Phi^{-1}(u_{d,t})$ for $d = 1, \dots, D$ and $t = 1, \dots, T$.
 - 15: **else** ▷ Student's- t errors
 - 16: Sample $\tilde{\nu}_d \sim p(\tilde{\nu}_d)$ for $d = 1, \dots, D$.
 - 17: Set $\epsilon_{d,t} = T_{\tilde{\nu}_d}^{-1}(u_{d,t})$ for $d = 1, \dots, D$ and $t = 1, \dots, T$.
 - 18: **end if**
 - 19: Sample GARCH parameters: $\alpha_{1,d} \sim p(\alpha_{1,d})$, $\alpha_{2,d} \sim p(\alpha_{2,d})$, and $\gamma_d \sim p(\gamma_d)$.
 - 20: Compute $\sigma_{d,t}^2$ using (10) for $d = 1, \dots, D$ and $t = 1, \dots, T$.
 - 21: Compute $y_{d,t}$ using (9) for $d = 1, \dots, D$ and $t = 1, \dots, T$.
 - Explanation:* If the goal is only to simulate the GARCH(1,1) marginals, then only Steps 19–21 are required, after generating innovations $\epsilon_{d,t}$ independently from either a standard Gaussian distribution or a Student's- t distribution.
 - 22: **return** the simulated time series, $y_{d,t}$, for $d = 1, \dots, D$ and $t = 1, \dots, T$.
-

S3 Convolutional Neural Networks for GARCH(1,1) models

Convolutional neural networks (CNNs) are most commonly used for image and other spatially structured data (Albawi et al., 2017). Here, we use a one-dimensional CNN to learn a mapping from a univariate time series \mathbf{y}_{mar} to the parameters of the approximate posterior

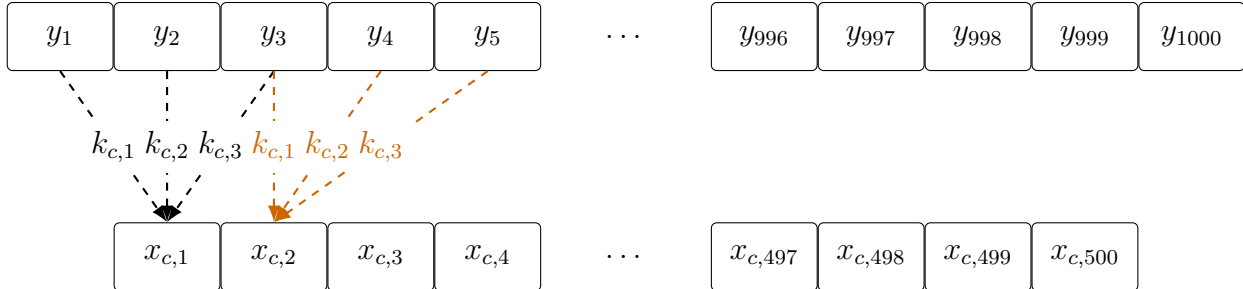


Figure 7: First (black) and second (orange) one-dimensional convolutional operations with 8 channels. Each channel applies a kernel of size 3 to the input time series y_t , for $t = 1, \dots, 1000$, producing the outputs x_c , for $c = 1, \dots, 8$. The second operation (orange) illustrates the shift induced by a stride of 2. The figure is adapted from Li et al. (2021).

distribution, $\lambda_{\text{mar}}(\mathbf{y}_{\text{mar}}; \boldsymbol{\gamma}_{\text{mar}})$, following Algorithm 1 in Section 3.2.1 of the main paper.

We now describe the 1D-CNN mechanism for the generic univariate time series y_t for $t = 1, \dots, 1000$. The 1D-CNN applies a 1D-kernel to adjacent observations in the time series, enabling the network to capture local temporal dependence. We use kernel size 3, stride 2, and padding 1 so that the sequence length is halved at each convolutional layer. The first convolutional operation can be written as

$$x_{c,1} = k_{c,1}y_1 + k_{c,2}y_2 + k_{c,3}y_3 + b_c,$$

where $c = 1, \dots, 8$ indexes the output channels, $k_{c,1}, k_{c,2}, k_{c,3}$ are the kernel weights for channel c , and b_c is the corresponding bias term. The second convolutional operation shifts the kernel forward by two time steps, reflecting the stride of 2. Figure 7 shows the first (black) and second (orange) convolution operations for the first 1D-CNN (`Conv1d`) layer in Table 6, which summarises the network architecture implemented in PyTorch (Paszke et al., 2019).

By stacking multiple one-dimensional convolutional layers, the network learns temporal dependencies and produces informative summary statistics. These features are flattened into a single vector and passed to three multilayer perceptron (MLP) heads that output the parameters of a Gaussian approximate posterior distribution.

Table 6: Neural network architecture for the GARCH(1,1) model with Gaussian errors, featuring a shared backbone and three output heads. The architecture is shown for a batch size of 32. **ReLU** activations are used throughout, except for the **Flatten** operation, which has no activation, and the final **Linear** layer of the middle output head, which uses a **SoftPlus** activation. The kernel size for the 1D-CNN (**Conv1d**) is 3.

Layer	Input Shape	Output Shape	# Parameters
Conv1d	[32, 1, 1000]	[32, 8, 500]	32
Conv1d	[32, 8, 500]	[32, 16, 250]	400
Conv1d	[32, 16, 250]	[32, 32, 125]	1,568
Flatten	[32, 32, 125]	[32, 4000]	-
Linear (Mean)	[32, 4000]	[32, 512]	2,048,512
Linear	[32, 512]	[32, 256]	131,328
Linear	[32, 256]	[32, 128]	32,896
Linear	[32, 128]	[32, 3]	387
Linear (Diagonal)	[32, 4000]	[32, 512]	2,048,512
Linear	[32, 512]	[32, 256]	131,328
Linear	[32, 256]	[32, 128]	32,896
Linear	[32, 128]	[32, 3]	387
Linear (Lower-triangular)	[32, 4000]	[32, 512]	2,048,512
Linear	[32, 512]	[32, 256]	131,328
Linear	[32, 256]	[32, 128]	32,896
Linear	[32, 128]	[32, 3]	387
Total trainable parameters			6,641,369

The Gaussian posterior approximation is parameterised by a mean vector and a covariance matrix; see Section 3.2.1 of the main paper. We reparameterise the covariance matrix via its Cholesky factor, so that the network outputs (i) the mean vector, (ii) the positive diagonal elements of the Cholesky factor, and (iii) the strictly lower-triangular elements, respectively. Table 6 reports the full architecture for the GARCH(1,1) model with Gaussian errors. For the GARCH(1,1) model with Student’s- t errors, we retain the same architecture but change the output dimensions of the final layers of the three MLP heads to [32, 4], [32, 4], and [32, 6], respectively.

S4 Deep Sets for copula models

This section describes Deep Sets network architecture of Zaheer et al. (2017), which is used to learn a mapping from copula “data” \mathbf{u} to the parameters of the approximate posterior distribution, $\boldsymbol{\lambda}_{\text{cop}}(\mathbf{u}; \boldsymbol{\gamma}_{\text{cop}})$, following Algorithm 2 in Section 3.2.2 of the main paper.

During training, for each sample $\tilde{\mathbf{G}}^{(n)}$, $n = 1, \dots, N$ with $N = 30,000$, we simulate $T = 1000$ i.i.d. realisations of $\mathbf{z}_t^{(n)}$ according to the procedure in Section S2.3. These replicates form the exchangeable set $\mathcal{Z}^{(n)} = \{\mathbf{z}_t^{(n)}\}_{t=1}^T$, and we compute the corresponding copula “data” $\mathcal{U}^{(n)} = \{\mathbf{u}_t^{(n)}\}_{t=1}^T$. Because the replicates are exchangeable, any permutation of $\mathcal{U}^{(n)}$ represents the same information, which aligns naturally with the permutation-invariant Deep Sets architecture.

The Deep Sets representation is

$$\boldsymbol{\lambda}_{\text{cop}}(\mathcal{U}^{(n)}; \boldsymbol{\gamma}_{\text{cop}}) = \boldsymbol{\phi}\left(\tilde{\mathbf{T}}(\mathcal{U}^{(n)}; \boldsymbol{\gamma}_{\psi}); \boldsymbol{\gamma}_{\phi}\right), \quad (37)$$

$$\tilde{\mathbf{T}}(\mathcal{U}^{(n)}; \boldsymbol{\gamma}_{\psi}) = \mathbf{a}\left(\left\{\boldsymbol{\psi}\left(\mathbf{u}_t^{(n)}; \boldsymbol{\gamma}_{\psi}\right)\right\}_{t=1}^T\right), \quad (38)$$

where $\boldsymbol{\psi}(\cdot; \boldsymbol{\gamma}_{\psi})$ and $\boldsymbol{\phi}(\cdot; \boldsymbol{\gamma}_{\phi})$ are neural networks and $\boldsymbol{\gamma}_{\text{cop}} = (\boldsymbol{\gamma}_{\phi}^{\top}, \boldsymbol{\gamma}_{\psi}^{\top})^{\top}$ collects all network parameters. Moreover, $\mathbf{a}(\cdot)$ is a permutation-invariant aggregation function, taken here to be the elementwise mean. The learned summary statistic $\tilde{\mathbf{T}}$ is then passed to the inference network $\boldsymbol{\phi}(\cdot; \boldsymbol{\gamma}_{\phi})$, which outputs $\boldsymbol{\lambda}_{\text{cop}}$. Deep Sets is known to be a universal approximator for continuous permutation-invariant set functions, provided the number of observations (T) is sufficiently large (Wagstaff et al., 2022). Figure 8 shows the schematic of the Deep Sets architecture.

Table 7 summarises the Deep Sets neural network architecture used for the one-factor Gaussian copula model, implemented in PyTorch. Each copula observation $\mathbf{u}_t^{(n)}$ is encoded independently using a shared sequence of fully connected layers, denoted by $\boldsymbol{\psi}(\cdot; \boldsymbol{\gamma}_{\psi})$. The resulting variables are then aggregated by taking the mean over the set dimension (the Mean layer, corresponding to the permutation-invariant function $\mathbf{a}(\cdot)$), producing the summary

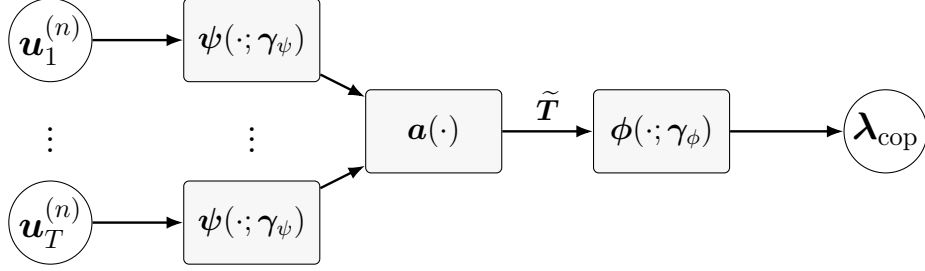


Figure 8: Schematic of the Deep Sets neural network architecture. Each independent realisation $\mathbf{u}_t^{(n)}$ is transformed independently by the function $\psi(\cdot; \gamma_\psi)$. The set of transformed inputs is then aggregated elementwise using a permutation-invariant function $\mathbf{a}(\cdot)$, yielding the summary statistic $\tilde{\mathbf{T}}$. Finally, the summary statistic is mapped to parameter estimates $\boldsymbol{\lambda}_{\text{cop}}$ by the function $\phi(\cdot; \gamma_\phi)$.

statistic $\tilde{\mathbf{T}}$. Finally, $\tilde{\mathbf{T}}$ is passed to two MLP output heads $\phi(\cdot; \gamma_\phi)$, implemented as fully connected layers with batch normalisation to stabilise training, which output the parameters of the Gaussian approximate posterior distribution $\boldsymbol{\lambda}_{\text{cop}}$.

The Gaussian posterior approximation is parameterised by a mean vector and a diagonal covariance matrix. Accordingly, the two output heads return (i) the mean vector and (ii) the diagonal entries (variances) of the covariance matrix, constrained to be positive via `SoftPlus`.

For higher-factor copula models, we replicate the network for each additional factor. For example, in the two-factor model, the first network outputs the approximate posterior parameters associated with the first column of $\tilde{\mathbf{G}}$, while the second network outputs the corresponding parameters for the second column. For the four-factor copula model, we include an additional `Linear` layer in the summary network to increase representational capacity when constructing the summary statistic. Tables 8 and 9 show the full neural network architecture for the four-factor Gaussian copula.

S5 Training neural-network models

This section provides additional implementation details on training the neural networks within the N-IFM framework, continuing on from Section 5.3 of the main paper. Figure 9

Table 7: Neural network architecture of the one-factor 20-dimensional Gaussian copula model, featuring a shared backbone and two output heads in a Deep Sets framework with a batch size of 32. ReLU activations are used throughout, except for the Mean operation (no activation) and the final Linear layer of the lower head (SoftPlus activation).

Layer	Input Shape	Output Shape	# Parameters
Linear	[32, 1000, 20]	[32, 1000, 64]	1,344
Linear	[32, 1000, 64]	[32, 1000, 128]	8,320
Linear	[32, 1000, 128]	[32, 1000, 256]	33,024
Linear	[32, 1000, 256]	[32, 1000, 512]	131,584
Mean	[32, 1000, 512]	[32, 512]	-
Linear (Mean)	[32, 512]	[32, 1024]	525,312
BatchNorm1d	[32, 1024]	[32, 1024]	2,048
Linear	[32, 1024]	[32, 512]	524,800
BatchNorm1d	[32, 512]	[32, 512]	1,024
Linear	[32, 512]	[32, 256]	131,328
BatchNorm1d	[32, 256]	[32, 256]	512
Linear	[32, 256]	[32, 128]	32,896
BatchNorm1d	[32, 128]	[32, 128]	256
Linear	[32, 128]	[32, 20]	2,580
Linear (Diagonal)	[32, 512]	[32, 1024]	525,312
BatchNorm1d	[32, 1024]	[32, 1024]	2,048
Linear	[32, 1024]	[32, 512]	524,800
BatchNorm1d	[32, 512]	[32, 512]	1,024
Linear	[32, 512]	[32, 256]	131,328
BatchNorm1d	[32, 256]	[32, 256]	512
Linear	[32, 256]	[32, 128]	32,896
BatchNorm1d	[32, 128]	[32, 128]	256
Linear	[32, 128]	[32, 20]	2,580
Total trainable parameters			2,615,784

displays the training and validation loss curves for the 20-dimensional one-factor Gaussian copula model in Section 5.4. The loss decreases rapidly in the early epochs, indicating that the network quickly captures the main structure in the training data, and then declines more gradually. The close agreement between the training and validation curves suggests good generalisation, with no evidence of overfitting.

Table 10 shows the training time for different copula and marginal models fitted using the N-IFM method. Training time increases with model complexity. For the Gaussian copula, increasing the number of factors from one to four raises the training time from

Table 8: Neural network architecture of the shared Deep Sets backbone for the four-factor, 20-dimensional Gaussian copula model. The backbone maps the input set of copula observations \mathbf{u} to a pooled summary representation. This shared representation is used by both output heads that return the approximate posterior mean vector and the diagonal covariance parameters, and it is replicated across all four factors. Only the final factor-specific output layers differ between factors (Table 9). The architecture is shown for a batch size of 32. ReLU activations are used throughout, except for the **Mean** operation (no activation) and the final layer leading to the factor-specific outputs.

Layer	Input Shape	Output Shape	# Parameters
Linear	[32, 1000, 20]	[32, 1000, 64]	1,344
Linear	[32, 1000, 64]	[32, 1000, 128]	8,320
Linear	[32, 1000, 128]	[32, 1000, 256]	33,024
Linear	[32, 1000, 256]	[32, 1000, 512]	131,584
Linear	[32, 1000, 512]	[32, 1024]	–
Linear (Mean)	[32, 1024]	[32, 1536]	1,574,400
BatchNorm1d	[32, 1536]	[32, 1536]	3,072
Linear	[32, 1536]	[32, 768]	1,180,416
BatchNorm1d	[32, 756]	[32, 756]	1,536
Linear	[32, 756]	[32, 512]	393,728
BatchNorm1d	[32, 512]	[32, 512]	1,024
Linear	[32, 512]	[32, 256]	131,328
BatchNorm1d	[32, 256]	[32, 256]	512
Linear	[32, 256]	Output (factor)	see Table 9
Linear (Diagonal)	[32, 1024]	[32, 1536]	1,574,400
BatchNorm1d	[32, 1536]	[32, 1536]	3,072
Linear	[32, 1536]	[32, 768]	1,180,416
BatchNorm1d	[32, 756]	[32, 756]	1,536
Linear	[32, 756]	[32, 512]	393,728
BatchNorm1d	[32, 512]	[32, 512]	1,024
Linear	[32, 512]	[32, 256]	131,328
BatchNorm1d	[32, 256]	[32, 256]	512
Linear	[32, 256]	Output (factor)	see Table 9
Total trainable parameters			7,271,616 + see Table 9

20,000 to 108,000 seconds. The t copula models are substantially more computationally demanding, requiring between 189,000 and 327,000 seconds. By comparison the GARCH marginal models train faster, taking 12,000 seconds under Gaussian errors and 27,000 seconds under Student’s- t errors.

Table 9: Factor-specific output heads for factors 1 to 4 in the four-factor, 20-dimensional Gaussian copula model. These layers correspond to the “Output (factor)” components shown in Table 8. The network is illustrated using a batch size of 32.

Factor	Head	Layer	Output Shape	# Parameters
1	Mean	Linear	[32, 20]	5,140
1	Diagonal	Linear	[32, 20]	5,140
2	Mean	Linear	[32, 19]	4,883
2	Diagonal	Linear	[32, 19]	4,883
3	Mean	Linear	[32, 18]	4,626
3	Diagonal	Linear	[32, 18]	4,626
4	Mean	Linear	[32, 17]	4,369
4	Diagonal	Linear	[32, 17]	4,369

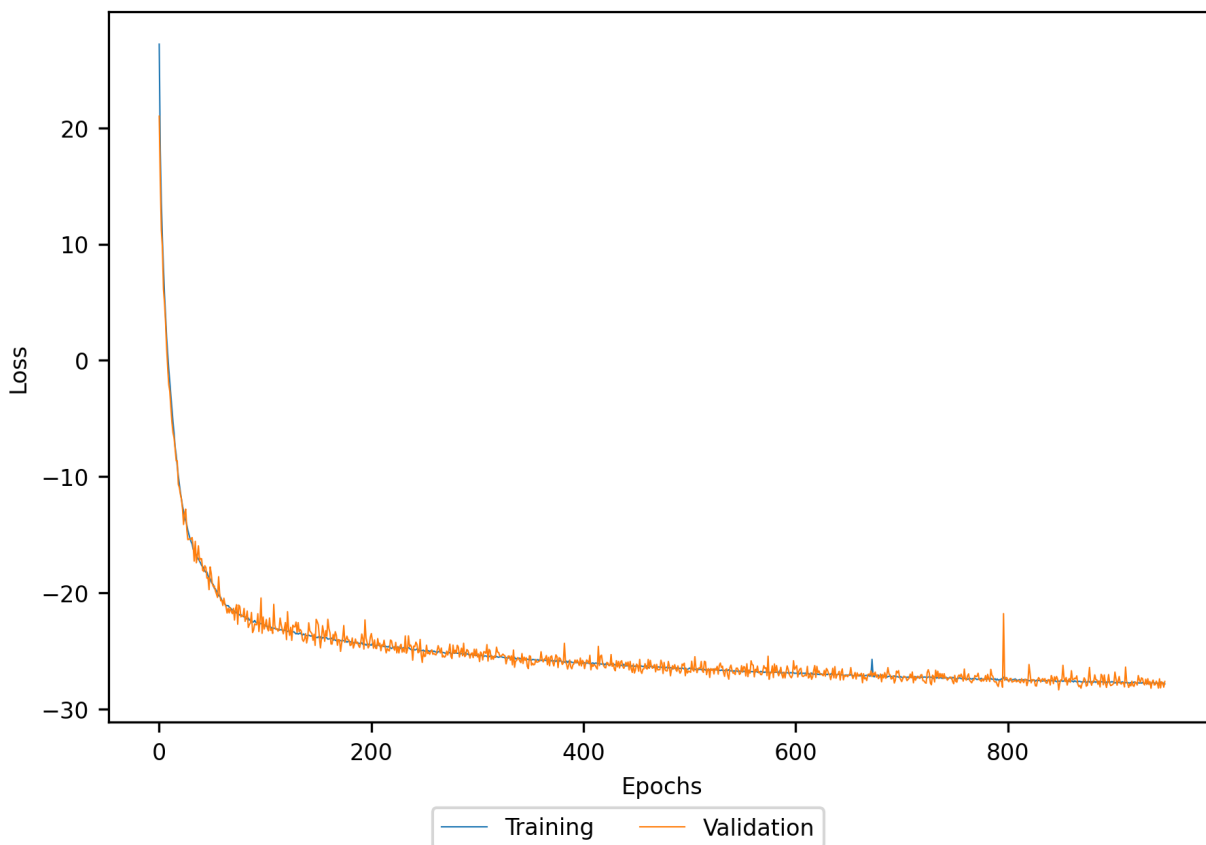


Figure 9: Training and validation loss curves for the 20-dimensional one-factor Gaussian copula over approximately 1000 epochs.

Table 10: Training time in seconds for different marginal and copula N-IFM models.

Models	Computing Time (in seconds)
GARCH(1,1) w/ Gaussian errors	12,000
GARCH(1,1) w/ Student's- t errors	27,000
Gaussian copula one-factor	20,000
Gaussian copula two-factors	55,000
Gaussian copula three-factors	75,000
Gaussian copula four-factors	108,000
t copula one-factor	199,000
t copula two-factors	189,000
t copula three-factors	327,000
t copula four-factors	325,000

S6 Additional results for the Gaussian copula simulation study (Section 5.4)

This section contains additional results for the Gaussian copula simulation study in Section 5.4 of the main paper. It presents additional figures and tables comparing N-IFM with HMC and HMC-IFM.

Similar to N-IFM, the HMC-IFM approach proceeds in two stages. First, it samples from the posterior distribution of the GARCH(1,1) parameters for each marginal series and computes their posterior means. Conditional on these posterior means, it then samples from the posterior distribution of the copula parameters. In contrast, HMC targets the joint posterior over all model parameters and updates the marginal and copula parameters simultaneously.

We consider HMC-IFM because full HMC can be computationally prohibitive for model selection, especially in sequential settings where each new data arrival requires rerunning the sampler to obtain draws from the posterior distribution of the model parameters and to compute one-step-ahead LPDS. To evaluate the accuracy of this two-stage approximation, we compare posterior estimates from N-IFM, HMC and HMC-IFM using simulated data generated from the one-factor Gaussian copula model.

Figures 10 to 12 display the posterior distributions of the GARCH(1, 1) parameters and show near identical results across the three methods. Likewise, Figure 13 shows that the posterior distributions of the Gaussian copula parameters are also in close agreement. Overall, these results indicate that the two-stage N-IFM and HMC-IFM procedures closely approximate the full joint posterior obtained by standard HMC, supporting the use of HMC-IFM as a computationally efficient alternative to full HMC for model selection.

For the HMC implementation in `Stan`, standard diagnostics such as the effective sample size (`n_eff`) and the potential scale reduction factor (\hat{R}) are used to assess convergence. As reported in Table 11, `n_eff` is large for all parameters and all \hat{R} values are close to 1, indicating good mixing and convergence across chains. For HMC-IFM (not reported), all \hat{R} values are close to 1, indicating good convergence, while `n_eff` is slightly lower for the GARCH(1,1) parameters and slightly higher for the copula parameters relative to HMC.

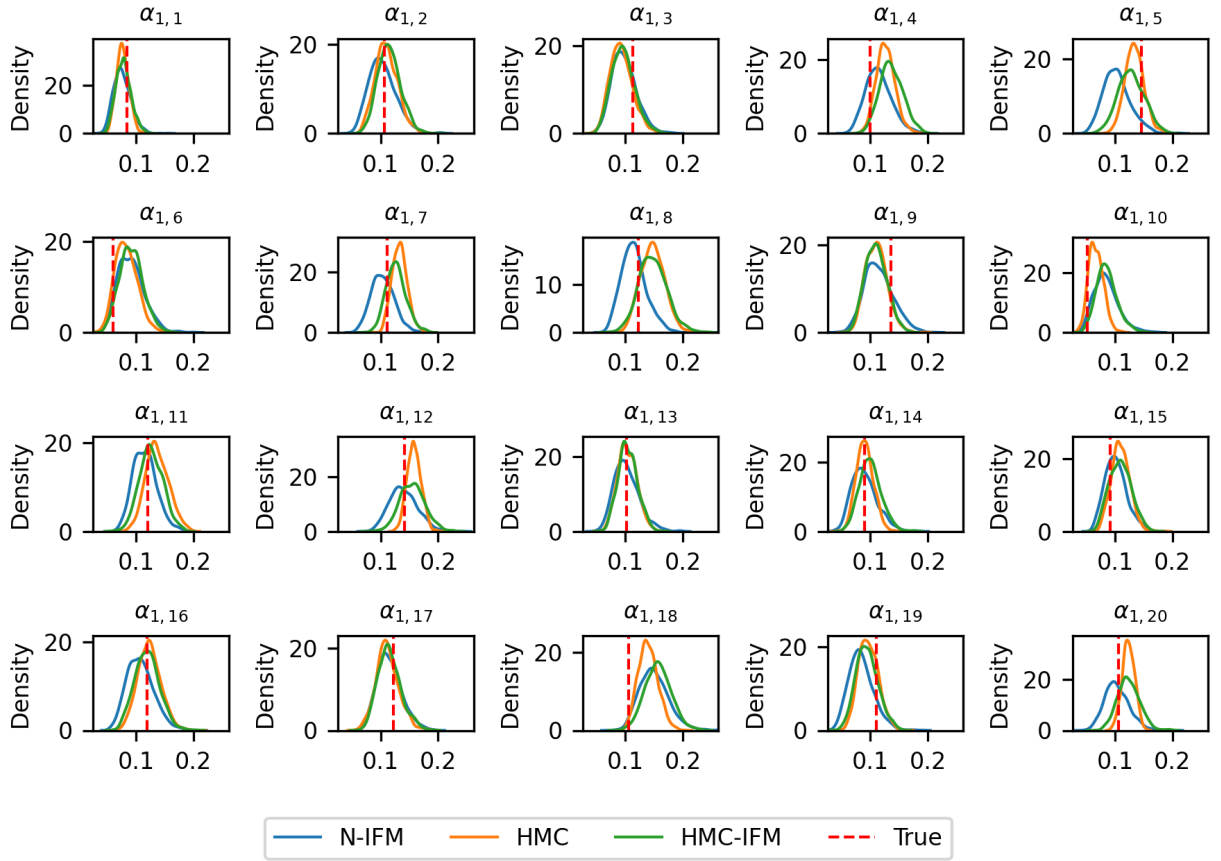


Figure 10: Posterior distributions of the GARCH(1,1) parameters $\alpha_{1,d}$ for $d = 1, \dots, D$, comparing N-IFM, HMC and HMC-IFM with the true values. The results are based on simulated data from a 20 dimensional one-factor Gaussian copula with GARCH(1,1) marginals with Gaussian errors.

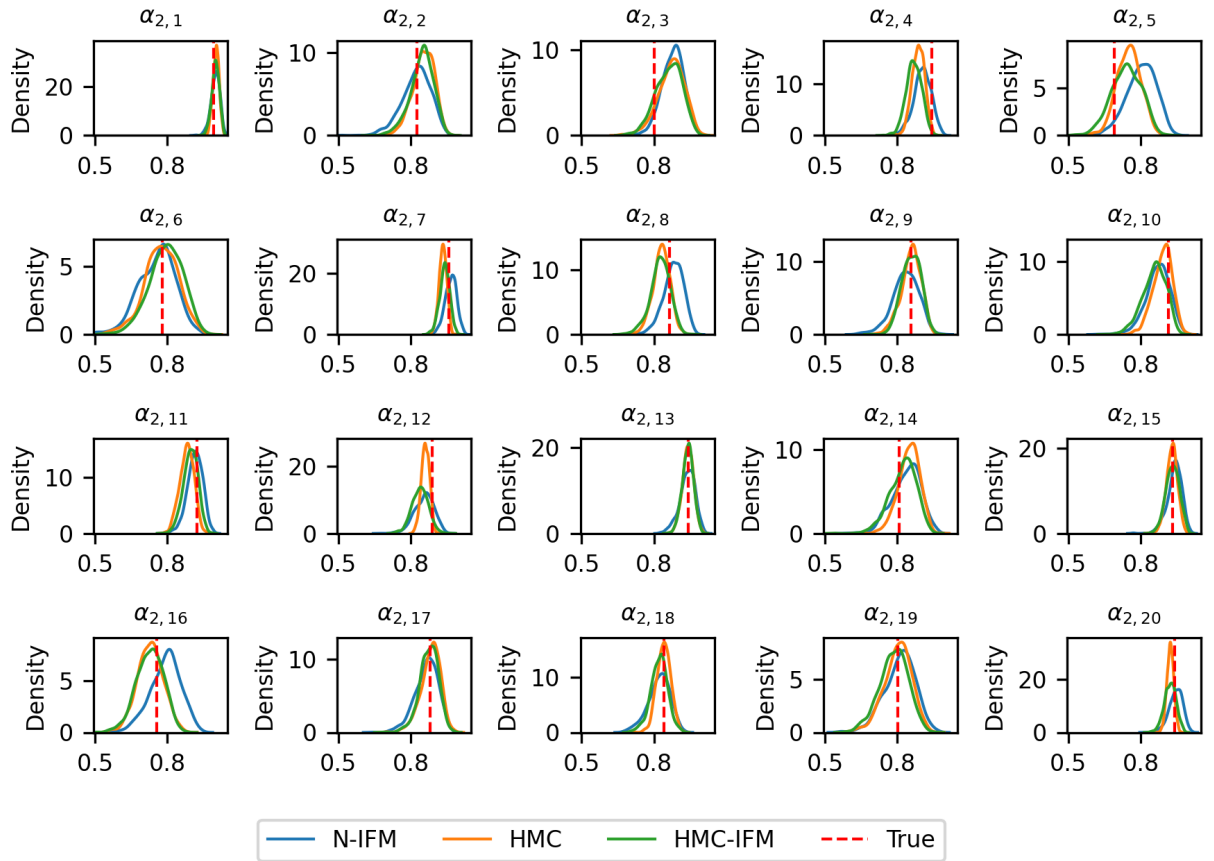


Figure 11: Posterior distributions of the GARCH(1,1) parameters $\alpha_{2,d}$ for $d = 1, \dots, D$, comparing N-IFM, HMC and HMC-IFM with the true values. The results are based on simulated data from a 20 dimensional one-factor Gaussian copula with GARCH(1,1) marginals with Gaussian errors.

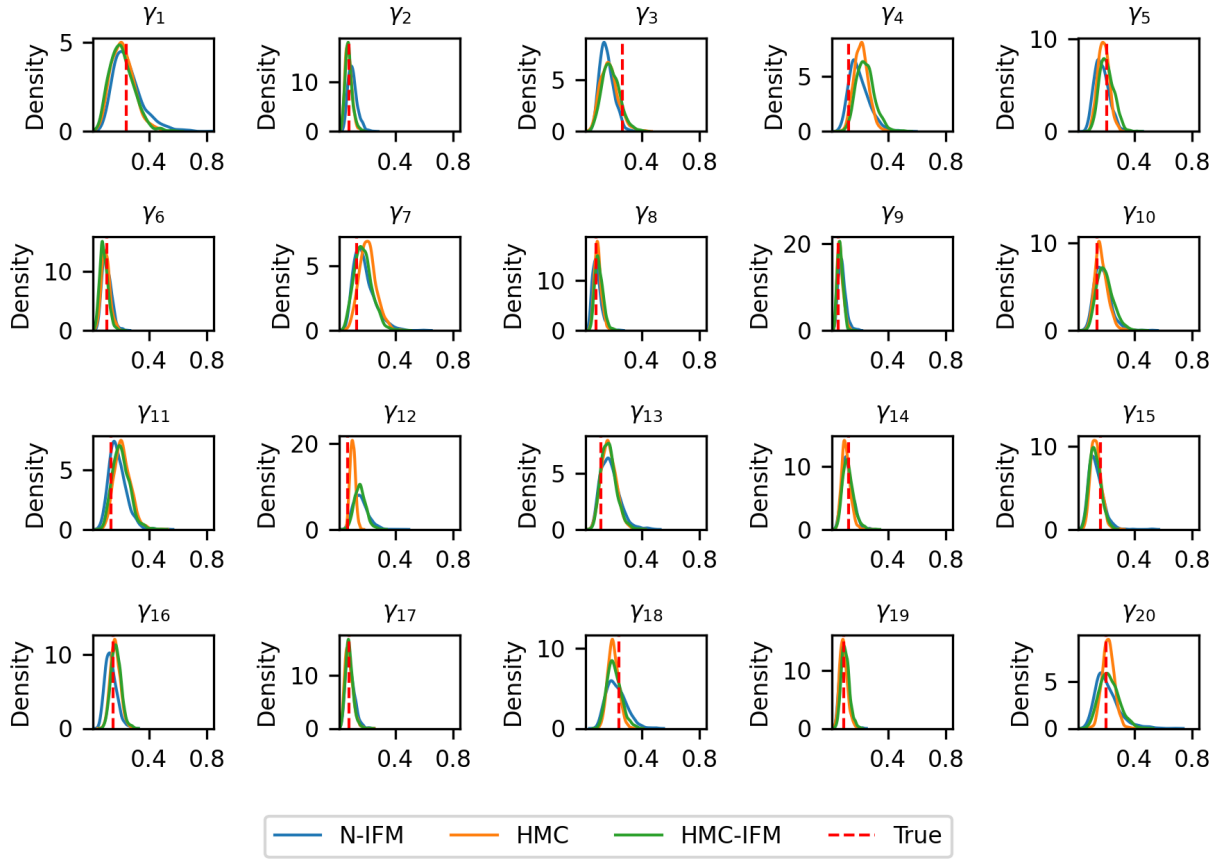


Figure 12: Posterior distributions of the GARCH(1,1) parameters γ_d for $d = 1, \dots, D$, comparing N-IFM, HMC and HMC-IFM with the true values. The results are based on simulated data from a 20 dimensional one-factor Gaussian copula with GARCH(1,1) marginals with Gaussian errors.

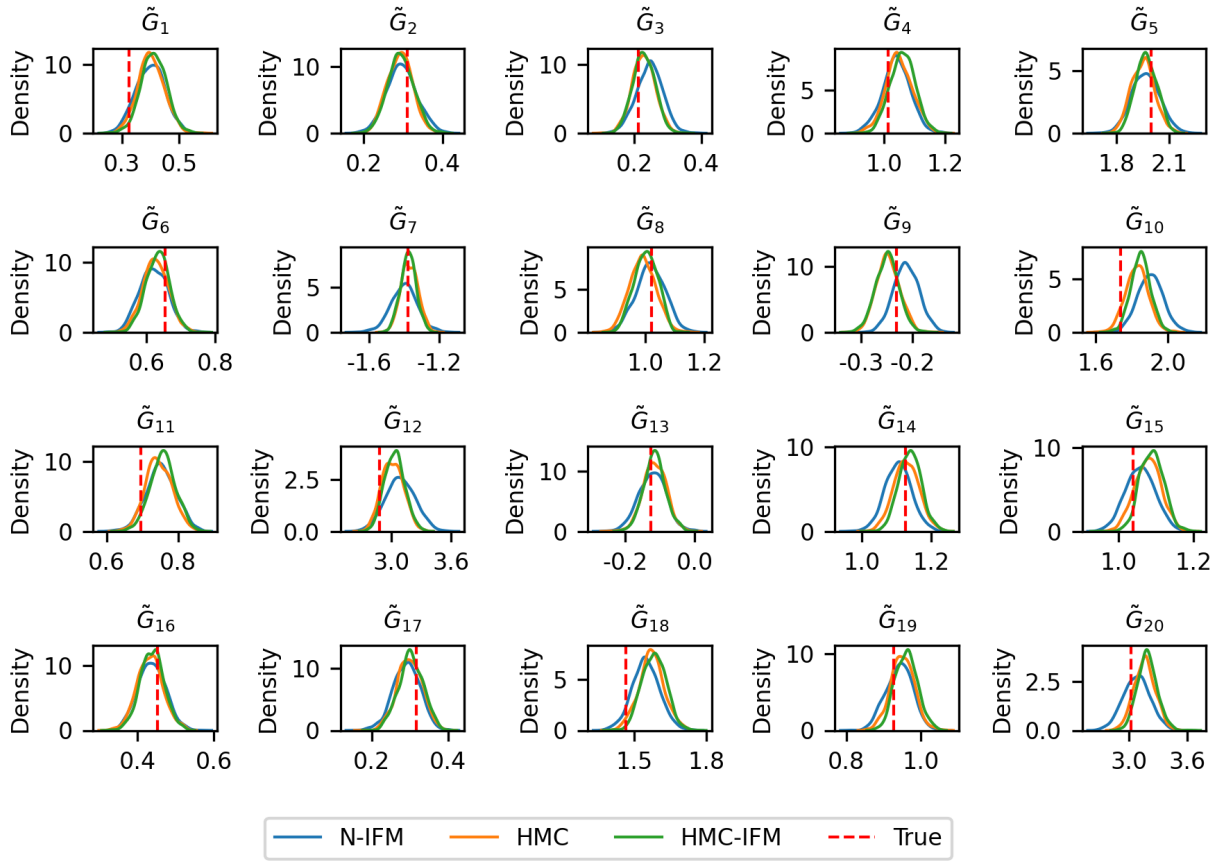


Figure 13: Posterior distributions of the copula parameters $\tilde{\mathbf{G}}$, comparing N-IFM, HMC and HMC-IFM with the true values. The results are based on simulated data from a 20 dimensional one-factor Gaussian copula with GARCH(1,1) marginals with Gaussian errors.

Table 11: Posterior diagnostics for model parameters estimated using HMC, based on simulated data from a 20-dimensional one-factor Gaussian copula model with GARCH(1, 1) marginals and Gaussian errors, including the effective sample size (n_{eff}) and the potential scale reduction factor ($\widehat{\mathbf{R}}$).

Parameter	n_{eff}	$\widehat{\mathbf{R}}$	Parameter	n_{eff}	$\widehat{\mathbf{R}}$
$\alpha_{1,1}$	7578	0.9997	γ_1	5552	1.0004
$\alpha_{1,2}$	5472	0.9999	γ_2	4631	1.0000
$\alpha_{1,3}$	5879	0.9998	γ_3	4467	0.9996
$\alpha_{1,4}$	4780	0.9995	γ_4	5396	1.0000
$\alpha_{1,5}$	5084	0.9996	γ_5	4790	1.0014
$\alpha_{1,6}$	6522	1.0000	γ_6	5698	0.9996
$\alpha_{1,7}$	6847	0.9997	γ_7	4260	0.9996
$\alpha_{1,8}$	4622	0.9996	γ_8	4929	0.9997
$\alpha_{1,9}$	5452	0.9999	γ_9	5764	0.9998
$\alpha_{1,10}$	5325	1.0000	γ_{10}	5463	0.9997
$\alpha_{1,11}$	5562	1.0002	γ_{11}	4950	0.9997
$\alpha_{1,12}$	3818	1.0003	γ_{12}	5575	1.0000
$\alpha_{1,13}$	5265	1.0000	γ_{13}	4667	0.9996
$\alpha_{1,14}$	5704	0.9999	γ_{14}	5470	0.9997
$\alpha_{1,15}$	5443	0.9999	γ_{15}	4753	1.0000
$\alpha_{1,16}$	6046	1.0003	γ_{16}	6173	0.9999
$\alpha_{1,17}$	3876	1.0001	γ_{17}	3242	1.0014
$\alpha_{1,18}$	4968	1.0003	γ_{18}	5865	0.9996
$\alpha_{1,19}$	6080	0.9998	γ_{19}	6235	0.9996
$\alpha_{1,20}$	3816	0.9997	γ_{20}	4701	1.0001
$\alpha_{2,1}$	8312	0.9996	\tilde{G}_1	3564	0.9996
$\alpha_{2,2}$	4743	0.9996	\tilde{G}_2	6387	0.9999
$\alpha_{2,3}$	4501	0.9997	\tilde{G}_3	7076	0.9996
$\alpha_{2,4}$	6233	0.9996	\tilde{G}_4	2874	1.0001
$\alpha_{2,5}$	4415	1.001	\tilde{G}_5	2822	1.0008
$\alpha_{2,6}$	5462	0.9996	\tilde{G}_6	4746	0.9997
$\alpha_{2,7}$	7521	0.9997	\tilde{G}_7	4313	1.0000
$\alpha_{2,8}$	5995	0.9997	\tilde{G}_8	3447	0.9996
$\alpha_{2,9}$	5613	0.9998	\tilde{G}_9	7620	0.9997
$\alpha_{2,10}$	4480	0.9998	\tilde{G}_{10}	2384	1.0000
$\alpha_{2,11}$	7179	0.9996	\tilde{G}_{11}	4010	0.9998
$\alpha_{2,12}$	6056	1.0000	\tilde{G}_{12}	3465	1.0000
$\alpha_{2,13}$	7363	0.9996	\tilde{G}_{13}	7219	0.9996
$\alpha_{2,14}$	4964	0.9998	\tilde{G}_{14}	3185	0.9998
$\alpha_{2,15}$	7393	0.9999	\tilde{G}_{15}	3425	0.9995
$\alpha_{2,16}$	5786	0.9999	\tilde{G}_{16}	5171	0.9996
$\alpha_{2,17}$	4805	1.0003	\tilde{G}_{17}	5264	1.0001
$\alpha_{2,18}$	6604	1.0000	\tilde{G}_{18}	2899	1.0000
$\alpha_{2,19}$	5919	0.9996	\tilde{G}_{19}	3228	0.9999
$\alpha_{2,20}$	6502	1.0001	\tilde{G}_{20}	3140	0.9998

Table 12: Computation time (in seconds) for parameter estimation in the simulation studies and real-data application using N-IFM, HMC and HMC-IFM.

Study	N-IFM	HMC	HMC-IFM
Simulation study (Gaussian copula)	0.55	1,904	984
Simulation study (t copula)	0.64	30,042	14,245
Real Data	1.07	37,034	19,238

S7 Computing time

This section reports the computational time required for parameter estimation in the simulation studies and the real data application described in Sections 5, 6 and S8. We compare three inference algorithms: N-IFM, HMC and HMC-IFM. The corresponding computing times are summarised in Table 12.

S8 Simulation study: t copula

This section compares the accuracy of N-IFM, HMC, and HMC-IFM in fitting the t -copula models with GARCH(1,1) marginals and Gaussian errors.. The simulated data is generated from a one-factor t copula model with GARCH(1,1) marginals with Gaussian errors, comprising $D = 20$ series of length $T = 1000$, following Algorithm 5 in Section S2.3.

Figures 14–18 shows posterior distributions of GARCH(1,1) parameters and t copula parameters estimated using the N-IFM, HMC and HMC-IFM methods for a one-factor t copula model with GARCH(1,1) marginals with Gaussian errors, comprising $D = 20$ series of length $T = 1000$. The figures shows that N-IFM and HMC-IFM produce very similar posterior distributions, with only small differences. For the copula parameters, the N-IFM and HMC-IFM results also closely match those from full HMC. By contrast, full HMC gives tighter posterior distributions for the GARCH(1,1) marginal parameters than N-IFM and HMC-IFM. This appears to be because HMC estimates the marginal and copula parameters jointly, whereas N-IFM and HMC-IFM estimate them in two steps. Notably, the degrees-of-freedom parameter ν of the t copula inferred using N-IFM is more tightly centred around

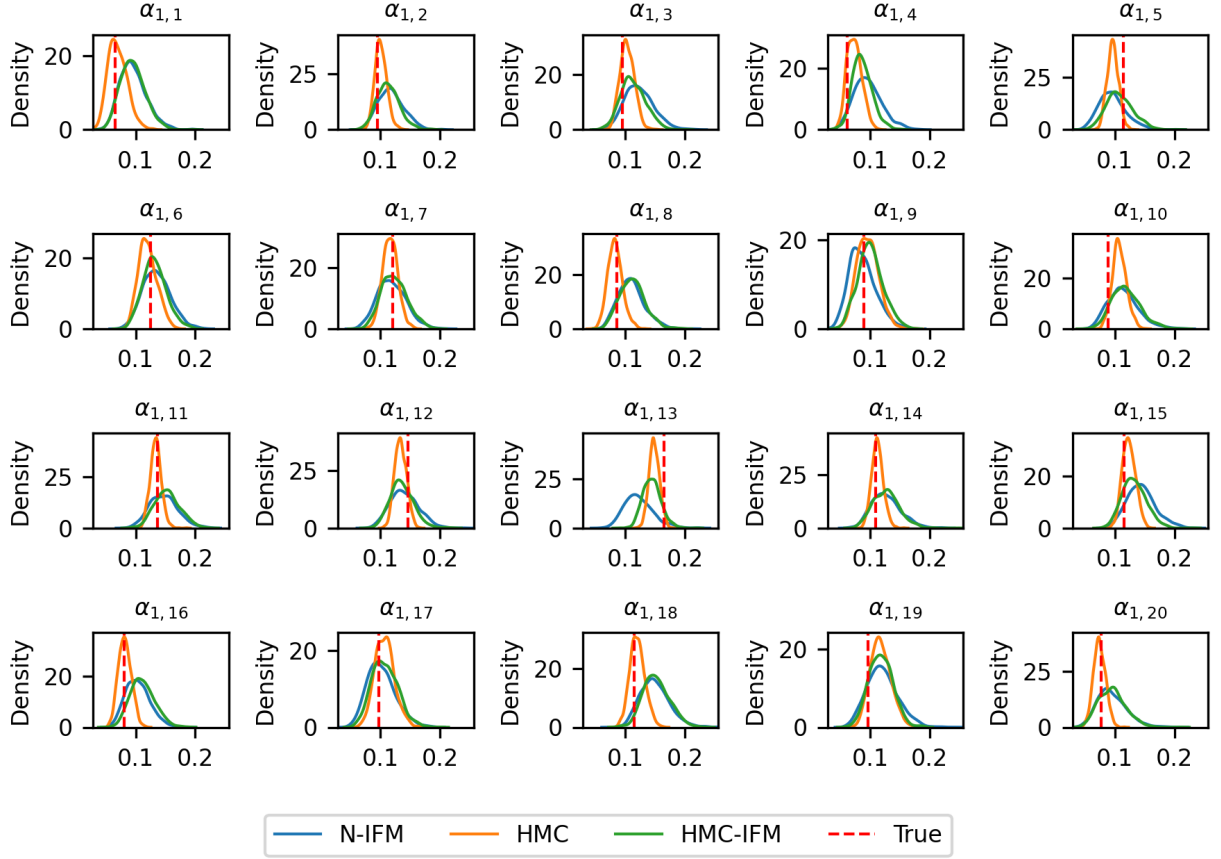


Figure 14: Posterior distributions of the GARCH(1, 1) parameters $\alpha_{1,d}$ for $d = 1, \dots, D$, comparing N-IFM, HMC and HMC-IFM with the true values. The results are based on simulated data from a 20 dimensional one-factor t copula with GARCH(1,1) marginals with Gaussian errors.

the true value than the corresponding HMC and HMC-IFM posteriors.

Figure 19 shows selected univariate and bivariate one-step-ahead posterior predictive densities obtained from N-IFM, HMC and HMC-IFM for a one-factor t copula model with GARCH(1,1) marginals with Gaussian errors. The predictive densities obtained from N-IFM, HMC and HMC-IFM are very similar. The lower triangular panels display the corresponding bivariate predictive distributions, which exhibit strong agreement across the three methods. In particular, the ellipses derived from N-IFM, HMC and HMC-IFM closely follow the true correlation structure. In terms of computational efficiency, as shown in Table 12 in Section S7, N-IFM is approximately 45,000 times faster than HMC and 22,000 times faster than

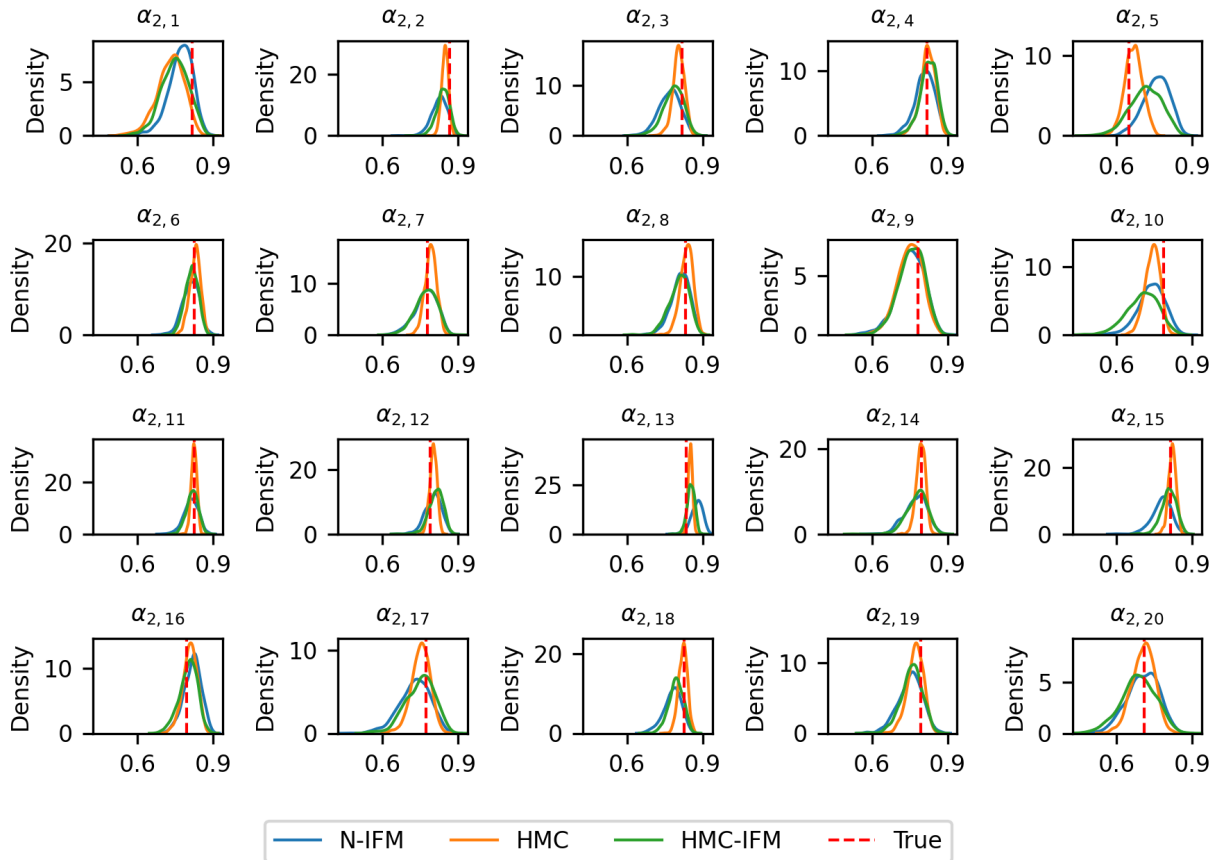


Figure 15: Posterior distributions of the GARCH(1,1) parameters $\alpha_{2,d}$ for $d = 1, \dots, D$, comparing N-IFM, HMC and HMC-IFM with the true values. The results are based on simulated data from a 20 dimensional one-factor t copula with GARCH(1,1) marginals with Gaussian errors.

HMC-IFM post-training, while delivering posterior estimates of comparable accuracy.

For the HMC implementation in `Stan`, standard diagnostics such as the effective sample size (`n_eff`) and the potential scale reduction factor (\widehat{R}) are used to assess convergence. As reported in Table 13, `n_eff` is large for all parameters and all \widehat{R} values are close to 1, indicating good mixing and convergence across chains. For HMC-IFM (not reported), all \widehat{R} values are close to 1, indicating good convergence, while `n_eff` is slightly lower for the GARCH(1,1) parameters and slightly higher for the copula parameters relative to HMC.

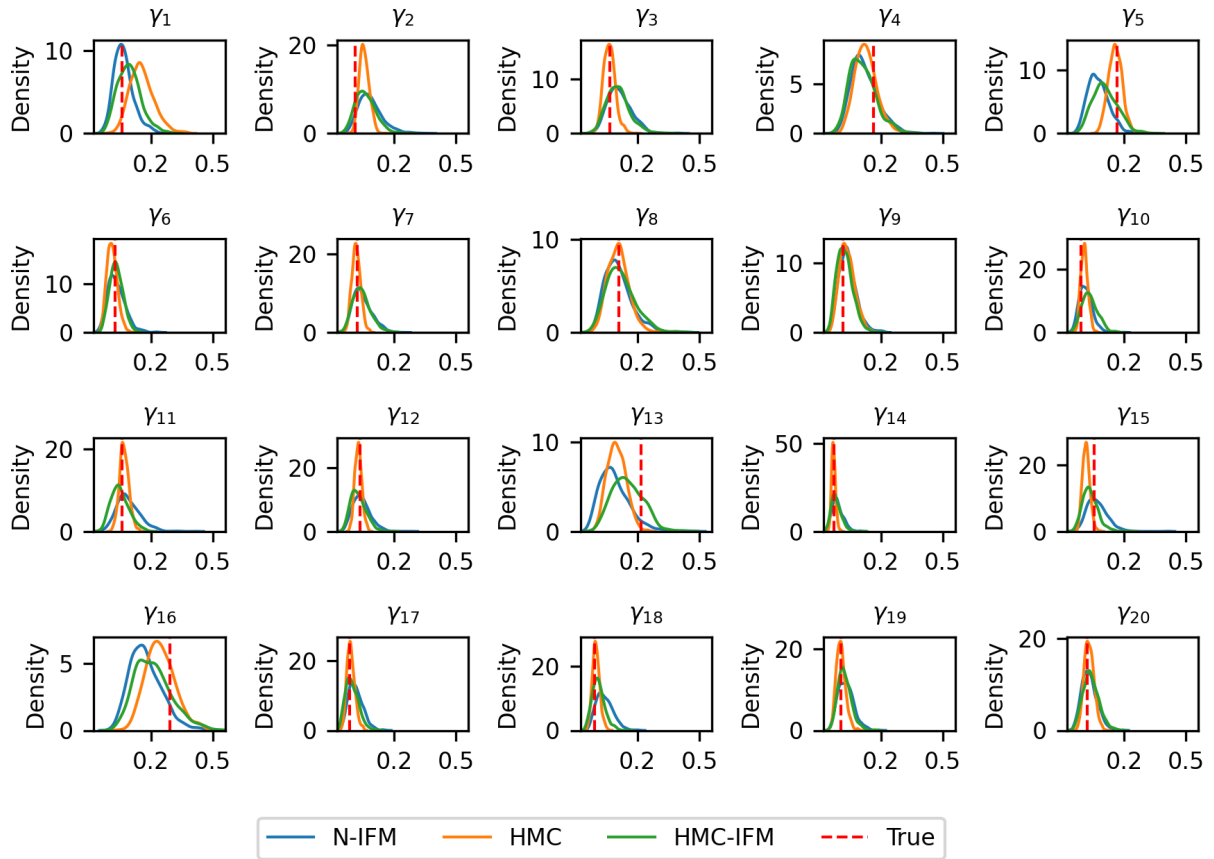


Figure 16: Posterior distributions of the GARCH(1,1) parameters γ_d for $d = 1, \dots, D$, comparing N-IFM, HMC and HMC-IFM with the true values. The results are based on simulated data from a 20 dimensional one-factor t copula with GARCH(1,1) marginals with Gaussian errors.

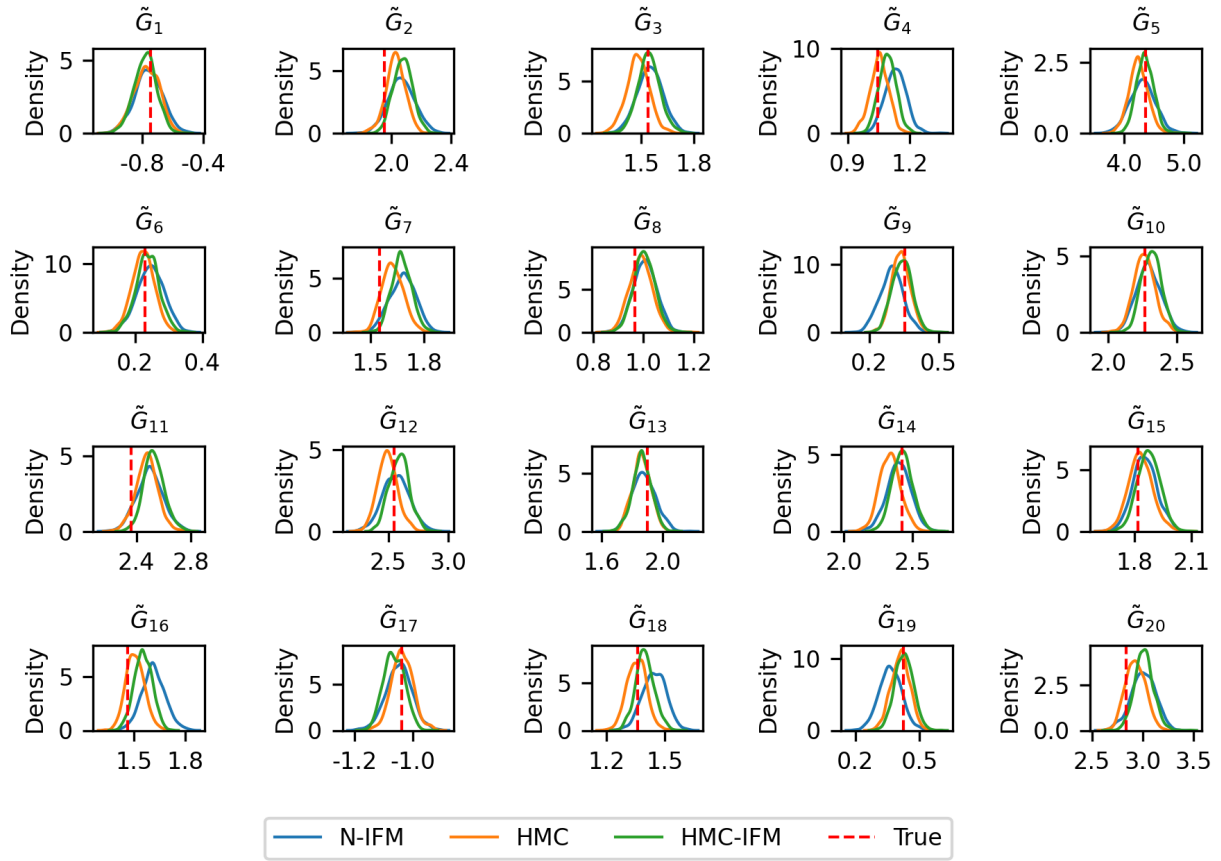


Figure 17: Posterior distributions of the t copula parameters $\tilde{\mathbf{G}}$, comparing N-IFM, HMC and HMC-IFM with the true values. The results are based on simulated data from a 20 dimensional one-factor t copula with GARCH(1,1) marginals with Gaussian errors.

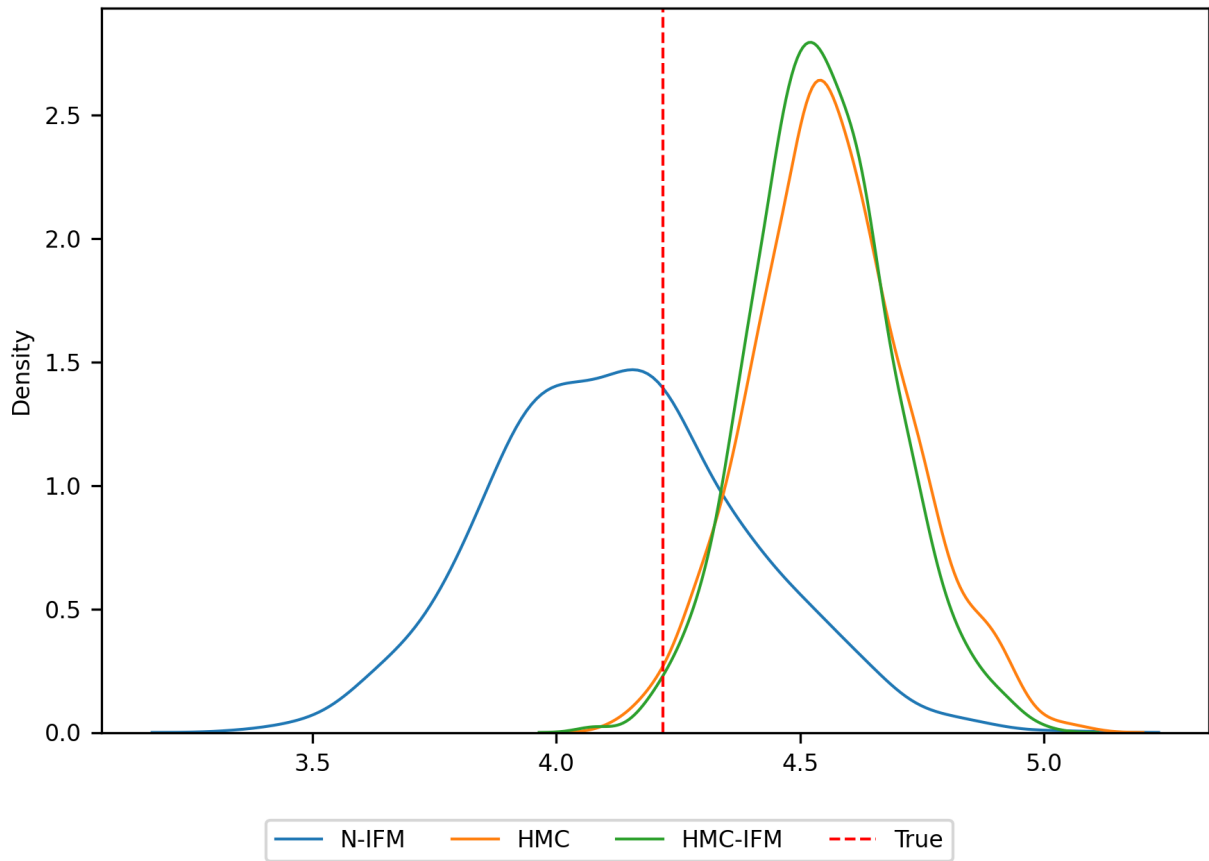


Figure 18: Posterior distributions of the t copula degrees-of-freedom parameter ν , comparing N-IFM, HMC and HMC-IFM with the true values. The results are based on simulated data from a 20 dimensional one-factor t copula with GARCH(1,1) marginals with Gaussian errors.

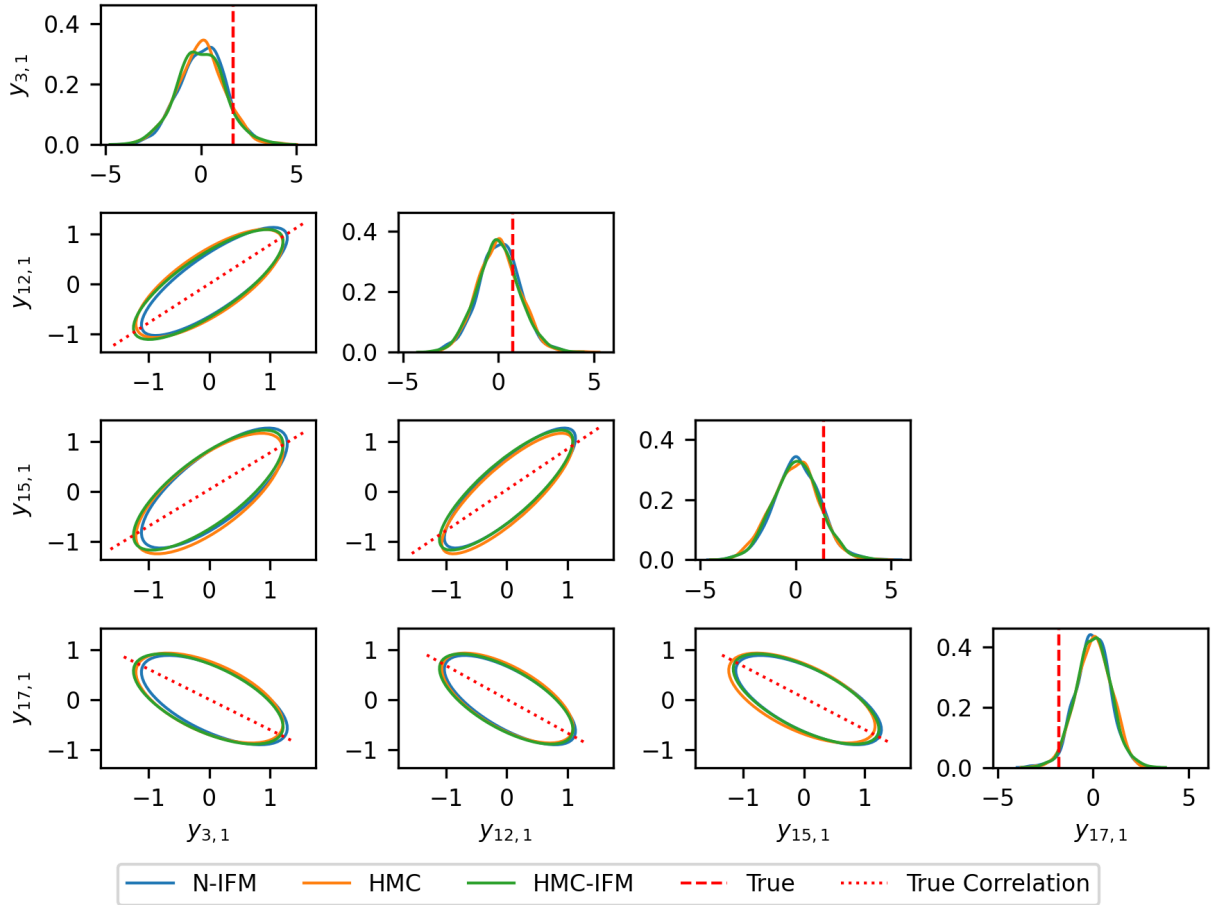


Figure 19: Selected one-step-ahead posterior predictive densities obtained from N-IFM, HMC and HMC-IFM for data simulated from a one-factor t copula model with GARCH(1,1) marginals with Gaussian errors, comprising $D = 20$ series of length $T = 1000$. Diagonal panels show the marginal predictive distributions, while off-diagonal panels display the corresponding bivariate predictive distributions. In the diagonal panels, the vertical lines indicate the true parameter values, while in the off-diagonal panels, the dotted lines represent the true correlation between each pair of series.

Table 13: Posterior diagnostics for model parameters estimated using HMC, based on simulated data from a 20 dimensional one factor t copula model with GARCH(1, 1) marginals with Gaussian errors, including the effective sample size (`n_eff`) and the potential scale reduction factor (\widehat{R}).

Parameter	<code>n_eff</code>	\widehat{R}	Parameter	<code>n_eff</code>	\widehat{R}
$\alpha_{1,1}$	7160	0.9996	γ_2	6135	0.9996
$\alpha_{1,2}$	5100	1.0002	γ_3	5215	0.9996
$\alpha_{1,3}$	5379	0.9997	γ_4	5483	0.9995
$\alpha_{1,4}$	6330	0.9997	γ_5	4254	0.9997
$\alpha_{1,5}$	4126	0.9998	γ_6	6012	1.0000
$\alpha_{1,6}$	4749	1.0006	γ_7	5275	0.9996
$\alpha_{1,7}$	5092	0.9996	γ_8	5983	0.9999
$\alpha_{1,8}$	5954	0.9999	γ_9	5936	0.9996
$\alpha_{1,9}$	6360	0.9997	γ_{10}	4410	0.9996
$\alpha_{1,10}$	4734	0.9997	γ_{11}	5376	1.0008
$\alpha_{1,11}$	2928	1.0009	γ_{12}	5265	1.0000
$\alpha_{1,12}$	3708	1.0008	γ_{13}	2031	1.0024
$\alpha_{1,13}$	5887	0.9997	γ_{14}	5123	0.9999
$\alpha_{1,14}$	3876	1.0000	γ_{15}	5802	0.9996
$\alpha_{1,15}$	4919	1.0002	γ_{16}	4660	0.9996
$\alpha_{1,16}$	4915	0.9996	γ_{17}	4529	0.9997
$\alpha_{1,17}$	4255	0.9997	γ_{18}	5715	1.0002
$\alpha_{1,18}$	4907	1.0000	γ_{19}	5803	0.9999
$\alpha_{1,19}$	5667	0.9998	γ_{20}	3611	1.0006
$\alpha_{1,20}$	4423	1.0000	\widetilde{G}_1	6554	0.9999
$\alpha_{2,1}$	5929	0.9999	\widetilde{G}_2	2504	1.0006
$\alpha_{2,2}$	5773	1.0002	\widetilde{G}_3	2310	1.0023
$\alpha_{2,3}$	5075	0.9998	\widetilde{G}_4	3187	1.0009
$\alpha_{2,4}$	5194	0.9996	\widetilde{G}_5	3163	1.0011
$\alpha_{2,5}$	4696	0.9998	\widetilde{G}_6	8707	0.9997
$\alpha_{2,6}$	7175	0.9996	\widetilde{G}_7	2540	1.0016
$\alpha_{2,7}$	5006	0.9997	\widetilde{G}_8	3187	1.0004
$\alpha_{2,8}$	5790	0.9999	\widetilde{G}_9	5728	0.9997
$\alpha_{2,9}$	5708	0.9996	\widetilde{G}_{10}	2201	1.0029
$\alpha_{2,10}$	4464	1.0003	\widetilde{G}_{11}	2336	1.0036
$\alpha_{2,11}$	6942	0.9995	\widetilde{G}_{12}	2509	1.0017
$\alpha_{2,12}$	6531	0.9997	\widetilde{G}_{13}	4066	1.0016
$\alpha_{2,13}$	5903	0.9997	\widetilde{G}_{14}	2018	1.0030
$\alpha_{2,14}$	5107	0.9995	\widetilde{G}_{15}	2484	1.0012
$\alpha_{2,15}$	6412	0.9997	\widetilde{G}_{16}	2755	1.0026
$\alpha_{2,16}$	4510	0.9999	\widetilde{G}_{17}	2882	1.0011
$\alpha_{2,17}$	4387	0.9995	\widetilde{G}_{18}	2861	1.0018
$\alpha_{2,18}$	6062	1.0005	\widetilde{G}_{19}	6286	1.0000
$\alpha_{2,19}$	6072	0.9998	\widetilde{G}_{20}	2139	1.0022
$\alpha_{2,20}$	3771	0.9999	ν	1798	1.0015
γ_1	5777	1.0000			

Table 14: Comparison of LPDS values for 100 one-step-ahead forecasts across the four candidate models C1–C4 evaluated on the four simulated datasets $M_{(1)}, \dots, M_{(4)}$. The values in bold indicate the best model.

Data Simulation	Criteria	C1	C2	C3	C4
$M_{(1)}$	LPDS	-2487	-2534	-2471	-2526
	Time (s)	131	137	167	174
$M_{(2)}$	LPDS	-1805	-1682	-1749	-1781
	Time (s)	149	146	169	162
$M_{(3)}$	LPDS	-2405	-2458	-2316	-2400
	Time (s)	100	106	111	115
$M_{(4)}$	LPDS	-1335	-1315	-1256	-1255
	Time (s)	136	136	137	153

S9 Simulation study 3: model selection

We investigate the performance of the N-IFM method to identify the true data-generating model, using the one-step-ahead log predictive density score (LPDS), computed under a rolling-window scheme with window length $T = 1000$, as in Section 5.4 of the main paper. The model achieving the highest LPDS is selected as the preferred model. We consider copula models with four factors under four specifications: (C1) a Gaussian copula with GARCH(1,1) marginals with Gaussian errors; (C2) a Gaussian copula with GARCH(1,1) marginals with Student’s- t errors; (C3) a t copula with GARCH(1,1) marginals with Gaussian errors; and (C4) a t copula with GARCH(1,1) marginals with Student’s- t errors.

We generate $D = 20$ dimensional multivariate time series of length $T = 1100$ from each of the four models described above, and denote them as $M_{(j)}$ for data generated from model j . For each simulated dataset $M_{(j)}$, $j = 1, \dots, 4$, we compare the four candidate models C1–C4 using the one-step-ahead LPDS. Table 14 reports the LPDS values and computation times for 100 one-step-ahead predictions. It compares the LPDS and computation times across the four candidate models C1–C4 for each simulated dataset $M_{(j)}$, for $j = 1, \dots, 4$. In each case, the highest LPDS is attained by the model that matches the true data-generating process. Computational time is lower for simpler models, with C1 exhibiting the shortest runtimes and C4 the longest.

S10 Additional details on the industry portfolio dataset

This section provides additional details on the industry portfolio dataset. Table 15 lists the industry sectors. The first $d = 1, \dots, 20$ sectors correspond to the 20 industry portfolios analysed in this study.

Figure 20 displays the de-meaned, average value-weighted returns for the 20 industry portfolios from 2 February 2015 to 20 December 2018. The agricultural industry is labelled as \mathbf{y}_1 . The \mathbf{y}_1 series has a minimum (-6.42) and maximum (7.66) return and shows the presence of some extreme movements and occasional large shocks. Several other series exhibit extreme movements and pronounced shocks, most notably \mathbf{y}_7 and \mathbf{y}_8 . The series \mathbf{y}_1 and \mathbf{y}_8 shows substantial excess kurtosis (8.23 and 33.16 respectively, compared with 0 under a Gaussian distribution), indicating heavy tails and a higher frequency of extreme observations. In addition, series \mathbf{y}_1 illustrates clear volatility clustering, highlighting the heteroskedastic nature of the data. These features support the use of GARCH-type volatility models with Student's- t errors rather than Gaussian errors.

Figure 21 presents histograms of the de-meaned, average value-weighted returns for all the 20 industry portfolios from 2 February 2015 to 20 December 2018. The series \mathbf{y}_1 , \mathbf{y}_6 , and \mathbf{y}_{14} exhibit the most pronounced spikes around zero, which is consistent with Figure 20. Overall, the histograms suggest leptokurtic return distributions, supporting the use of Student's- t innovations with relatively small degrees of freedom.

Table 15: List of industry portfolios.

<i>d</i>	Code	Industry Name
1	Agric	Agriculture, forestry, and fishing
2	Mines	Mining
3	Oil	Oil and Gas Extraction
4	Stone	Nonmetallic Minerals Except Fuels
5	Cnstr	Construction
6	Food	Food and Kindred Products
7	Smoke	Tobacco Products
8	Txtls	Textile Mill Products
9	Apprl	Apparel and Other Textile Products
10	Wood	Lumber and Wood Products
11	Chair	Furniture and Fixtures
12	Paper	Paper and Allied Products
13	Print	Printing and Publishing
14	Chems	Chemicals and Allied Products
15	Ptrlm	Petroleum and Coal Products
16	Rubbr	Rubber and Miscellaneous Plastics Products
17	Lethr	Leather and Leather Products
18	Glass	Stone, Clay and Glass Products
19	Metal	Primary Metal Industries
20	MtlPr	Fabricated Metal Products
21	Machn	Machinery, Except Electrical
22	Elctr	Electrical and Electronic Equipment
23	Cars	Transportation Equipment
24	Instr	Instruments and Related Products
25	Manuf	Miscellaneous Manufacturing Industries
26	Trans	Transportation
27	Phone	Telephone and Telegraph Communication
28	TV	Radio and Television Broadcasting
29	Utils	Electric, Gas, and Water Supply
30	Garbg	Sanitary Services
31	Steam	Steam Supply
32	Water	Irrigation Systems
33	Whsl	Wholesale
34	Rtail	Retail Stores
35	Money	Finance, Insurance, and Real Estate
36	Srvc	Services
37	Govt	Public Administration
38	Other	Almost Nothing

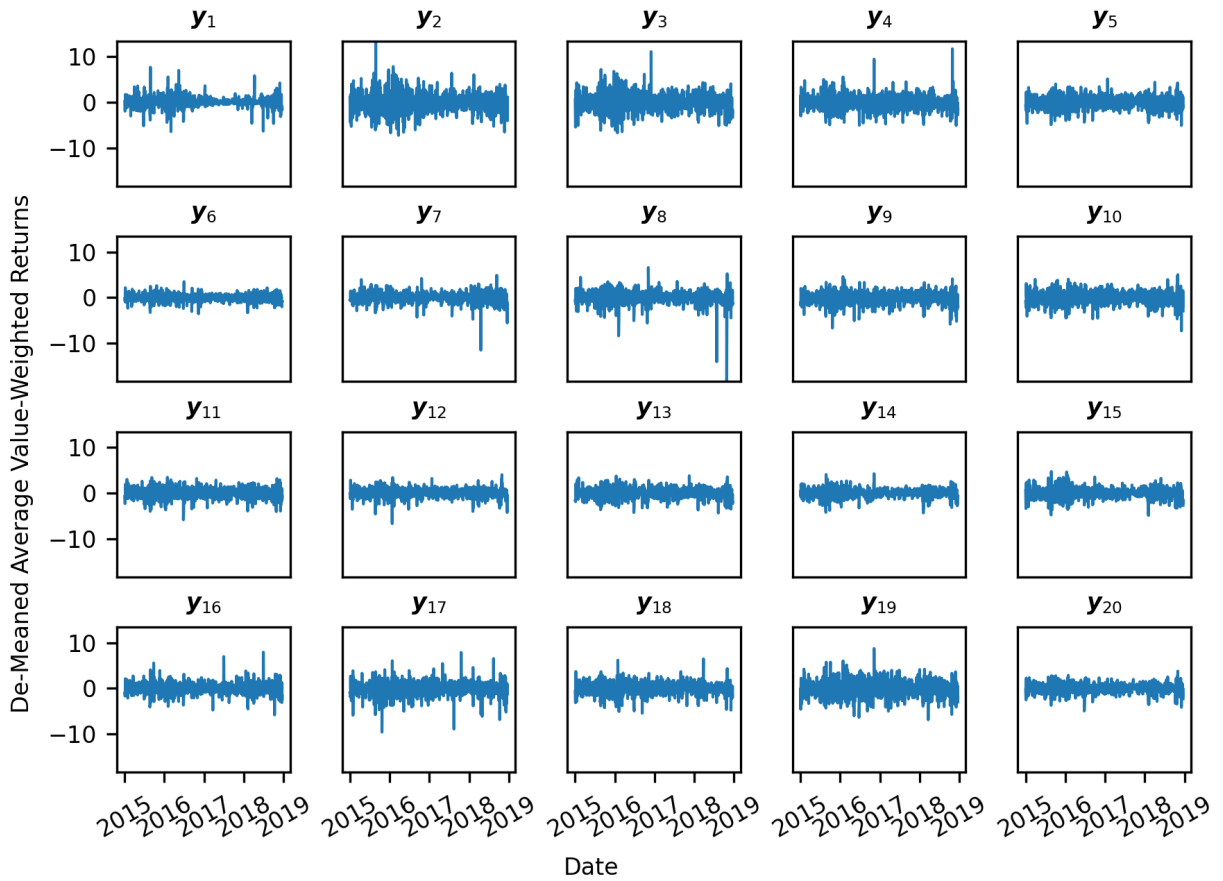


Figure 20: De-meaned, average value-weighted returns for the 20 industry portfolios from 2 February 2015 to 20 December 2018.

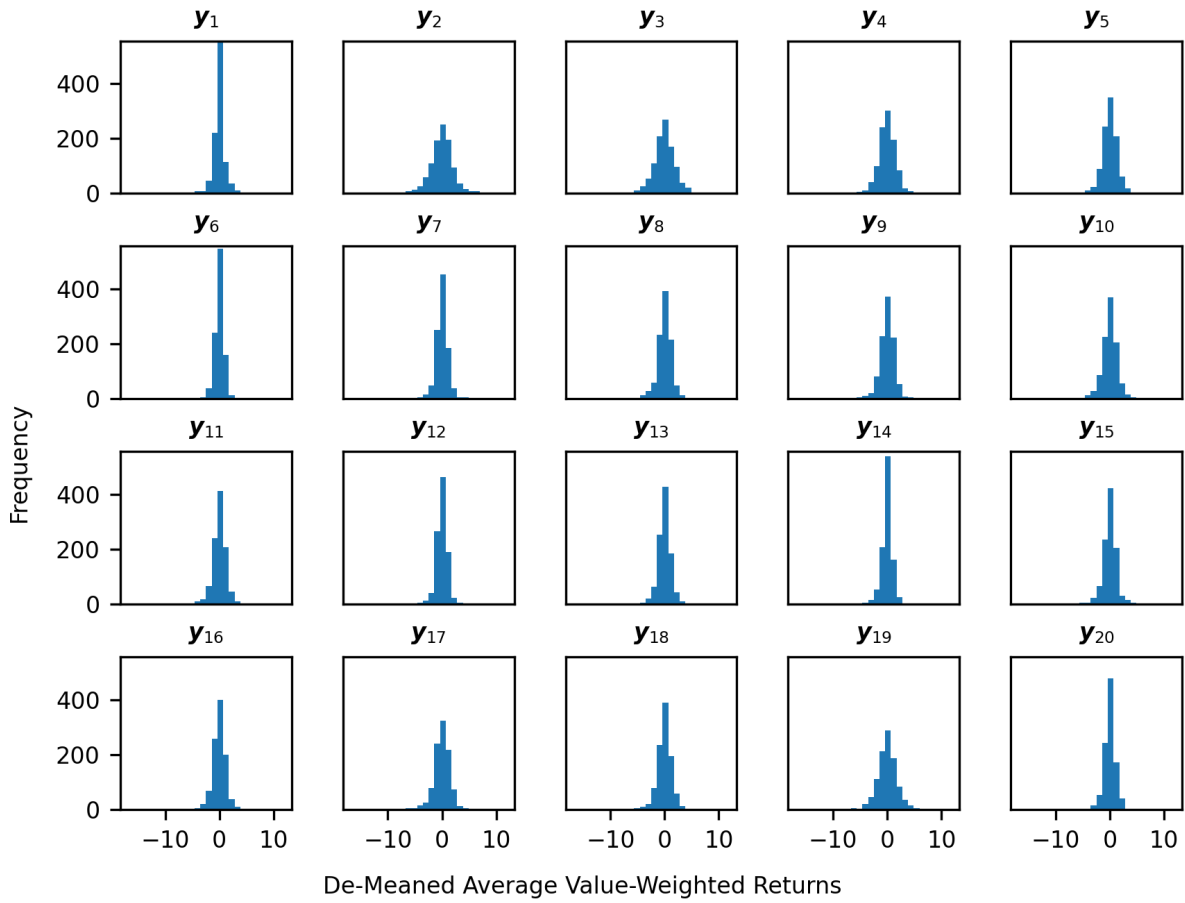


Figure 21: Histograms of de-meaned, average value-weighted returns for the 20 industry portfolios from 2 February 2015 to 20 December 2018.

S11 Additional results for the real data application

(Section 6)

In Section 6 of the main paper, we find that the best model on the real dataset is the four-factor Gaussian copula with GARCH(1,1) marginals with Student's- t errors. The posterior distributions of the parameters of the GARCH(1,1) model with Student's- t errors, obtained using N-IFM, HMC and HMC-IFM, are shown in Figures 22 to 25. Overall, the methods produce broadly similar posteriors. However, noticeable discrepancies appear for some marginal model parameters. In particular, the N-IFM approximation for some $\alpha_{1,d}$ parameters, and to a lesser extent for $\alpha_{2,d}$ and γ_d , differs from the corresponding HMC, while still having strong agreement with HMC-IFM, agreeing with findings from the simulation studies.

A noticeable difference occurs for the degrees-of-freedom parameter of the GARCH(1,1) errors. Figure 25 shows the posterior distribution of the degrees-of-freedom parameters. The N-IFM posterior distribution for the first degree-of-freedom parameter, $\tilde{\nu}_1$, is shifted to the right, whereas the HMC and HMC-IFM posterior distributions are tightly concentrated around 2. The posterior distributions for the Gaussian copula parameters are displayed in Figures 26 to 29. These results, except in a few cases, agree between N-IFM, HMC and HMC-IFM.

For the HMC implementation in `Stan`, we assess posterior sampling quality using standard MCMC diagnostics, including the effective sample size (`n_eff`) and the potential scale reduction factor ($\widehat{\mathbf{R}}$), which compares within-chain and between-chain variability for each parameter. These diagnostics are reported in Table 16. Overall, `n_eff` is large across parameters and the $\widehat{\mathbf{R}}$ values are very close to 1, indicating that the chains have mixed well. Although a small number of `n_eff` values for the $\tilde{\mathbf{G}}$ parameters fall below 1000, they remain sufficiently large to support reliable posterior inference. For HMC-IFM (results not reported), the $\widehat{\mathbf{R}}$ values are close to 1, indicating that the chains have mixed well, while `n_eff` is slightly lower for the GARCH(1,1) parameters and slightly higher for the copula

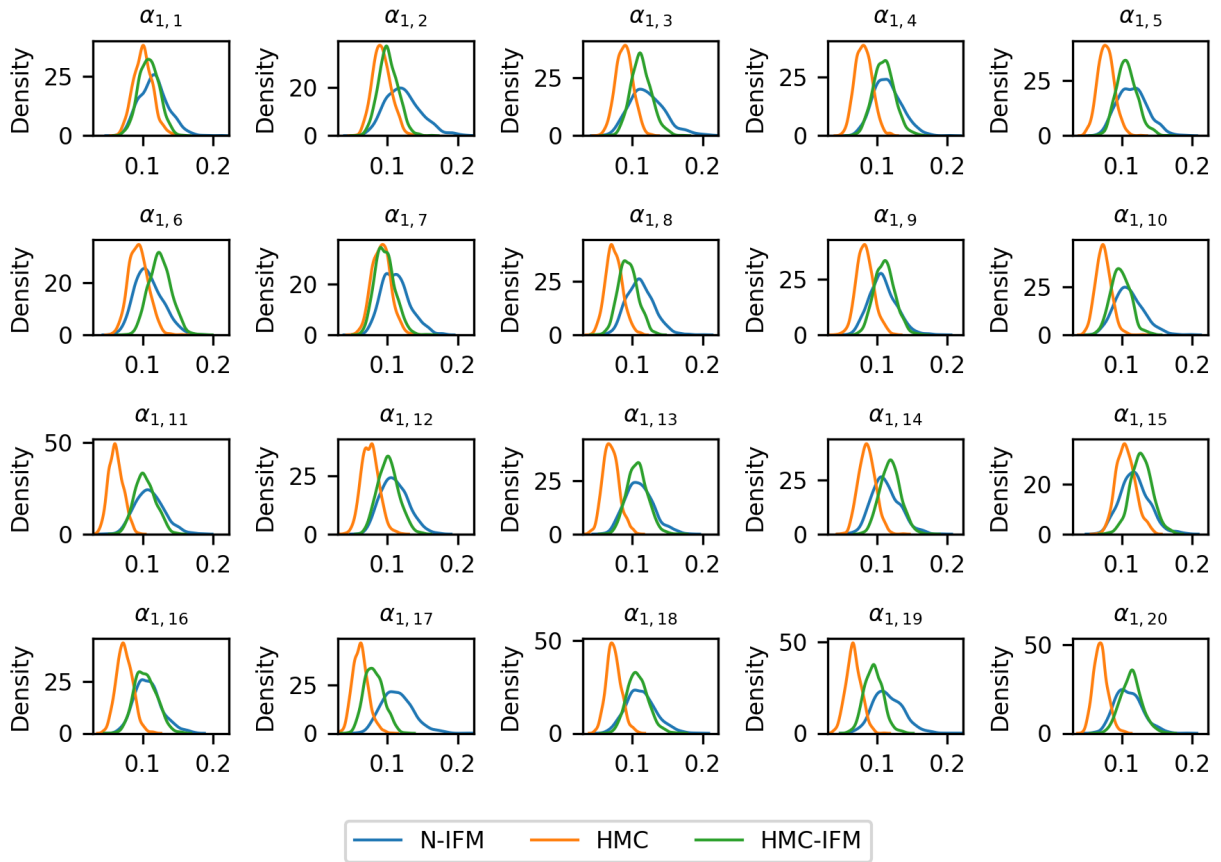


Figure 22: Posterior distributions of the GARCH(1, 1) parameters $\alpha_{1,d}$ for $d = 1, \dots, D$, comparing N-IFM with HMC and HMC-IFM for the industry portfolio data.

parameters relative to HMC. HMC-IFM required 20,000 iterations per chain for the copula model to obtain an adequate `n_eff`.

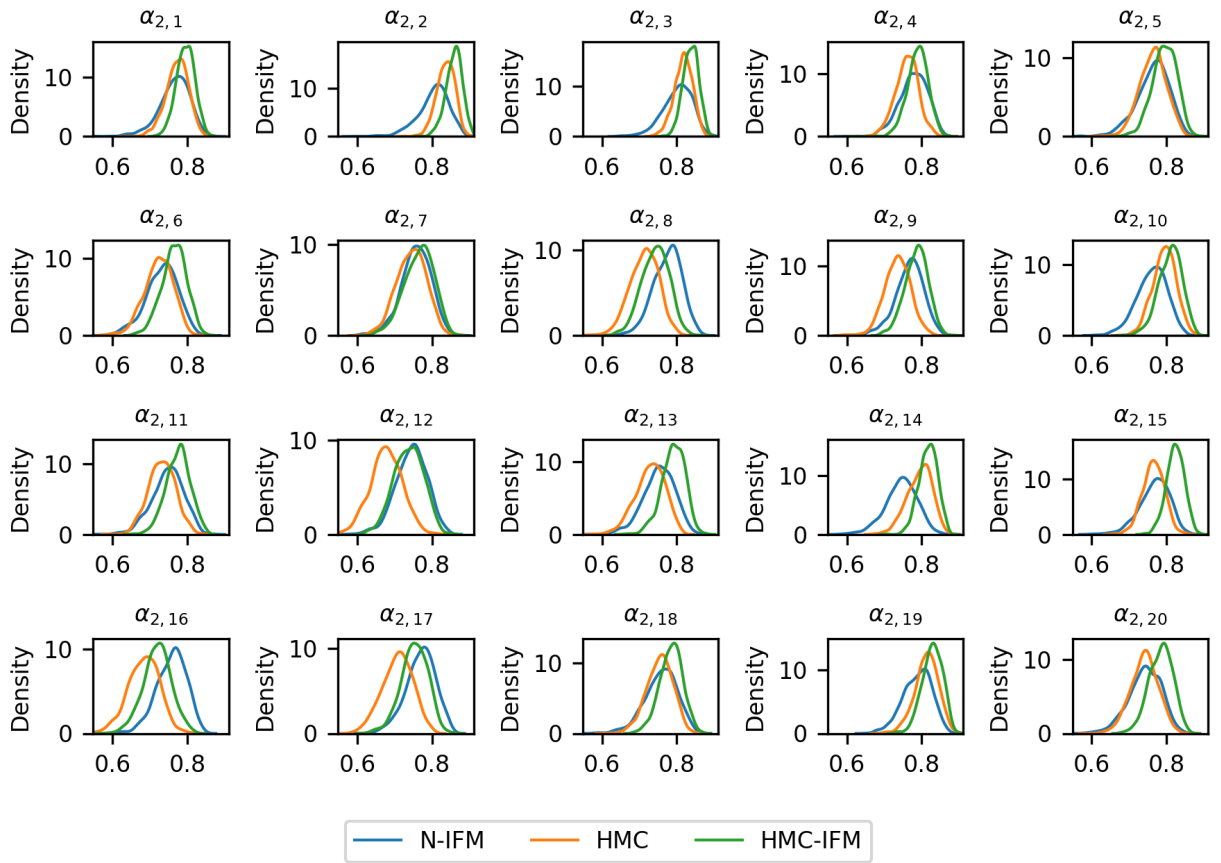


Figure 23: Posterior distributions of the GARCH(1, 1) parameters $\alpha_{2,d}$ for $d = 1, \dots, D$, comparing N-IFM with HMC and HMC-IFM for the industry portfolio data.

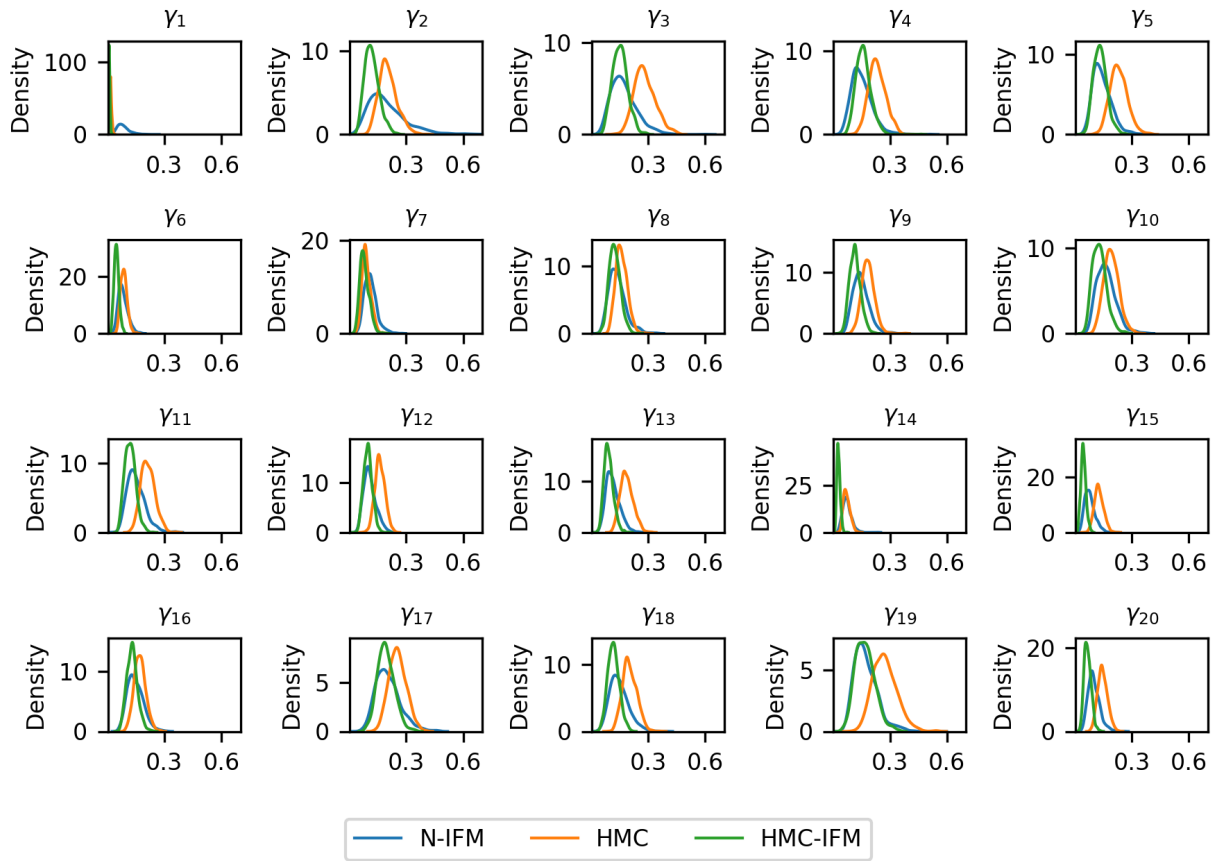


Figure 24: Posterior distributions of the GARCH(1,1) parameters γ_d for $d = 1, \dots, D$, comparing N-IFM with HMC and HMC-IFM for the industry portfolio data.

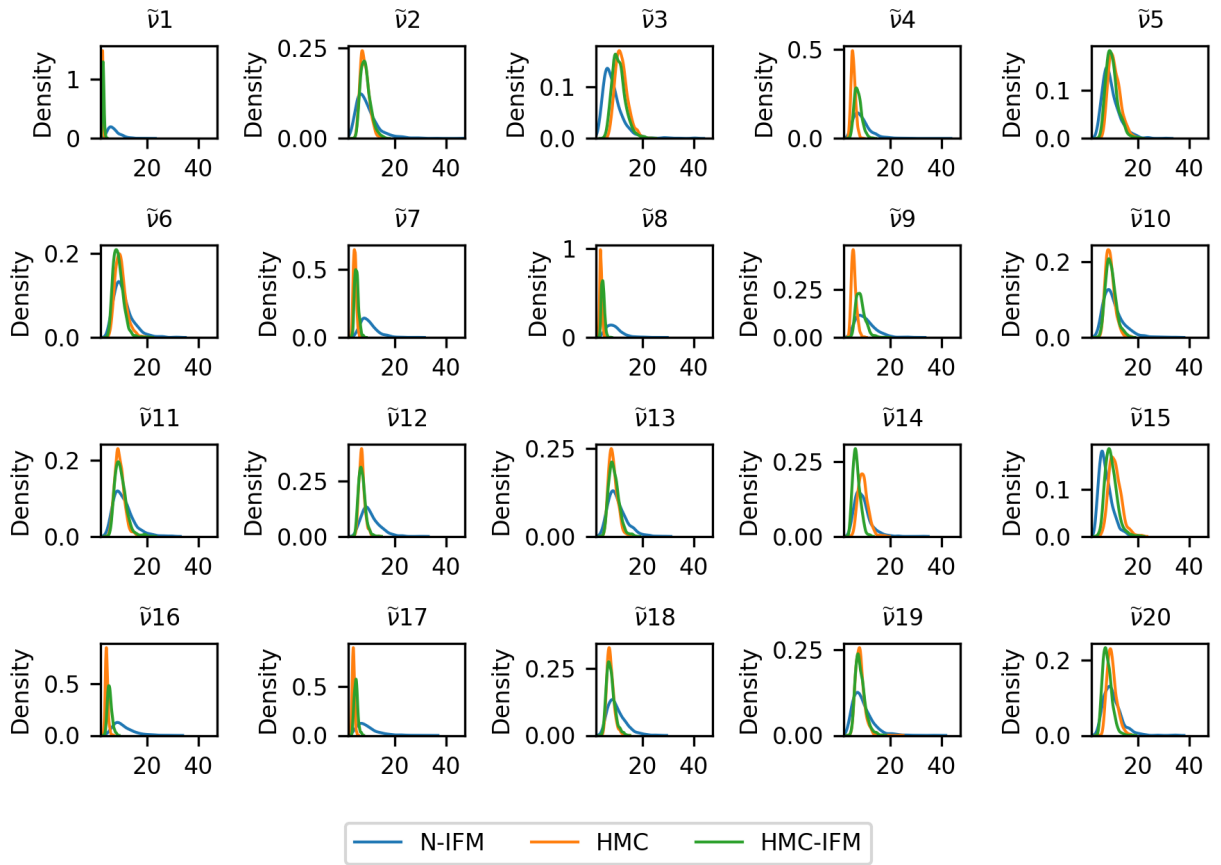


Figure 25: Posterior distributions of the GARCH(1,1) parameters $\tilde{\nu}_d$ for $d = 1, \dots, D$, comparing N-IFM with HMC and HMC-IFM for the industry portfolio data.

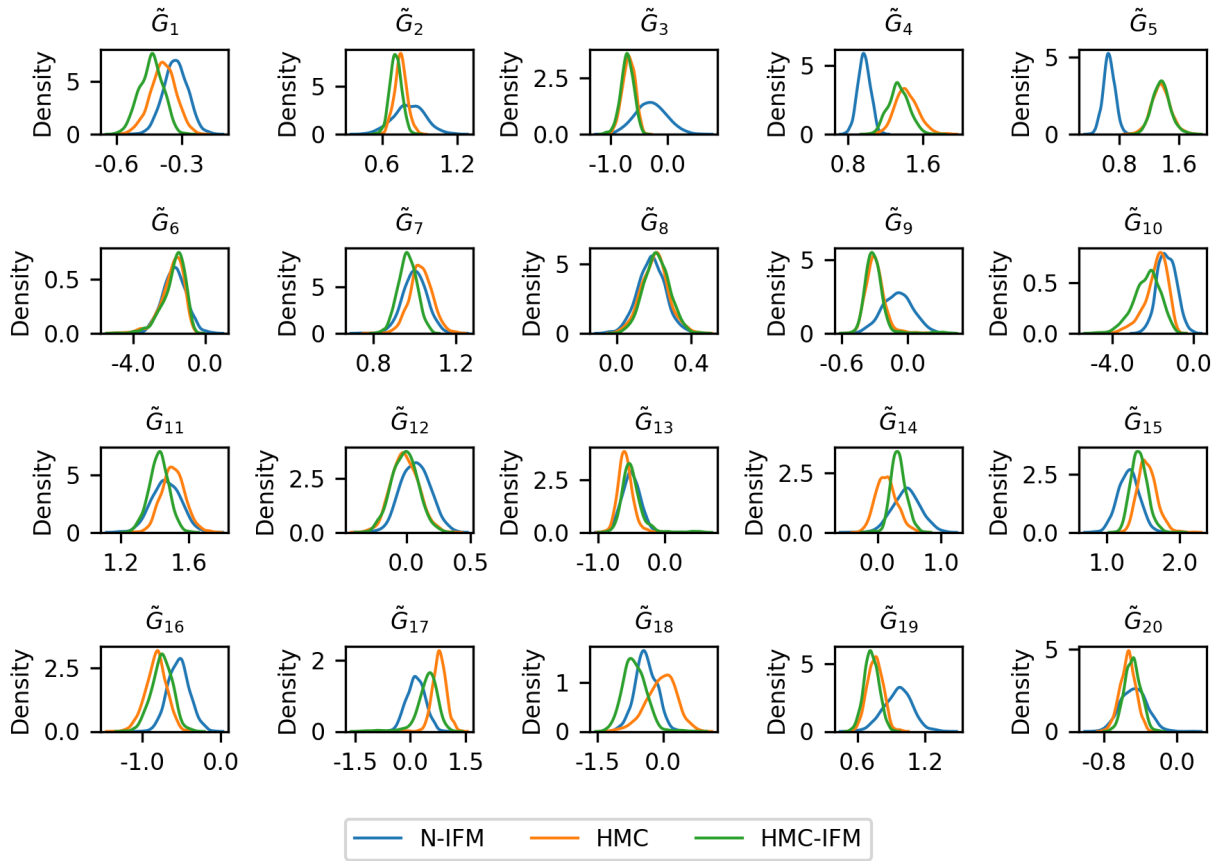


Figure 26: Posterior distributions of the 1st factor of copula parameters $\tilde{\mathbf{G}}$ for, comparing N-IFM with HMC and HMC-IFM for the industry portfolio data.

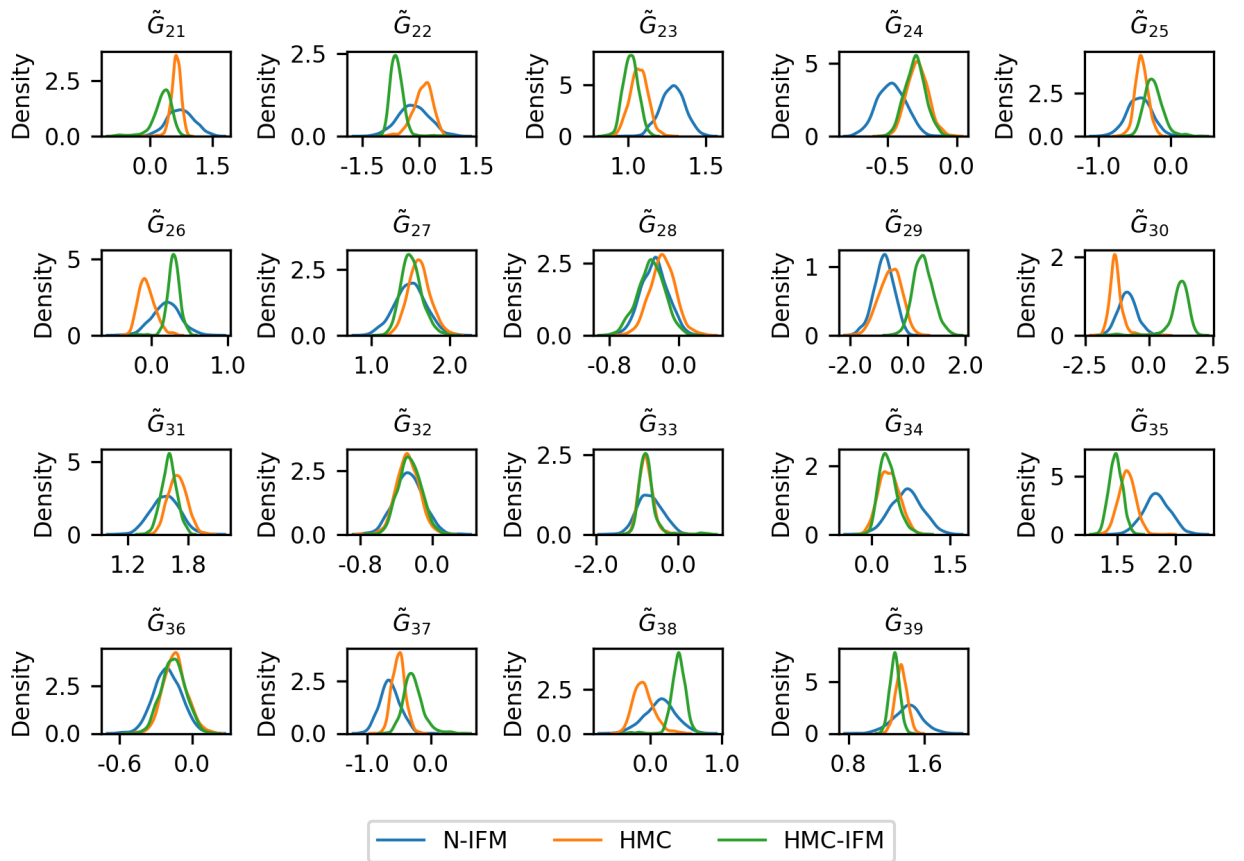


Figure 27: Posterior distributions of the 2nd factor of copula parameters \tilde{G} for, comparing N-IFM with HMC and HMC-IFM for the industry portfolio data.

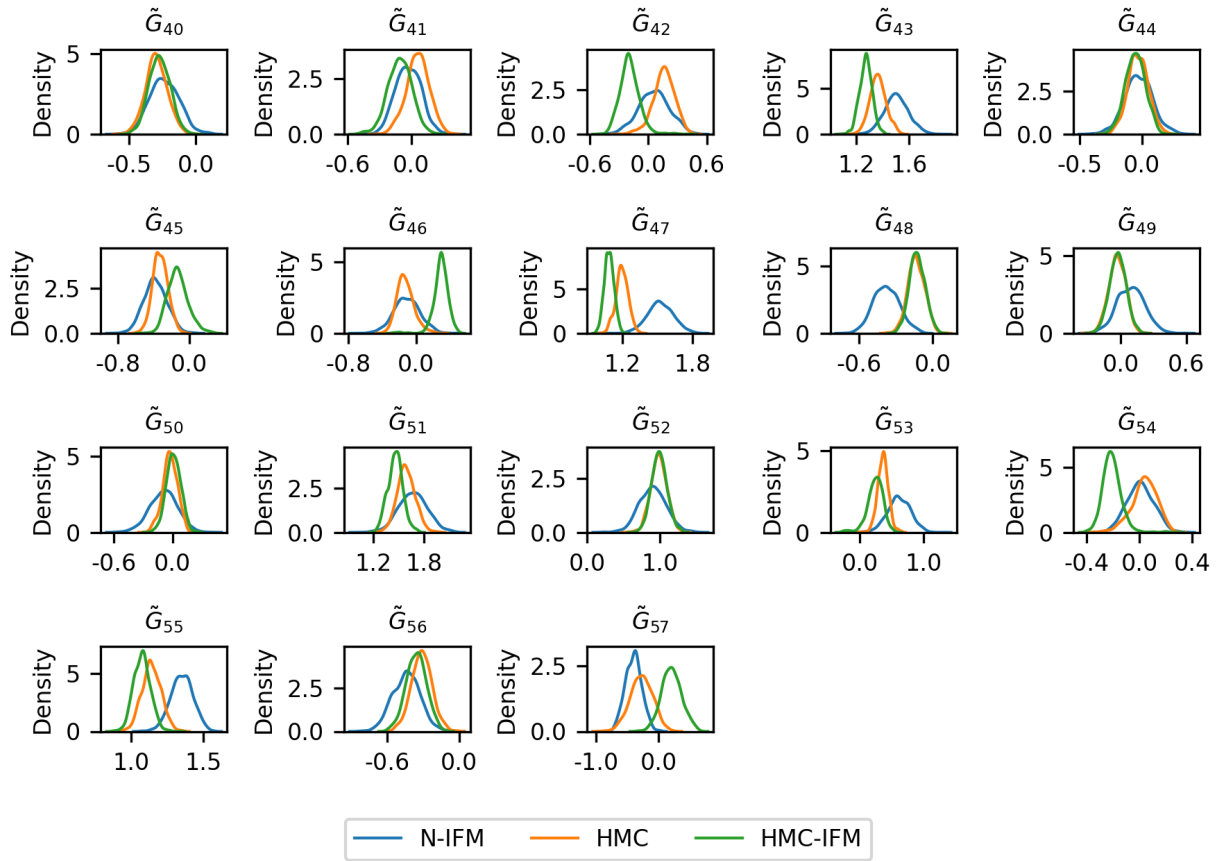


Figure 28: Posterior distributions of the 3rd factor of copula parameters \tilde{G} for, comparing N-IFM with HMC and HMC-IFM for the industry portfolio data.

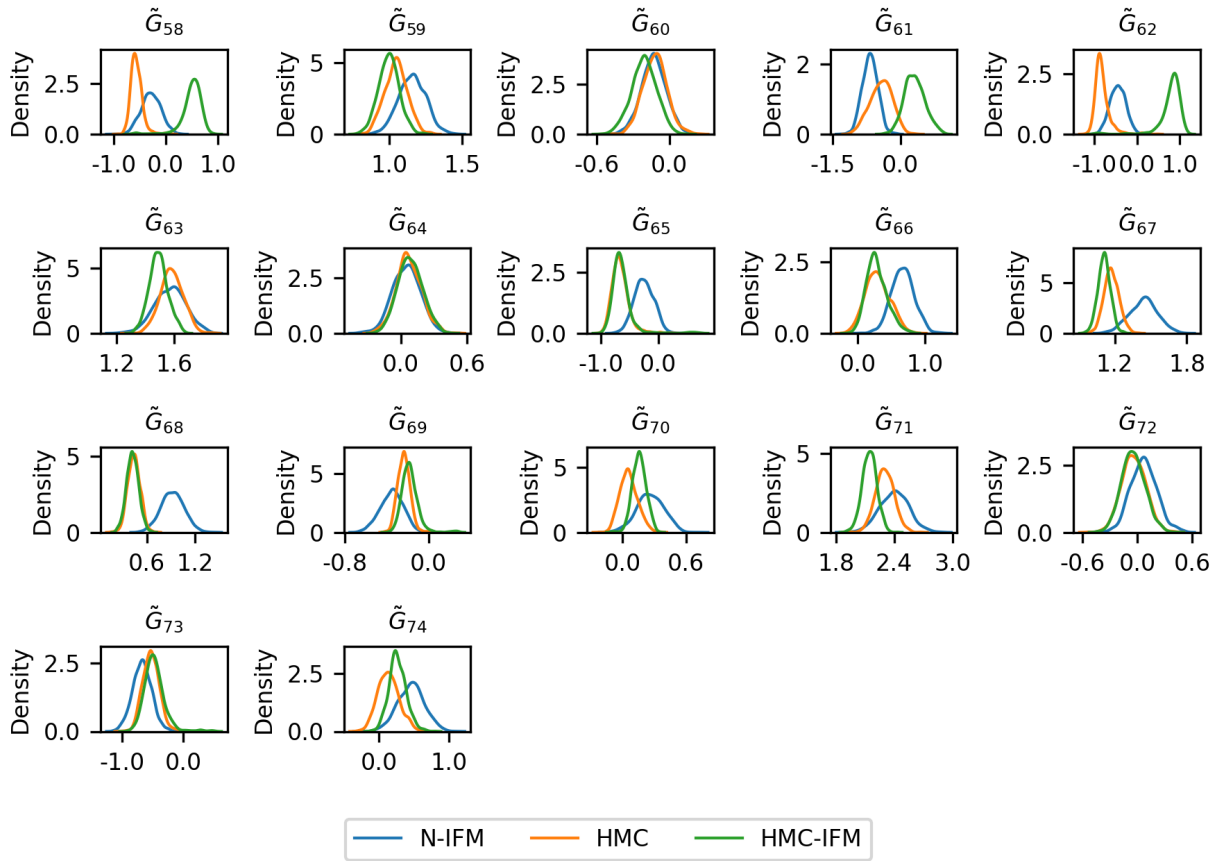


Figure 29: Posterior distributions of the 4th factor of copula parameters \tilde{G} for, comparing N-IFM with HMC and HMC-IFM for the industry portfolio data.

Table 16: Posterior diagnostics for model parameters estimated using HMC for the real data application, showing effective sample size (n_{eff}) and \hat{R} , for the Gaussian copula model with GARCH(1,1) marginals with Student's- t errors.

Parameter	n_{eff}	\hat{R}	Parameter	n_{eff}	\hat{R}	Parameter	n_{eff}	\hat{R}
$\alpha_{1,1}$	7771	0.9999	γ_{13}	7082	0.9999	\tilde{G}_{24}	1327	0.9997
$\alpha_{1,2}$	6481	0.9997	γ_{14}	5368	0.9997	\tilde{G}_{25}	1427	1.0008
$\alpha_{1,3}$	5986	0.9996	γ_{15}	6028	0.9996	\tilde{G}_{26}	800	1.0041
$\alpha_{1,4}$	6171	1.0001	γ_{16}	6339	0.9999	\tilde{G}_{27}	3329	0.9997
$\alpha_{1,5}$	5909	1.0001	γ_{17}	7157	0.9996	\tilde{G}_{28}	1460	1.0000
$\alpha_{1,6}$	6356	0.9998	γ_{18}	7216	0.9997	\tilde{G}_{29}	725	1.0030
$\alpha_{1,7}$	5847	1.0008	γ_{19}	5965	1.0002	\tilde{G}_{30}	657	1.0035
$\alpha_{1,8}$	5758	1.0004	γ_{20}	6754	0.9998	\tilde{G}_{31}	2361	0.9997
$\alpha_{1,9}$	5904	0.9997	$\tilde{\nu}_1$	6073	0.9997	\tilde{G}_{32}	1163	1.0002
$\alpha_{1,10}$	6647	0.9998	$\tilde{\nu}_2$	5756	0.9997	\tilde{G}_{33}	694	1.0040
$\alpha_{1,11}$	5917	0.9997	$\tilde{\nu}_3$	6192	0.9998	\tilde{G}_{34}	770	1.0029
$\alpha_{1,12}$	5468	1.0002	$\tilde{\nu}_4$	6439	1.0003	\tilde{G}_{35}	2393	0.9996
$\alpha_{1,13}$	6286	0.9998	$\tilde{\nu}_5$	6000	0.9997	\tilde{G}_{36}	1244	0.9995
$\alpha_{1,14}$	5463	1.0000	$\tilde{\nu}_6$	6948	0.9997	\tilde{G}_{37}	1466	1.0002
$\alpha_{1,15}$	5604	1.0005	$\tilde{\nu}_7$	5840	0.9998	\tilde{G}_{38}	775	1.0028
$\alpha_{1,16}$	5316	1.0005	$\tilde{\nu}_8$	6840	0.9998	\tilde{G}_{39}	3364	0.9997
$\alpha_{1,17}$	5962	0.9996	$\tilde{\nu}_9$	6495	0.9996	\tilde{G}_{40}	1700	0.9999
$\alpha_{1,18}$	6501	0.9998	$\tilde{\nu}_{10}$	5494	0.9998	\tilde{G}_{41}	1076	1.0028
$\alpha_{1,19}$	6463	0.9997	$\tilde{\nu}_{11}$	5680	0.9998	\tilde{G}_{42}	1502	1.0009
$\alpha_{1,20}$	6325	0.9998	$\tilde{\nu}_{12}$	7050	0.9998	\tilde{G}_{43}	2574	0.9998
$\alpha_{2,1}$	8532	0.9999	$\tilde{\nu}_{13}$	6695	0.9998	\tilde{G}_{44}	1256	0.9998
$\alpha_{2,2}$	6861	0.9998	$\tilde{\nu}_{14}$	6752	0.9996	\tilde{G}_{45}	1573	1.0001
$\alpha_{2,3}$	6628	0.9997	$\tilde{\nu}_{15}$	5724	0.9997	\tilde{G}_{46}	867	1.0026
$\alpha_{2,4}$	6682	0.9998	$\tilde{\nu}_{16}$	5948	0.9999	\tilde{G}_{47}	3184	0.9995
$\alpha_{2,5}$	8041	0.9997	$\tilde{\nu}_{17}$	5773	0.9996	\tilde{G}_{48}	1545	0.9996
$\alpha_{2,6}$	6024	0.9996	$\tilde{\nu}_{18}$	5574	0.9999	\tilde{G}_{49}	1588	1.0008
$\alpha_{2,7}$	7389	0.9998	$\tilde{\nu}_{19}$	6489	0.9999	\tilde{G}_{50}	2536	0.9996
$\alpha_{2,8}$	7130	0.9999	$\tilde{\nu}_{20}$	6638	0.9996	\tilde{G}_{51}	2933	1.0002
$\alpha_{2,9}$	7127	1.0001	\tilde{G}_1	4607	0.9998	\tilde{G}_{52}	2129	1.0000
$\alpha_{2,10}$	6537	0.9996	\tilde{G}_2	2799	1.0003	\tilde{G}_{53}	3160	1.0009
$\alpha_{2,11}$	6612	0.9997	\tilde{G}_3	2237	1.0002	\tilde{G}_{54}	776	1.0026
$\alpha_{2,12}$	7922	0.9996	\tilde{G}_4	2542	0.9996	\tilde{G}_{55}	2894	0.9997
$\alpha_{2,13}$	7776	0.9998	\tilde{G}_5	2831	0.9997	\tilde{G}_{56}	1455	1.0001
$\alpha_{2,14}$	5663	0.9998	\tilde{G}_6	1938	1.0016	\tilde{G}_{57}	850	1.0021
$\alpha_{2,15}$	6261	0.9998	\tilde{G}_6	1938	1.0016	\tilde{G}_{58}	878	1.0029
$\alpha_{2,16}$	6675	0.9996	\tilde{G}_7	2651	0.9996	\tilde{G}_{59}	2590	0.9996
$\alpha_{2,17}$	7193	0.9996	\tilde{G}_8	1477	0.9999	\tilde{G}_{60}	1549	1.0008
$\alpha_{2,18}$	7100	0.9997	\tilde{G}_9	751	1.0034	\tilde{G}_{61}	722	1.0029
$\alpha_{2,19}$	6711	1.0001	\tilde{G}_{10}	938	1.0030	\tilde{G}_{62}	615	1.0048
$\alpha_{2,20}$	7056	0.9999	\tilde{G}_{11}	2230	0.9998	\tilde{G}_{63}	2373	0.9996
γ_1	7037	0.9997	\tilde{G}_{12}	1181	1.0001	\tilde{G}_{64}	1186	0.9998
γ_2	6188	0.9999	\tilde{G}_{13}	897	1.0032	\tilde{G}_{65}	713	1.0045
γ_3	5940	0.9997	\tilde{G}_{14}	732	1.0035	\tilde{G}_{66}	732	1.0031
γ_4	6260	0.9998	\tilde{G}_{15}	3425	1.0000	\tilde{G}_{67}	2413	0.9998
γ_5	7715	0.9998	\tilde{G}_{16}	2244	1.0006	\tilde{G}_{68}	1465	1.0001
γ_6	5245	0.9998	\tilde{G}_{17}	1409	1.0004	\tilde{G}_{69}	1765	1.0004
γ_7	6374	0.9996	\tilde{G}_{18}	750	1.0029	\tilde{G}_{70}	821	1.0022
γ_8	6980	1.0000	\tilde{G}_{19}	2359	1.0003	\tilde{G}_{71}	2717	1.0000
γ_9	6581	0.9998	\tilde{G}_{20}	2217	0.9999	\tilde{G}_{72}	1227	0.9998
γ_{10}	6610	0.9997	\tilde{G}_{21}	1528	1.0006	\tilde{G}_{73}	1041	1.0016
γ_{11}	5733	0.9998	\tilde{G}_{22}	689	1.0035	\tilde{G}_{74}	1032	1.0019
γ_{12}	6759	0.9996	\tilde{G}_{23}	2640	0.9996			